MODE EXCITATION AND PROPAGATION IN WAVEGUIDES CONTAINING ANISOTROPIC PLASMAS

Thesis by

Alfred George Lieberman

In Partial Fulfillment of the Requirements

For the Degree of

Doctor of Philosophy

California Institute of Technology

Pasadena, California

1964

ACKNOWLEDGEMENT

The author wishes to express his sincere gratitude to the faculty of the California Institute of Technology for their assistance and advice during the course of this investigation. The author is particularly indebted to Professor Roy W. Gould for his interest and very capable guidance. The author also extends thanks to Dr. D. Gary Swanson for his suggestions and aid in preparing certain computer programs. Kiku Matsumoto and Harry Glover of the Caltech Computing Center are also thanked for their time and effort. Mrs. Ruth Stratton's very able and professional assistance in preparing this manuscript should not be overlooked. Last, but not least, the author thanks all his friends for their encouragement and goodwill.

ABSTRACT

An analysis is presented of perfectly-conducting cylindrical structures completely filled with cold, anisotropic plasmas. Major, but not exclusive, consideration is directed to the circular waveguide containing a lossless, longitudinally magnetized plasma. The modes are generally a mixture of TE and TM fields with the result that the conventional orthogonality relations must be replaced by appropriate generalizations. The orthogonality relations are used to determine the fields excited in a longitudinally magnetized plasmaguide* by a coaxial current loop. At cut-off, resonance, and at limiting values of the system's parameters, the modes reduce to simple TE or TM waves. The field configuration and dispersion are examined at these limiting conditions as well as at intermediate values of the parameters. Numerical results are provided for the cut-off frequencies and dispersion relation.

*Plasmaguide is the generic name given to any metallic waveguide containing an anisotropic plasma. In this manuscript it will refer to the longitudinally-magnetized, plasma-filled waveguide.

MODE EXCITATION AND PROPAGATION IN WAVEGUIDES

CONTAINING ANISOTROPIC PLASMAS

Table of Contents

ABSTRACT

INTRODUCTION 1

I. FUNDAMENTAL PRINCIPLES 4

The Physical Plasma Model 4

Derivation of the Conductivity and Permittivity Tensors 8

Properties of the Dielectric Tensor and Its Relation to Plane Waves 10

II. THE WAVEGUIDE FORMULATION 19

Maxwell's Equations in a Cylindrical Geometry 19

Boundary Conditions and Separable Waveguide Solutions 23

The Circular Waveguide 30

Reflection Symmetry 33

III. WAVE RESONANCE AND CUT-OFF IN THE CIRCULAR PLASMAGUIDE 36

Wave Resonance 36

Cyclotron resonance 37

Plasma resonance 40

The Cut-Off Frequencies 43

The circularly symmetric cut-off frequencies 51

The angularly dependent cut-off frequencies 63

IV. LIMITING FORMS OF WAVE PROPAGATION IN THE CIRCULAR PLASMAGUIDE 85

Limiting Magnetic Fields 86

No magnetic bias ($\underline{B}_o = 0$) 86

Infinite magnetic bias ($\underline{B}_o \to \infty$) 91

Geometric Limits 99

Plane waves in an unbounded plasma 99

The narrow waveguide limit and the quasi-static approximation 110

Guided Magnetohydrodynamic Waves 122

The Alfvén waves 123

The whistler mode of propagation 126

The MHD dispersion curves 130

V. WAVE DISPERSION IN THE CIRCULAR PLASMAGUIDE 134

VI. MODE ORTHOGONALITY, POWER FLOW AND PLASMAGUIDE EXCITATION 145

Notation 145

Mode Orthogonality for a Lossless Plasma 146

Power Flow 150

Wave Excitation in a Lossless Plasma 152

Mode Orthogonality for a Dissipative Plasma

Wave Excitation in a Dissipative Plasma

CONCLUSION 172

BIBLIOGRAPHY 174

APPENDIX 177

LIST OF SYMBOLS 179

INTRODUCTION

Plane waves in anisotropic plasmas of infinite extent have been treated exhaustively, but until now the bounded plasma has been studied only under very restricted conditions in domains that hardly overlap. The most common approximations usually concern the signal frequency, the plasma density and the applied magnetic field strength. Other assumptions involve the wave velocity, the field configuration, the relative magnitudes of the displacement and conduction currents, or the neglect of the electron to ion mass ratio.

The following manuscript presents a systematic account of wave excitation and propagation within perfectly conducting cylindrical waveguides containing anisotropic plasmas. The circular waveguide homogeneously filled with a longitudinally magnetized plasma is emphasized, but often more general results are given. The plasma is idealized as a cold, collisionless, electrically neutral gas consisting of electrons and a single species of ions. By neglecting the finite temperature of the plasma and the collision mechanism, ion-acoustic waves and dissipation losses are excluded from the theory. The plasma sheath formed at the waveguide wall and the effect of Landau damping are thereby also omitted.

The techniques developed by Kales (1), Suhl and Walker (2), Gamo (3), Van Trier (4), and Epstein (5), for investigating wave propagation in ferrites are employed in Chapter II, to solve Maxwell's equations in anisotropic plasmas. As in an ordinary waveguide, the transverse fields are derived from the longitudinal field components.

Now, however, the longitudinal electric and magnetic field components are coupled, and the variety of geometries which support separable wave solutions is substantially reduced. A careful investigation of the conditions leading to separable solutions indicates errors in two well-known papers (6,7).

Various limiting situations for which the waves divide into TE and TM modes are studied and compared in Chapter IV to the existing literature. For example, the validity of Trivelpiece's quasi-static approach (8) is determined, and the theory of guided MHD waves developed by Newcomb (9), Gajewski (10), Gould (11), Schmoys and Mishkin (12), is verified and extended. In another case the presence of an infinite magnetostatic field reduces the coupled waveguide modes to the familiar space-charge waves of microwave tube design. Finally, the fields of the lowest angular dependent modes are shown to approach plane waves as the waveguide radius is made infinite.

Numerical results are presented in Chapters III and V for various experimental observables such as the cut-off frequencies, resonance, and wave dispersion. These results are computed as functions of the waveguide radius, magnetostatic field strength and plasma density. Under suitable conditions the dispersion near plasma resonance may involve backward or even complex waves. The backward wave, first discussed by Trivelpiece and Gould (13), has oppositely directed phase and group velocities. The complex wave, whose existence was predicted by Chorney (14), has a propagation constant which is complex even in the absence of losses.

In the final chapter, several orthogonality relations are derived and then used to study waveguide excitation and power flow. The technique for determining the fields excited by a current source in an isotropic waveguide are well-known, however the same problem in a bounded anisotropic dielectric has not been solved until now. Formulas are obtained for evaluating the mode amplitudes excited by a coaxial current loop within the longitudinally-magnetized, plasma-filled circular waveguide. The loop is of arbitrary size and the plasma may be dissipative.

To recapitulate, this manuscript presents for the first time a systematic analysis of plasmaguide propagation that is valid over the entire frequency spectrum. As such, many of the existing partial theories are combined within the framework of a simple anisotropic dielectric description of the plasma. Much of the published literature consists of special limiting cases of our analysis. Walker's orthogonality relations (31), which were later extended by Bressler et al.(32) to include dissipative plasmas, are rederived here by a different scheme. When these relations are interpreted in terms of power flow, Chorney's results (14) are recovered. However, perhaps the most important contribution presented in this study is the technique by which the orthogonality relations are used to determine the plasmaguide fields excited by a given current source.

CHAPTER I. FUNDAMENTAL PRINCIPLES

The Physical Plasma Model

The dynamics of the plasma are complicated by the statistical nature of the interactions that each particle experiences. By restricting the analysis to an averaged or macroscopic description, the basic wave phenomenon is brought to the foreground. The macroscopic equations of motion, the so-called transfer equations of kinetic theory, are obtained as the moments (15,16) of a particle conservation law in phase space. The Boltzmann equation is the simplest statement of this law.

The plasma to be considered will consist of electrons and ions of a single species. The generalization to more than one ion species is straightforward but will not be considered in this text. On the whole, the medium is electrically neutral. It is further assumed that the particles are interpenetrable and that the only forces exerted on the particles are through the electric and magnetic fields. The presence of a neutral constituent is irrelevant when collisions are neglected. The thermal velocities which appear superimposed upon the collective motion of the plasma are also ignored.

A Boltzmann equation exists for each type of charge carrier present in the plasma. If one introduces the definitions

$$\rho = n_i q_i - n_e e \qquad \text{and} \qquad \underline{J} = n_i q_i \underline{v}_i - n_e e \, \underline{v}_e \qquad \text{(I-1)}$$

the "zeroth" moment of each Boltzmann equation may be combined to give the continuity relation

$$\nabla \cdot \underline{J} + \frac{\partial \rho}{\partial t} = 0 \qquad \text{(I-2)}$$

$\underline{J}$, ρ, and n are respectively the averaged current, charge and number densities at a point $\underline{r}$ and time t for particles of charge $+q_i$ and $-e$. $\underline{v}_i(\underline{r},t)$ and $\underline{v}_e(\underline{r},t)$ are the average velocities with which the ions and electrons pass through $\underline{r}$ at the instant t. Because the continuity equation I-2 is already contained in Maxwell's version of Ampere's and Gauss' laws:

$$\nabla \times \underline{H} = \underline{J} + \frac{\partial \underline{D}}{\partial t} \qquad \text{and} \qquad \nabla \cdot \underline{D} = \rho \qquad \text{(I-3)}$$

it need not appear in the explicit formulation of the plasma equations.

The first moment of the Boltzmann equation leads to a Newtonian equation of motion modified by a pressure and a collision term

$$n_i m_i (\frac{\partial}{\partial t} + \underline{v}_i \cdot \nabla)\underline{v}_i = n_i \underline{F}_i - \nabla \cdot \underline{\underline{\Psi}}_i + \underline{P}_{ie} \quad .$$

A similar equation exists for the electrons. The significance of the assumptions defining the plasma behavior now becomes evident. The pressure tensor $\underline{\underline{\Psi}}_i$ is a measure of the random deviations of the particle velocities from the organized motion. When the thermal motion is neglected, $\underline{\underline{\Psi}}_i$ vanishes. $\underline{P}_{ie}$ is the momentum transferred per unit time and volume from the ions to the electrons by collisions. The assumed interpenetrability of particles eliminates this force. This leaves only the Lorentz force

$$\underline{F}_i = q_i(\underline{E} + \underline{v}_i \times \underline{B}) \quad .$$

Hence the equation which will describe the ion motion is

$$m_i (\frac{\partial}{\partial t} + \underline{v}_i \cdot \nabla)\underline{v}_i = q_i(\underline{E} + \underline{v}_i \times \underline{B}) \quad . \qquad \text{(I-4)}$$

The analogous expression for electrons is obtained by replacing the ion mass m_i by m_e, the charge q_i by $-e$, and the velocity $\underline{v}_i$ by $\underline{v}_e$.

The nonlinear nature of equations I-1 and I-4 accounts for the dearth of exact solutions and the multiplicity of approximations. Thus a final and very essential assumption regarding the magnitude of the wave disturbance must be presented. The postulate known as the "small signal approximation" implies such slight perturbations from an otherwise steady condition that second-order product terms are negligible. In this fashion equations I-1 and I-4 are linearized and the principle of superposition becomes applicable. If the perturbations are then Fourier analyzed, each harmonic component will separately satisfy the linearized set of equations.

To comply with this assumption, let

$$\underline{E}(r,t) = \underline{E}_o(\underline{r}) + \underline{E}_1(\underline{r},t)$$

$$\underline{B}(\underline{r},t) = \underline{B}_o(\underline{r}) + \underline{B}_1(\underline{r},t)$$

$$n(\underline{r},t) = n_o(\underline{r}) + n_1(\underline{r},t)$$

$$\underline{v}(\underline{r},t) = \underline{v}_o(\underline{r}) + \underline{v}_1(\underline{r},t)$$

$$\underline{J}(\underline{r},t) = \underline{J}_o(\underline{r}) + \underline{J}_1(\underline{r},t) \quad .$$

The zero subscripts denote the steady or d.c. components of the field and plasma variables, while the subscript 1 refers to small time-dependent perturbations from these averages. Accordingly, equations

I-1 and I-4 are decomposed into a self-consistent set of static and small-signal equations:

$$\underline{J}_o = q_i n_{io} \underline{v}_{io} - e\, n_{eo} \underline{v}_{eo} \tag{I-5a}$$

$$\underline{J}_1 = q_i (n_{io} \underline{v}_{i1} + n_{i1} \underline{v}_{io}) - e(n_{eo} \underline{v}_{e1} + n_{e1} \underline{v}_{eo}) \tag{I-5b}$$

$$m_i (\underline{v}_{io} \cdot \nabla) \underline{v}_{io} = q_1 (\underline{E}_o + \underline{v}_{io} \times \underline{B}_o) \tag{I-6a}$$

$$m_i \left[\left(\frac{\partial}{\partial t} - \underline{v}_{io} \cdot \nabla \right) \underline{v}_{i1} + (\underline{v}_{i1} \cdot \nabla) \underline{v}_{io} \right] = q_i (\underline{E}_1 + \underline{v}_{i1} \times \underline{B}_o + \underline{v}_{io} \times \underline{B}_1) \tag{I-6b}$$

The resultant static electric field within the plasma is zero, since the induced field set up by the free charge cancels the applied electric field. In the problem about to be considered, the plasma is at rest and the drift velocities $\underline{v}_{io}$ and $\underline{v}_{eo}$, together with the direct current $\underline{J}_o$, are therefore zero. As a result the static equations I-5a and I-6a vanish, whereas equations I-5b and I-6b reduce to

$$\underline{J}_1 = q_i n_{io} \underline{v}_{i1} - e\, n_{eo} \underline{v}_{e1} \tag{I-7}$$

$$m_i \frac{\partial \underline{v}_{i1}}{\partial t} = q_i (\underline{E}_1 + \underline{v}_{i1} \times \underline{B}_o) \quad . \tag{I-8}$$

The analogous equation of motion for the electron is

$$m_e \frac{\partial \underline{v}_{e1}}{\partial t} = -\, e(\underline{E}_1 + \underline{v}_{e1} \times \underline{B}_o) \quad . \tag{I-9}$$

Although highly restrictive, the small signal assumption is of great importance, for it exhibits the basic wave behavior. Within its limitations, one can consider a variety of situations distinguished by diverse stationary conditions. The static equations retain the

nonlinearity of the original equations so that in general the assortment of rigorous static solutions is meager. In our particular problem the static equations conveniently vanish.

Derivation of the Conductivity and Permittivity Tensors

The conductivity of the plasma is governed by the motion of the charges through the applied field. If the stimulus has an $e^{j\omega t}$ time dependence the steady-state response of the linearized system must also be sinusoidal. The equations of motion, I-8 and I-9, are therefore

$$j\omega m_i \underline{v}_i = q_i(\underline{E} + \underline{v}_i \times \underline{B}_o) \tag{I-10a}$$

$$j\omega m_e \underline{v}_e = -e(\underline{E} + \underline{v}_e \times \underline{B}_o) \quad . \tag{I-10b}$$

Since all the plasma and field variables except $\underline{B}_o$ are time-dependent the subscript 1 has been deleted. By solving equations I-10 for the velocities and substituting the result into I-7, a tensorial current-field relation is obtained.

$$\begin{pmatrix} J_r \\ J_\theta \\ J_z \end{pmatrix} = \begin{pmatrix} \sigma_1 & +j\sigma_2 & 0 \\ -j\sigma_2 & \sigma_1 & 0 \\ 0 & 0 & \sigma_2 \end{pmatrix} \begin{pmatrix} E_r \\ E_\theta \\ E_z \end{pmatrix} \tag{I-11}$$

with

$$\sigma_1 = j\omega\epsilon_o \left\{ \frac{\Omega_e^2}{\omega_e^2 - \omega^2} + \frac{\Omega_i^2}{\omega_i^2 - \omega^2} \right\} \tag{I-12a}$$

$$\sigma_2 = j\omega\epsilon_o \left\{ \frac{\Omega_e^2 \omega_e}{\omega(\omega_e^2 - \omega^2)} - \frac{\Omega_i^2 \omega_i}{\omega(\omega_i^2 - \omega^2)} \right\} \tag{I-12b}$$

$$\sigma_3 = - j\omega\epsilon_o \left\{ \frac{\Omega_e^2 + \Omega_i^2}{\omega^2} \right\} \quad . \tag{I-12c}$$

The z axis is along the direction of the magnetostatic field $\underline{B}_o$. σ_1 and σ_3 are the conductivities perpendicular and parallel to the magnetostatic field and σ_2 is the Hall conductivity. $\omega_e = \frac{eB_o}{m_e}$ and $\omega_i = \frac{q_i B_o}{m_i}$ are the electron and ion cyclotron frequencies, whereas $\Omega_e = (\frac{n_{eo}\, e^2}{m_e \epsilon_o})^{1/2}$ and $\Omega_i = (\frac{n_{io}\, q_i^2}{m_i \epsilon_o})^{1/2}$ are the corresponding plasma frequencies.

The fields are determined in a self-consistent manner by solving equations I-11 and I-12 simultaneously with Maxwell's equations:

$$\nabla \times \underline{E} = - j\omega \mu_o \underline{H} \tag{I-13}$$

$$\nabla \times \underline{H} = \underline{J} + j\omega\epsilon_o \underline{E} \quad . \tag{I-14}$$

For convenience the convection and displacement currents are combined as one term by writing

$$\underline{J} + j\omega\epsilon_o \underline{E} = j\omega(\frac{\underline{\underline{\sigma}}}{j\omega} + \epsilon_o \underline{\underline{1}}) \cdot \underline{E} = j\omega\underline{\underline{\epsilon}} \cdot \underline{E} = j\omega\underline{D} \tag{I-15}$$

so that

$$\nabla \times \underline{H} = j\omega\underline{\underline{\epsilon}} \cdot \underline{E} \quad . \tag{I-16}$$

In this manner the complex permittivity tensor is defined by

$$\begin{pmatrix} D_r \\ D_\theta \\ D_z \end{pmatrix} = \begin{pmatrix} \epsilon_1 & +j\epsilon_2 & 0 \\ -j\epsilon_2 & \epsilon_1 & 0 \\ 0 & 0 & \epsilon_3 \end{pmatrix} \begin{pmatrix} E_r \\ E_\theta \\ E_z \end{pmatrix} \tag{I-17}$$

with

$$\epsilon_1 = \epsilon_o \left\{ 1 + \frac{\Omega_e^2}{\omega_e^2 - \omega^2} + \frac{\Omega_i^2}{\omega_i^2 - \omega^2} \right\} \tag{I-18a}$$

$$\epsilon_2 = \epsilon_o \left\{ \frac{\Omega_e^2 \, \omega_e}{\omega(\omega_e^2 - \omega^2)} - \frac{\Omega_i^2 \, \omega_i}{\omega(\omega_i^2 - \omega^2)} \right\} \tag{I-18b}$$

$$\epsilon_3 = \epsilon_o \left\{ 1 - \frac{\Omega_e^2 + \Omega_i^2}{\omega^2} \right\} \quad . \tag{I-18c}$$

Properties of the Dielectric Tensor and Its Relation to Plane Waves

The permittivity tensor of equation I-17 exhibits the following symmetries with respect to the magnetostatic field:

$$\underline{\underline{\epsilon}}(+\underline{B}_o) = \underline{\underline{\tilde{\epsilon}}}(-\underline{B}_o) \tag{I-19}$$

and

$$\epsilon_{ik} = \epsilon^*_{ki} \quad . \tag{I-20}$$

Equation I-20, describing the Hermitian character of $\underline{\underline{\epsilon}}$, follows directly from the conservation of energy (Poynting's theorem) in a dissipationless plasma. However, while equation I-20 applies only to a lossless plasma, Landau and Lifshitz (17,18) show that equation I-19 remains valid even if the medium is dissipative. The tilde above the permittivity tensor indicates that reversing the magnetic field transposes the matrix representation of $\underline{\underline{\epsilon}}$. The subscripts i,k designate the position of an element in the matrix, and the asterisk implies complex conjugation. The elements of the lossless permittivity tensor are real along the main diagonal, while the elements symmetrically disposed to the diagonal are complex conjugates.

Combining equations I-19 and I-20 one concludes that in a lossless plasma

$$\text{Re } \epsilon_{ik}(+\underline{B}_o) = \text{Re } \epsilon_{ki}(+\underline{B}_o) = \text{Re } \epsilon_{ik}(-\underline{B}_o) \tag{I-21}$$

$$\text{Im } \epsilon_{ik}(+\underline{B}_o) = -\text{Im } \epsilon_{ki}(+\underline{B}_o) = -\text{Im } \epsilon_{ik}(-\underline{B}_o) \ . \tag{I-22}$$

The real part of $\underline{\underline{\epsilon}}$ is a symmetric tensor and an even function of the magnetic field. The imaginary part of $\underline{\underline{\epsilon}}$ is an antisymmetric tensor and an odd function of B_o .

Certain fundamental characteristics of the magneto-ionic plasma and the anisotropy of $\underline{\underline{\epsilon}}$ are illustrated by plane wave propagation. For this class of waves each field component contains the factor $e^{j(\omega t - \underline{\beta} \cdot \underline{r})}$. $\underline{r}$ is the radius vector from the origin to a point in the field, and $\underline{\beta}$ is the propagation vector which determines the direction and phase of the wave. Maxwell's equations I-13 and I-16 for a plane monochromatic wave are simply

$$\underline{\beta} \times \underline{E} = \omega \mu_o \underline{H} \tag{I-23}$$

$$\underline{\beta} \times \underline{H} = -\omega \underline{D} = -\omega \underline{\underline{\epsilon}} \cdot \underline{E} \ . \tag{I-24}$$

The scalar product of $\underline{\beta}$ with equation I-23 shows $\underline{\beta}$ to be perpendicular to $\underline{H}$, while equation I-24 guarantees that $\underline{D}$, $\underline{H}$ and $\underline{\beta}$ form a mutually orthogonal group. $\underline{E}$ is confined to lie in the plane determined by $\underline{\beta}$ and $\underline{D}$.

If $\underline{H}$ is eliminated between equations I-23 and I-24 then

$$\underline{D} = \frac{-1}{\omega^2 \mu_o} [\underline{\beta} \times (\underline{\beta} \times \underline{E})] = \frac{+1}{\omega^2 \mu_o} [\beta^2 \underline{E} - \underline{\beta}(\underline{\beta} \cdot \underline{E})] = \underline{\underline{\epsilon}} \cdot \underline{E} \ .$$

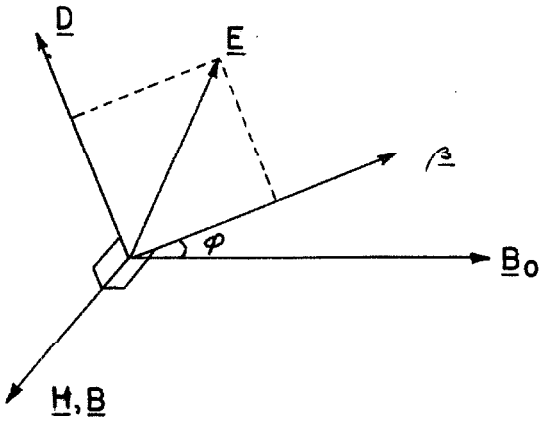

Figure I-1. The Component Vectors of a Plane Wave

This expression can be restated in the form

$$[\omega^2 \mu_o \underline{\underline{\epsilon}} + \underline{\beta}\,\underline{\beta} - \beta^2 \underline{\underline{1}}] \cdot \underline{E} = 0 \quad . \tag{I-25}$$

For the electric field not identically zero, it is necessary that

$$\det[\omega^2 \mu_o \underline{\underline{\epsilon}} + \underline{\beta}\,\underline{\beta} - \beta^2 \underline{\underline{1}}] = 0 \quad . \tag{I-26}$$

This determinant relates the propagation vector $\underline{\beta}$ to the existing frequency ω. Consequently it is a statement of the wave dispersion.

Without loss of generality, a Cartesian reference system is introduced which places $\underline{\beta}$ in the yz coordinate plane at an angle ϕ with respect to the z axis.

$$\underline{\beta} = \beta(\sin \phi\, \underline{e}_y + \cos \phi\, \underline{e}_z) \quad . \tag{I-27}$$

Substituting I-27 for $\underline{\beta}$ and equation I-17 for the elements of $\underline{\underline{\epsilon}}$ leads, upon expansion of I-26, to the customary Fresnel equation

$$\tan^2\phi = \frac{-\epsilon_3 [\beta^2 - \omega^2\mu_o(\epsilon_1 - \epsilon_2)] [\beta^2 - \omega^2\mu_o(\epsilon_1 + \epsilon_2)]}{[\beta^2 - \omega^2\mu_o\epsilon_3] [\epsilon_1\beta^2 - \omega^2\mu_o(\epsilon_1 - \epsilon_2^2)]} \quad . \tag{I-28}$$

For propagation at a specified angle ϕ with respect to the magnetic field, this is a quadratic equation for β^2 with real coefficients. Hence the magnitude of $\underline{\beta}$ assumes either of two values for each direction of wave transmission.

If the plane wave propagates parallel to the magnetostatic flux, then $\phi = 0$ and the dispersion relations are simply

$$\epsilon_3 = 0 \qquad \text{or} \qquad \omega = \sqrt{\Omega_e^2 + \Omega_i^2} = \Omega_p \tag{I-29a}$$

and

$$\beta_{\pm}^2 = \omega^2\mu_o(\epsilon_1 \pm \epsilon_2) \quad . \tag{I-29b}$$

Equation I-29a corresponds to an electrostatic oscillation of the plasma which has, by equation I-25, $\underline{E}$ parallel to $\underline{B}_o$ and $\underline{\beta}$; and as a result of equation I-23 has $\underline{H}$ equal to zero. Equation I-29a leaves $\underline{\beta}$ indeterminate. Consequently the group velocity $d\omega/d\beta = 0$ and the field remains local to the disturbance.

The wave polarizations associated with the factors of I-29b are determined with ease. Substituting via I-17 for $\underline{\underline{\epsilon}}$ and setting $\underline{\beta} = \sqrt{\omega^2\mu_o(\epsilon_1 \pm \epsilon_2)}\ \underline{e}_z$, gives as the x component of I-25:

$$\omega^2\mu_o [\epsilon_1 E_x + j\epsilon_2 E_y - (\epsilon_1 \pm \epsilon_2)E_x] = 0 \quad ,$$

or simply, $E_y = \mp jE_x$.

The compatibility determinant I-26 requires the y component also to reduce to the same result. However, the z component of I-25

$$\omega^2 \mu_o \epsilon_3 E_z = 0$$

demands in general that $E_z = 0$. Table I-1 summarizes the plane wave behavior for propagation along the magnetostatic field, $(\underline{\beta} \,//\, \underline{B}_o \,//\, \underline{e}_z)$.

Propagation Vector	Electric Field	Wave Polarization
$\beta_+^2 = \omega^2 \mu_o (\epsilon_1 + \epsilon_2)$	$E_y = -jE_x \quad E_z = 0$	Right circular polarized TEM plane wave.
$\beta_-^2 = \omega^2 \mu_o (\epsilon_1 - \epsilon_2)$	$E_y = +jE_x \quad E_z = 0$	Left circular polarized TEM plane wave
β indeterminate, $\omega = \Omega_p$	$E_x = E_y = 0 \quad E_z \neq 0$	Longitudinal electrostatic oscillation of the field

Table I-1. Plane Wave Behavior for Propagation along $\underline{B}_o$

The simplicity of these dispersion relations suggests a review of Figure I-1 along with equations I-17, I-23 and I-24. Notice that a plane wave propagating along B_o having $E_z = 0$, or else $E_x = E_y = 0$, has the electric vector parallel to the dielectric displacement. Three electric vectors that satisfy this requirement have the directions

$$\underline{E}_1 = \hat{E}_1 (\underline{e}_x - j\underline{e}_y)$$

$$\underline{E}_2 = \hat{E}_2 (\underline{e}_x + j\underline{e}_y)$$

$$\underline{E}_3 = \hat{E}_3 \, \underline{e}_z$$

of the right and left circularly polarized plane waves and the

longitudinal electrostatic field. The corresponding displacement vectors, by equation I-17 are

$$\underline{D}_1 = (\epsilon_1 + \epsilon_2)\,\underline{E}_1$$

$$\underline{D}_2 = (\epsilon_1 - \epsilon_2)\,\underline{E}_2$$

$$\underline{D}_3 = \epsilon_3\,\underline{E}_3 \quad .$$

In other words, $\underline{E}_1$, $\underline{E}_2$ and $\underline{E}_3$ are the eigenvectors of the permittivity tensor; $(\epsilon_1 + \epsilon_2)$, $(\epsilon_1 - \epsilon_2)$ and ϵ_3 are its eigenvalues. In the coordinate system defined by the two counter-rotating basis vectors $\underline{e}_1 = (\underline{e}_x - j\underline{e}_y)$, $\underline{e}_2 = (\underline{e}_x + j\underline{e}_y)$ and the fixed basis vector $\underline{e}_3 = \underline{e}_z$, the permittivity tensor is diagonal.

$$\begin{pmatrix} \hat{D}_1 \\ \hat{D}_2 \\ \hat{D}_3 \end{pmatrix} = \begin{pmatrix} (\epsilon_1 + \epsilon_2) & 0 & 0 \\ 0 & (\epsilon_1 - \epsilon_2) & 0 \\ 0 & 0 & \epsilon_3 \end{pmatrix} \begin{pmatrix} \hat{E}_1 \\ \hat{E}_2 \\ \hat{E}_3 \end{pmatrix} \quad .$$

These preferred directions for which $\underline{E}$ and $\underline{D}$ are parallel, are known in crystal optics as the <u>principal dielectric axes</u>.

For reference purposes Figure I-2 summarizes the limiting forms of plane wave propagation parallel and perpendicular to the magnetostatic field of an anisotropic plasma. Frames a and b refer to propagation along the magnetostatic field $\underline{B}_o$. Frames c and d correspond to plane wave propagation normal to this preferred direction.

When, as in frame a or c, the electric field is parallel to the

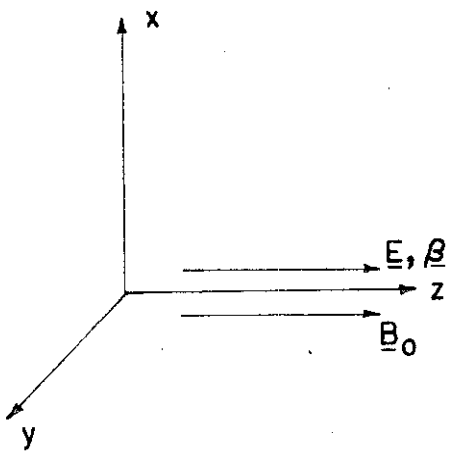

a) Longitudinal plasma oscillation $\epsilon_3 = 0$, i.e.,
$\omega = \sqrt{\Omega_e^2 + \Omega_i^2} = \Omega_p$

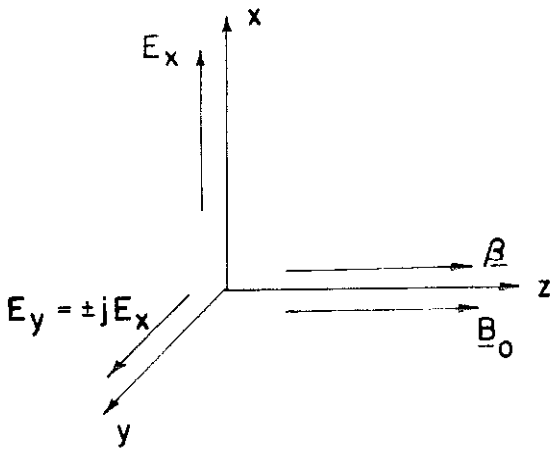

b) Circularly polarized transverse wave $\beta_{\pm}^2 = \omega^2 \mu_o (\epsilon_1 \pm \epsilon_2)$

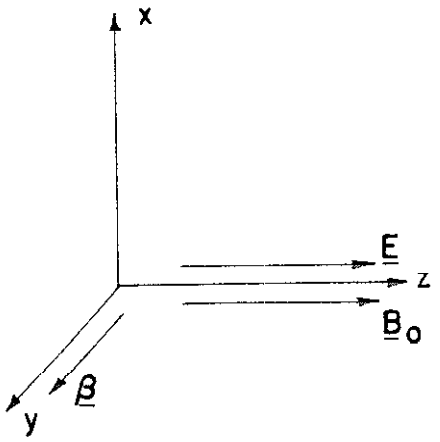

c) Linearly polarized transverse wave
$\beta^2 = \omega^2 \mu_o \epsilon_3$

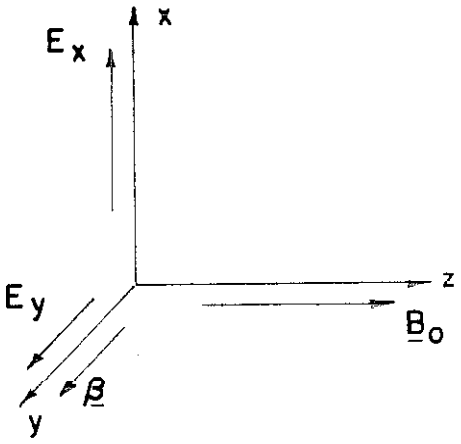

d) Elliptically polarized hybrid wave
$\beta^2 = \omega^2 \mu_o \left(\frac{\epsilon_1^2 - \epsilon_2^2}{\epsilon_1} \right)$

Figure I-2. Limiting forms of plane wave propagation

magnetostatic bias $\underline{B}_o$, the latter has no effect on the wave; the dielectric permittivity behaves as the simple scalar

$$\epsilon = \epsilon_3 = \epsilon_o \left(1 - \frac{\Omega_e^2 + \Omega_i^2}{\omega^2}\right) \quad .$$

Note that the relative dielectric constant ϵ/ϵ_o is always less than one; for most materials the dielectric constant exceeds unity. Since the phase velocity is inversely proportional to the square root of the dielectric constant, the waves of frame c exceed the speed of light and are known as "fast waves". On the other hand, the longitudinal waves of frame a have a dispersion relation $\omega = \Omega_p$ which is independent of the wave number β . Longitudinal waves therefore have zero group velocity $(\frac{d\omega}{d\beta} = 0)$, whereas their phase velocity (ω/β) is completely arbitrary. One concludes that the longitudinal waves are stationary natural oscillations of the medium at the plasma frequency. When the applied frequency of the linearly polarized transverse wave, frame c, equals Ω_p , it too assumes the characteristics of the longitudinal wave. Further examination reveals that the medium will not support transverse waves below the plasma frequency where ϵ_3 is negative.

Frames b and d are more complicated forms of plane wave propagation. In each case an electric field E_x normal to both the direction of propagation $\underline{\beta}$ and the magnetization $\underline{B}_o$ is coupled by means of a conduction current $\underline{J}$ to an electric field in the y direction. The coupling originates when the plasma current J_x induced by field component E_x is diverted by the magnetostatic force $(\underline{J}_x \times \underline{B}_o)$ into the y direction. This new current component produces an electric field E_y which is in phase quadrature with E_x .

If, as in frame b, $\underline{\beta}$ and $\underline{B}_o$ are parallel, then E_y is transverse and two oppositely-polarized circular plane waves result. Because these waves have different propagation constants, a linearly polarized plane wave experiences Faraday rotation.

When $\underline{\beta}$ and $\underline{B}_o$ are perpendicular, E_y lies parallel to $\underline{\beta}$ as in frame d. The electric field now has both a transverse and a longitudinal component ($\underline{D}$, $\underline{H}$ and $\underline{\beta}$ still remain mutually orthogonal) hence it is called a "hybrid wave". When $\underline{B}_o = 0$, the coupling between the transverse wave and the longitudinal wave is removed and one recovers the linearly polarized transverse wave of frame c and the longitudinal oscillations of frame a.

The presence of the static magnetic field in frames b and d extends the region of propagation down to zero frequency. At the very lowest frequencies these waves reduce to the familiar Alfvén waves of magnetohydrodynamic theory, for as $\epsilon_2 \to 0$, β_+ becomes equal to β_-. The two oppositely-polarized circular waves combine to form a single linearly polarized plane wave free of Faraday rotation.

CHAPTER II. THE WAVEGUIDE FORMULATION

Maxwell's Equations in a Cylindrical Geometry

This chapter establishes the conditions and relations for guided propagation in a gyroelectric medium described by equation I-17 and bounded by a longitudinally invariant, perfectly conducting wall. For the moment the waveguide cross-section is arbitrary, but eventually the results are specialized to a circular cylindric geometry. In every case the magnetostatic field is applied parallel to the waveguide axis.

The source-free modes of an infinite, longitudinally invariant waveguide are orthogonal (c.f., Chapter VI) and so provide a basis for expanding any source-induced field. The longitudinal invariance of the guide also insures that the axial and transverse dependence of a mode are separable. For an e^{-hz} axial dependence, $h = \alpha + j\beta$, Maxwell's equations I-13 and I-16 become:

$$\underline{H}_t = \frac{1}{j\omega\mu_o}\left[(\underline{e}_z \times \nabla_t E_z) + h(\underline{e}_z \times \underline{E}_t)\right] \tag{II-1a}$$

$$H_z = \frac{-1}{j\omega\mu_o}(\nabla_t \times \underline{E}_t) \cdot \underline{e}_z \tag{II-1b}$$

$$j\omega\epsilon_1 \underline{E}_t + \omega\epsilon_2(\underline{e}_z \times \underline{E}_t) = -(\underline{e}_z \times \nabla_t H_z) - h(\underline{e}_z \times \underline{H}_t) \tag{II-2a}$$

$$E_z = \frac{1}{j\omega\epsilon_3}(\nabla_t \times \underline{H}_t) \cdot \underline{e}_z \quad . \tag{II-2b}$$

The transverse part of the field is denoted by the subscript t. The two-dimensional gradient operator is $\nabla_t = \nabla - (-h)\underline{e}_z$. Before proceeding to simplify the above equations it will prove convenient to

list certain sets of parameters that repeatedly appear. Let

$$\gamma_1 = -(h^2 + \omega^2 \mu_o \epsilon_1) \qquad \text{and} \qquad \gamma_2 = \omega^2 \mu_o \epsilon_2 \tag{II-3}$$

also define

$$a = \frac{-jh\,\gamma_1}{\gamma_1^2 - \gamma_2^2}\,, \qquad b = \frac{\omega \mu_o \gamma_2}{\gamma_1^2 - \gamma_2^2}\,, \qquad c = \frac{-\,jh\,\gamma_2}{\gamma_1^2 - \gamma_2^2}\,,$$

$$d = \frac{-\,\omega\mu_o\,\gamma_1}{\gamma_1^2 - \gamma_2^2}\,, \qquad f = \frac{h^2 \omega \epsilon_2}{\gamma_1^2 - \gamma_2^2}\,, \qquad g = \frac{\omega(\epsilon_1\gamma_1 + \epsilon_2\gamma_2)}{\gamma_1^2 - \gamma_2^2}\,. \tag{II-4}$$

The coefficients satisfy the following identities:

$$ab + cd = 0 \qquad \text{and} \qquad fd - ac = 0 \tag{II-5}$$

To continue the derivation, multiply equation II-1a vectorially by $\underline{e}_z$ and expand the resulting triple vector products.

$$(\underline{e}_z \times \underline{H}_t) = \frac{-1}{j\omega\mu_o}(\nabla_t E_z + h\,\underline{E}_t)\,.$$

Next, substitute this expression into II-2a and obtain

$$-\,j\gamma_1 \underline{E}_t + \gamma_2(\underline{e}_z \times \underline{E}_t) = -\,\omega\mu_o(\underline{e}_z \times \nabla_t H_z) - jh\,\nabla_t E_z\,. \tag{II-6}$$

The vector product of $\underline{e}_z$ with II-6 in turn leads to

$$-\,\gamma_2 \underline{E}_t - j\gamma_1(\underline{e}_z \times \underline{E}_t) = \omega\mu_o \nabla_t H_z - jh(\underline{e}_z \times \nabla_t E_z)\,. \tag{II-7}$$

Multiplying equation II-6 by $j\gamma_1$ and adding γ_2 times equation II-7 yields

$$\underline{E}_t = ja\nabla_t E_z + b\nabla_t H_z + c(\underline{e}_z \times \nabla_t E_z) + jd(\underline{e}_z \times \nabla_t H_z) \quad . \qquad \text{(II-8)}$$

The insertion of II-8 into equation II-1a immediately provides

$$\underline{H}_t = f\nabla_t E_z + ja\nabla_t H_z + jg(\underline{e}_z \times \nabla_t E_z) + c(\underline{e}_z \times \nabla_t H_z) \quad . \qquad \text{(II-9)}$$

Equations II-8 and II-9 define the transverse fields in terms of the longitudinal fields. Equations II-1b and II-2b express the longitudinal fields in terms of the transverse fields. To treat the transverse vectors as fundamental (19) has purely formal merit; certainly from a practical standpoint the scalar longitudinal fields are more wieldy. The equations satisfied by the longitudinal fields are derived next.

Substituting equation II-8 into equation II-1b and using a number of well-known vector identities, gives

$$c\nabla_t^2 E_z + jd\nabla_t^2 H_z + j\omega\mu_o H_z = 0 \quad . \qquad \text{(II-10)}$$

In a similar way, the substitution of equation II-9 into II-2b yields

$$c\nabla_t^2 H_z + jg\nabla_t^2 E_z - j\omega\epsilon_3 E_z = 0 \quad . \qquad \text{(II-11)}$$

These differential equations couple E_z to H_z; if either longitudinal field is zero, the other also vanishes. Under certain limiting conditions discussed in Chapters III and IV, the coupling coefficient c vanishes and E_z becomes independent of H_z. Except for such situations, the TE or TM description of a mode is not applicable.

As with any system of equations, there are several methods (1,2, 3,4,5) by which a solution may be attained. For example, by eliminating either longitudinal field between relations II-10 and II-11 one finds that E_z and H_z satisfy the same fourth order partial differential equation.

$$\left\{(\nabla_t^2)^2 + \omega\left(\frac{\mu_o g - d\epsilon_3}{gd + c^2}\right)\nabla_t^2 - \left(\frac{\omega^2\mu_o\epsilon_3}{gd + c^2}\right)\right\}\begin{pmatrix} H_z \\ \\ E_z \end{pmatrix} = 0 \quad . \qquad \text{(II-12)}$$

Since E_z and H_z exhibit the same spatial behavior, take $H_z = \Phi$ and $E_z = \tau\Phi$; τ is an admittance function which is independent of the coordinates and time.

Equation II-12 can be factored into:

$$(\nabla_t^2 + T_1^2)(\nabla_t^2 + T_2^2)\Phi = 0 \quad . \qquad \text{(II-13)}$$

Designating the two solutions of this equation by Φ_1 and Φ_2

$$H_z = \Phi_1 + \Phi_2 \qquad \text{(II-14a)}$$

$$E_z = \tau_1\Phi_1 + \tau_2\Phi_2 \quad . \qquad \text{(II-14b)}$$

Comparing II-12 with II-13 it is evident that T_1 and T_2 are the two roots of

$$T^4 - \omega\left(\frac{\mu_o g - d\epsilon_3}{gd + c^2}\right)T^2 - \left(\frac{\omega^2\mu_o\epsilon_3}{gd + c^2}\right) = 0 \quad . \qquad \text{(II-15)}$$

Substituting for c, d and g from II-4 , we obtain

$$\left[\gamma_1^2 - \gamma_2^2 + \gamma_1 T^2\right] - \frac{T^2}{\omega^2\mu_o\epsilon_3}\left[\gamma_1^2 - \gamma_2^2 + \gamma_1 T^2 + h^2(\gamma_1 + T^2)\right] = 0 \qquad \text{(II-16)}$$

and a factor $(\gamma_1^2 - \gamma_2^2)$. Equations II-8 and II-9 suggest that if $(\gamma_1^2 - \gamma_2^2) = 0$, then E_z and H_z must vanish for $\underline{E}_t$ and $\underline{H}_t$ to remain finite. Such TEM fields cannot exist within a waveguide whose cross-section is simply connected unless $\epsilon_2 = 0$ and the longitudinal conductivity is infinite (e.g., Alfvén waves near $\omega = 0$) .

To determine how τ and T are related, substitute $H_z = \Phi$, $E_z = \tau\Phi$ in the coupled wave equations, and by equation II-13 replace ∇_t^2 by $-T^2$. Equation II-10 yields

$$\tau = j\left(\frac{\omega\mu_o}{cT^2} - \frac{d}{c}\right) \qquad \text{(II-17a)}$$

while equation II-11 gives

$$\tau = \frac{j}{\left(\frac{\omega\epsilon_3}{cT^2} + \frac{g}{c}\right)} . \qquad \text{(II-17b)}$$

The equivalence of I-17a and II-17b is demonstrated at once by equating these two expressions and obtaining as a result equation II-15.

Boundary Conditions and Separable Waveguide Solutions

The pertinent relations for a longitudinally magnetized plasma-guide of arbitrary cross section have been established in the last section. In particular, the set of coupled equations for the longitudinal fields have been replaced by a pair of two-dimensional Helmholtz equations

$$\nabla_t^2 \Phi_i + T_i^2 \Phi_i = 0 \quad , \quad i = 1,2 \quad . \qquad \text{(II-18)}$$

The first step is to find all possible solutions to this equation; the second step is to choose from among these solutions the particular

combinations that satisfy the boundary conditions. The boundary conditions are that the tangential electric field and the normal magnetic vector vanish at the conducting waveguide wall. In terms of Φ this means, according to equations II-14a,b, II-8 and II-9, that on the waveguide surface

$$\tau_1\Phi_1 + \tau_2\Phi_2 = 0 \qquad \text{(II-19a)}$$

$$\sum_{i=1}^{2} \left\{(c\tau_i + jd)(\underline{n}\cdot\nabla_t\Phi_i) + (ja\tau_i + b)(\underline{n}\times\nabla_t\Phi_i)\cdot\underline{e}_z\right\} = 0 \qquad \text{(II-19b)}$$

$$\sum_{i=1}^{2} \left\{(f\tau_i + ja)(\underline{n}\cdot\nabla_t\Phi_i) - (jg\tau_i + c)(\underline{n}\times\nabla_t\Phi_i)\cdot\underline{e}_z\right\} = 0 \qquad \text{(II-19c)}$$

$\underline{n}$ is the unit vector normal to each element of waveguide surface and orthogonal to $\underline{e}_z$. From Maxwell's equation

$$\nabla \times \underline{E} = -j\omega\mu_o\underline{H}$$

it may be verified that equation II-19c is a consequence of II-19a and II-19b, and not an independent condition.

A standard method for solving the Helmholtz equation is the separation of variables technique. The separation is different for each coordinate system and the number of coordinate systems in which separation can be accomplished is limited. The two-dimensional Helmholtz equation II-18 is separable in only four coordinate systems (20): rectangular, polar, elliptic and parabolic. Boundary conditions II-19 restrict the number of applicable systems still further.

Let u and v be the orthogonal curvilinear coordinates appropriate to any one of these four separable systems. If ℓ_u and ℓ_v are the corresponding metric coefficients, the element of length is

$$ds = \sqrt{(\ell_u du)^2 + (\ell_v dv)^2} \qquad \text{(II-20)}$$

and the gradient and Laplacian operators are respectively

$$\nabla_t = \underline{e}_u \frac{1}{\ell_u} \frac{\partial}{\partial u} + \underline{e}_v \frac{1}{\ell_v} \frac{\partial}{\partial v} \qquad \text{(II-21a)}$$

$$\nabla_t^2 = \frac{1}{\ell_u \ell_v} \left[\frac{\partial}{\partial u} \left(\frac{\ell_v}{\ell_u} \frac{\partial}{\partial u}\right) + \frac{\partial}{\partial v} \left(\frac{\ell_u}{\ell_v} \frac{\partial}{\partial v}\right) \right] . \qquad \text{(II-21b)}$$

The separated solutions to the Helmholtz equation are then of the variety

$$\Phi_i(u,v) = U_i(u)\, V_i(v) , \quad i = 1,2 \quad .$$

For the boundary conditions to take their simplest forms, and for the separation technique to be practical, it is necessary to have each segment of waveguide wall congruous to a coordinate surface. If such a segment coincides with the coordinate surface $u = u_o$ then, as will be shown, the only function $V_i(v)$ which satisfies the boundary requirements at u_o is an exponential, viz.

$$V_1(v) = V_2(v) = e^{Kv} \qquad \text{(II-22)}$$

where K is independent of u,v and index i .

At the waveguide wall corresponding to the coordinate surface u_o , $\underline{n}$ equals $\underline{e}_u$ and boundary conditions II-19a,b become

$$\tau_1 U_1(u_o)\, V_1(v) + \tau_2\, U_2(u_o)\, V_2(v) = 0 \qquad \text{(II-23a)}$$

$$\sum_{i=1} \left\{ (c\tau_i + jd)\, \frac{1}{\ell_u}\bigg|_{u_o} \frac{dU_i(u_o)}{du_o}\, V_i(v) + (ja\tau_i + b)\, U_i(u_o)\, \frac{1}{\ell_v}\bigg|_{u_o} \frac{dV_i(v)}{dv} \right\} = 0 . \qquad \text{(II-23b)}$$

The left side of equation II-23a cannot vanish for all values of v unless

(a) $U_1(u_o) = U_2(u_o) = 0$, or else

(b) V_1 and V_2 are proportional, i.e., $V_1(v) = pV_2(v)$, and $\tau_1 U_1(u_o) + p\,\tau_2 U_2(u_o) = 0$. The proportionality factor p is independent of the coordinates u and v .

If, as in the first case $U_1(u_o) = U_2(u_o) = 0$, then equation II-23b reduces to

$$\left[(c\tau_1 + jd)\, \frac{dU_1(u_o)}{du_o} \right] V_1(v) + \left[(c\tau_2 + jd)\, \frac{dU_2(u_o)}{du_o} \right] V_2(v) = 0 .$$

This relation cannot be fulfilled at every point unless $\frac{dU_1(u_o)}{du_o} = \frac{dU_2(u_o)}{du_o} = 0$. By means of the Helmholtz equation II-18 and its successive derivatives, it follows that every derivative of $U_1(u_o)$ and $U_2(u_o)$ vanishes. As a result of Taylor's theorem, the functions $U_1(u)$ and $U_2(u)$ are identically zero, not only on the surface $u = u_o$, but everywhere. Therefore assumption (a) leads to non-existent fields.

On the other hand, if $V_1 = pV_2$, equations II-23 become:

$$\tau_1 U_1(u_o) + p\tau_2 U_2(u_o) = 0 \qquad \text{(II-24a)}$$

$$\left[(c\tau_1 + jd)\frac{dU_1(u_o)}{du_o} + p(c\tau_2 + jd)\frac{dU_2(u_o)}{du_o}\right]\frac{1}{\ell_u}\bigg|_{u_o} V + \left[(ja\tau_1 + b)U_1(u_o) + p(ja\tau_2 + b)U_2(u_o)\right]\frac{1}{\ell_v}\bigg|_{u_o}\frac{dV}{dv} = 0 \; . \qquad \text{(II-24b)}$$

Equation II-24b cannot be satisfied for all v on the surface u_o unless

$$\frac{dV}{dv} = K\frac{\ell_v}{\ell_u}\bigg|_{u_o} V \quad , \qquad \text{(II-25)}$$

where for any given physical condition

$$K = -\frac{\left[(c\tau_1 + jd)\frac{dU_1(u_o)}{du_o} + p(c\tau_2 + jd)\frac{dU_2(u_o)}{du_o}\right]}{\left[(ja\tau_1 + b)U_1(u_o) + p(ja\tau_2 + b)U_2(u_o)\right]} \qquad \text{(II-26)}$$

is a complex constant independent of v . By replacing the metric coefficient ℓ_v/ℓ_u with its function behavior and integrating equation II-25 in each of the four separable coordinate frames, the functions $V(v)$ listed in Table II-1 are generated. These functions are compared to the solutions obtained by separating variables in the Helmholtz equation. When, for a given geometry, the functions obtained by the two methods match, the boundary conditions can be satisfied by separated wave solutions. Table II-1 shows that when the conductors occupy any of the radial coordinate surfaces of a polar cylindrical frame, or any of the parallel coordinate planes of a rectangular system, separated wave solutions can be found.

Cylindrical Coordinate System	Coordinates		Metric Coefficient		Function V by Integrating II-25	Function V by Separating II-18
	u_o	v	ℓ_u	ℓ_v		
rectangular	x_o	y	1	1	$Y = e^{Ky}$	exponential
polar	r_o	θ	1	r_o	$\Theta = e^{(Kr_o)\theta}$	exponential
	θ_o	r	r	1	$R = r^K$	Bessel function
parabolic	ξ_o	η	$\sqrt{\xi_o^2 + \eta^2}$	$\sqrt{\xi_o^2 + \eta^2}$	$N = e^{K\eta}$	Confluent Hypergeometric Function
	η_o	ξ	$\sqrt{\xi^2 + \eta_o^2}$	$\sqrt{\xi^2 + \eta_o^2}$	$\Xi = e^{K\xi}$	Confluent Hypergeometric Function
elliptic	ξ_o	η	$\sqrt{\frac{\xi_o^2 - \eta^2}{\xi_o^2 - 1}}$	$\sqrt{\frac{\xi_o^2 - \eta^2}{1 - \eta^2}}$	$N = e^{K\sqrt{\xi_o^2 - 1}\sin^{-1}\eta}$	Mathieu Function
	η_o	ξ	$\sqrt{\frac{\xi^2 - \eta_o^2}{1 - \eta_o^2}}$	$\sqrt{\frac{\xi^2 - \eta_o^2}{\xi^2 - 1}}$	$\Xi = \frac{\xi + \sqrt{\xi^2 - 1}}{K\sqrt{1 - \eta_o^2}}$	Mathieu Function

Table II-1. A Comparison of the Separable Coordinate Systems

Furthermore, the functional behavior along any direction parallel to the conductor must always be exponential. Thus only those configurations illustrated in Figure II-1 and their degenerations support separated waves.

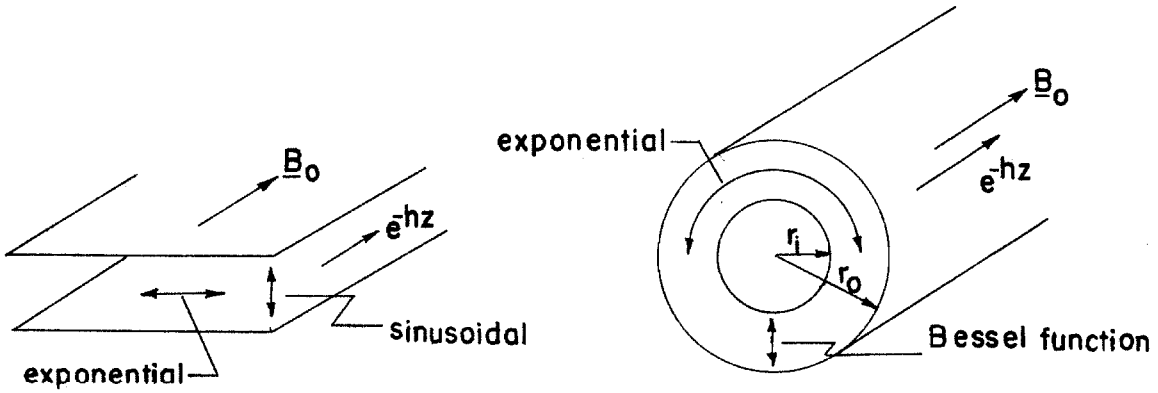

Figure II-1. Geometries for which separable wave solutions can be found, and the behavior of the separated functions in these systems.

Unlike the parallel plate transmission line, the fields of the rectangular waveguide require a sinusoidal behavior in each transverse direction in order that E_z may vanish on opposing pairs of conducting walls. However, this requirement conflicts with boundary condition II-19b, or equivalently II-25, which demands exponential functions of both x and y. Consequently the longitudinally magnetized rectangular waveguide does not support separated waves. In a similar manner, the angular periodicity of the circular waveguide requires behaviors of the type $e^{\pm jn\theta}$ with n an integer. In contrast to the exponential, the trigonometric functions $\cos n\theta$ and $\sin n\theta$ do not satisfy

the boundary conditions. Physically, the magnetostatic field removes the degeneracy associated with the positive and negative exponents of the transverse function. The waves corresponding to these exponents have different transverse field configurations and different longitudinal propagation factors.

Unaware of these special requirements, Wang and Hopson (6) chose to describe propagation by a trigonometric angular dependence, $\cos(n\theta + \delta_n)$, and erroneously concluded that angular dependent waves do not propagate in a circular plasmaguide. Their error lies entirely with their choice of function. A valid dispersion relation for the angular dependent modes will be derived in the next section.

Within the framework of the quasi-static approximation, Laplace's equation is substituted for the coupled wave equations II-10 and II-11, and simpler relations replace boundary conditions II-19. Because the boundary conditions are relaxed, separated quasi-static solutions can be found in structures which do not actually support separated waves. Smullin and Chorney (7) obtain a quasi-static dispersion relation for the longitudinally magnetized rectangular waveguide which they compare with equation II-16 using an assumed value of T . The comparison is of questionable merit, even for non-separated wave solutions, because T_1 and T_2 are themselves functions of the frequency which are determined by the boundary conditions.

The Circular Waveguide

The geometry under consideration resembles the coaxial waveguide of Figure II-1 without its internal conductor; i.e., r_i is to be zero According to the preceding discussion Φ_1 and Φ_2 have the same

exponential dependence. Therefore assume at the outset that

$$\Phi_i = R_i(r)\, e^{j(\omega t - n\theta) - hz} \quad , \quad i = 1,2 \qquad \text{(II-27)}$$

Substituting Φ_i into equation II-18 and cancelling the common exponential factor gives Bessel's equation in the variable $v = T_i r$

$$\frac{1}{v}\frac{d}{dv}\left(v\frac{dR_i}{dv}\right) + \left(1 - \frac{n^2}{v^2}\right) R_i = 0 \quad .$$

Bessel's equation has solutions of the form

$$R_i(r) = A_i J_n(T_i r) + B_i Y_n(T_i r) \quad . \qquad \text{(II-28)}$$

In a coaxial geometry both radial functions are required by the boundary conditions. However, in a circular waveguide the axis $r = 0$ is accessible and B_i must vanish if Φ_i is to remain finite. Thus

$$\Phi_i = A_i J_n(T_i r)\, e^{j(\omega t - n\theta) - hz} \quad . \qquad \text{(II-29)}$$

For convenience the following vector function is defined:

$$\underline{\Psi}(T_i r) \equiv \left(\frac{1}{A_i\, e^{j(\omega t - n\theta) - hz}}\right) \nabla_t \Phi_i \qquad \text{(II-30)}$$

$$= \frac{1}{r}\left[(T_i r)\, J_n'(T_i r)\, \underline{e}_r - jn\, J_n(T_i r)\, \underline{e}_\theta\right] .$$

In accordance with equations II-14, the longitudinal fields are

$$H_z = \Phi_1 + \Phi_2 = \left[A_1 J_n(T_1 r) + A_2 J_n(T_2 r)\right] e^{j(\omega t - n\theta) - hz} \qquad \text{(II-31)}$$

$$E_z = \tau_1\Phi_1 + \tau_2\Phi_2 = \left[A_1\tau_1 J_n(T_1r) + A_2\tau_2 J_n(T_2r)\right] e^{j(\omega t - n\theta) - hz} . \tag{II-32}$$

Equations II-8 and II-9 show that the transverse fields are

$$\underline{E}_t = \sum_{i=1}^{2} A_i \left\{(ja\,\tau_i + b)\,\underline{\psi}(T_ir) + (c\tau_i + jd)\underline{e}_z \times \underline{\psi}(T_ir)\right\} e^{j(\omega t - n\theta) - hz} \tag{II-33}$$

$$\underline{H}_t = \sum_{i=1}^{2} A_i \left\{(f\tau_i + ja)\,\underline{\psi}(T_ir) + (jg\tau_i + c)\underline{e}_z \times \underline{\psi}(T_ir)\right\} e^{j(\omega t - n\theta) - hz} . \tag{II-34}$$

The boundary conditions demand that the tangential electric field vanish everywhere along the perfectly conducting waveguide wall. Using equation II-32 and the θ component of II-33 it follows that

$$A_1\tau_1 J_n(T_1r_o) + A_2\tau_2 J_n(T_2r_o) = 0 \tag{II-35a}$$

$$\sum_{i=1}^{2} A_i \left\{n(a\tau_i - jb)\,J_n(T_ir_o) + (c\tau_i + jd)(T_ir_o)J_n'(T_ir_o)\right\} = 0 . \tag{II-35b}$$

Similar equations result from conditions II-19. For there to exist a non-trivial solution to these two homogeneous equations, the determinant constructed from the coefficients of A_1 and A_2 must vanish. Equations II-4 and II-17a permit the simplification of this determinant which finally becomes the dispersion relation

$$bn(T_1^2 - T_2^2) + (\omega\mu_o - dT_1^2)\frac{(T_2r_o)J_n'(T_2r_o)}{J_n(T_2r_o)} - (\omega\mu_o - dT_2^2)\frac{(T_1r_o)J_n'(T_1r_o)}{J_n(T_1r_o)} = 0 . \tag{II-36}$$

This relation, together with equation II-16,

$$\left[\gamma_1^2 - \gamma_2^2 + \gamma_1 T_i^2\right] - \frac{T_i^2}{\omega^2 \mu_o \epsilon_3}\left[\gamma_1^2 - \gamma_2^2 + \gamma_1 T_i^2 + h^2(\gamma_1 + T_i^2)\right] = 0$$

defines wave transmission in the circular plasmaguide. Replacing h by -h does not alter either equation II-16 or equation II-36. This property, known as "reflection symmetry", is the subject of the next section. The simultaneous solution of II-16 and II-36 is postponed until Chapter V.

Reflection Symmetry

The conditions for which a wave will travel in either of two opposite directions with the same propagation factor h are now investigated. A configuration which exhibits this property is said to display reflection symmetry.

For a wave with an $e^{j\omega t - hz}$ dependence propagating in a medium described by a general second rank dielectric tensor, Maxwell's equations in component form are

$$\left(\frac{\partial E_z}{\partial y} + h E_y\right) = - j\omega \mu_o H_x \qquad \text{(II-37)}$$

$$\left(hE_x + \frac{\partial E_z}{\partial x}\right) = + j\omega \mu_o H_y \qquad \text{(II-38)}$$

$$\left(\frac{\partial E_y}{\partial x} - \frac{\partial E_x}{\partial y}\right) = - j\omega \mu_o H_z \qquad \text{(II-39)}$$

$$\left(\frac{\partial H_z}{\partial y} + hH_y\right) = j\omega(\epsilon_{xx}E_x + \epsilon_{xy}E_y + \epsilon_{xz}E_z) \qquad \text{(II-40)}$$

$$\left(hH_x + \frac{\partial H_z}{\partial x}\right) = - j\omega(\epsilon_{yx}E_x + \epsilon_{yy}E_y + \epsilon_{yz}E_z) \qquad \text{(II-41)}$$

$$\left(\frac{\partial H_y}{\partial x} - \frac{\partial H_x}{\partial y}\right) = j\omega(\epsilon_{zx}E_x + \epsilon_{zy}E_y + \epsilon_{zz}E_z) \quad . \qquad \text{(II-42)}$$

Replacing h by -h in equation II-39 leaves E_x, E_y and H_z unaffected, whereas equations II-37 and II-38 require E_z, H_x and H_y to change sign. These changes are consistent with equation II-40 if $\epsilon_{xz} = 0$, with equation II-41 if $\epsilon_{yz} = 0$, and lastly with equation II-42 if $\epsilon_{zx} = \epsilon_{zy} = 0$. One concludes, for $\epsilon_{xz} = \epsilon_{zx} = \epsilon_{yz} = \epsilon_{zy} = 0$, that the transformation

$$(\underline{E}_t, E_z, \underline{H}_t, H_z, h) \longrightarrow (\pm \underline{E}_t, \mp E_z, \mp \underline{H}_t, \pm H_z, -h) \quad \text{(II-43)}$$

leaves Maxwell's equations invariant. Furthermore, any given frequency which propagates in the positive z direction also propagates in the negative z direction with the same velocity and a similar field configuration.

A magneto-active plasma exhibits reflection symmetry whenever the static field $\underline{B}_o$ and the direction of propagation are aligned (c.f. equation I-17). If the magnetostatic field parallels the x axis, the permittivity tensor has the form

$$\underline{\underline{\epsilon}} = \begin{pmatrix} \epsilon_3 & 0 & 0 \\ 0 & \epsilon_1 & j\epsilon_2 \\ 0 & -j\epsilon_2 & \epsilon_1 \end{pmatrix}$$

This tensor does not, in general, display reflection symmetry with respect to a wave propagating in the z direction. A notable exception is the plane wave which, by not possessing any transverse derivatives

$(\frac{\partial}{\partial x} = \frac{\partial}{\partial y} = 0)$, is able to propagate symmetrically in either direction along the z axis. The fields within a rectangular waveguide containing a transversely magnetized plasma are never reflection symmetric unless $\underline{E}$ and $\underline{B}_o$ are parallel, in which case $\underline{\underline{\epsilon}}$ behaves like the scalar ϵ_3 .

The fields of the longitudinally magnetized plasmaguide always comply with transformation II-43. Consequently, if a waveguide is terminated in the plane $z = 0$ by a perfectly conducting wall, the boundary conditions are satisfied by furnishing a reflected wave having an h, $\underline{E}_t$ and H_z of opposite sign to the incident wave. For $h = j\beta$, the exponentials of the incident and reflected $\underline{E}_t$ and H_z components combine as $\sin \beta z$. A circular cylindrical cavity can be constructed from a waveguide by inserting two such conducting planes a distance L apart. The boundary conditions at both ends are satisfied when $\beta = m\pi/L$ and m is an integer. The resonant frequencies of this cavity are determined by placing $\beta = m\pi/L$ in equation II-16 and solving the radial boundary condition II-36 for T and ω . The circular plasma resonator with an axial magnetic field has been studied by Buchsbaum, Mower and Brown (21,22). In contrast, the absence of reflection symmetry in the transversely magnetized rectangular waveguide requires, at a conducting termination, an infinite number of reflected waves for each incident wave.

Reflection symmetry will be very useful in Chapter VI. It is the means for simplifying the mode orthogonality relations which apply to waveguides containing longitudinally magnetized plasmas.

CHAPTER III. WAVE RESONANCE AND CUT-OFF IN THE CIRCULAR PLASMAGUIDE

At resonance the electromagnetic field experiences an intense interaction with the plasma which causes the magnitude of the longitudinal propagation factor h to increase without bound. As a result the group and phase velocities of the resonant wave vanish, and the fields are purely reactive. The resonant frequencies are found to depend only upon the plasma variables and not upon the geometry of the waveguide.

In contrast, waveguide cut-off coincides with a vanishing longitudinal propagation factor. The phase velocity of the cut-off wave is infinite, but again the fields are reactive. The cut-off frequencies are transcendental functions of the plasma parameters and the waveguide cross-section, thus making it more difficult to investigate the behavior of a waveguide cut-off than to study a wave resonance.

The cut-off and resonant frequencies define the dispersion limits for the propagating mode and, in so doing, govern the conduct of the wave. Furthermore, the ease with which these critical frequencies are observed suggest that they may be useful to the experimentalist for reference measurements.

Wave Resonance

The resonant frequencies can be determined directly from equation II-16. Making use of definitions II-3, equation II-16 gives

$$h^2=\left[\frac{1}{2}\left(1+\frac{\epsilon_1}{\epsilon_3}\right)T^2-\omega^2\mu_o\epsilon_1\right]\pm\sqrt{(\omega^2\mu_o\epsilon_2)^2-(\omega^2\mu_o\epsilon_2)\frac{\epsilon_2}{\epsilon_3}T^2+\frac{1}{4}\left(1-\frac{\epsilon_1}{\epsilon_3}\right)^2T^4}\,. \tag{III-1}$$

The singularities of h, which occur at the zero of ϵ_3 and at the poles of ϵ_1 and ϵ_2, are the resonant frequencies of the system. Equations I-18 for the permittivity tensor show that these resonances occur at the plasma frequency Ω_p and at the two cyclotron frequencies ω_i and ω_e.

Prior to investigating the fields near resonance, the behavior of γ_1 and γ_2 must be understood. Since the ratio

$$\frac{\gamma_2}{\gamma_1} = \frac{-\omega^2\mu_o\epsilon_2}{h^2+\omega^2\mu_o\epsilon_1} = -\left(\frac{h^2}{\omega^2\mu_o\epsilon_2}+\frac{\epsilon_1}{\epsilon_2}\right)^{-1} \qquad \text{(III-2)}$$

has different limits at each resonance, the plasma and cyclotron frequencies are discussed separately.

Cyclotron resonance. At the cyclotron frequencies

$$\frac{\epsilon_1}{\epsilon_2} \to \pm 1 \qquad \text{(III-3)}$$

the upper sign corresponds to electron cyclotron resonance, the lower sign refers to ion cyclotron resonance. Because both ϵ_2 and h^2 are infinite at cyclotron resonance, the quantity (h^2/ϵ_2) appearing in equation III-2 remains indeterminate until the relative orders of the infinities are established. To this end let

$$\frac{h^2}{\gamma_2} = \frac{h^2}{\omega^2\mu_o\epsilon_2} \to k \qquad \text{(III-4)}$$

at cyclotron resonance. As yet k is unknown; it may be zero, infinite or finite. The value of k is fixed by the boundary

conditions on the fields.

The resonant behavior of the electromagnetic field is obtained from equations II-8 through II-11 by examining the limiting forms of the coefficients specified by equation II-4. Upon substituting III-3 and III-4, equation III-2 becomes

$$\frac{\gamma_2}{\gamma_1} \rightarrow \frac{-1}{(k \pm 1)} \quad . \tag{III-5}$$

As a result the field coefficients approach the following limits at cyclotron resonance:

$$a \rightarrow +j \left(\frac{k \pm 1}{k \pm 2}\right) \frac{1}{h} \qquad b \rightarrow \frac{\omega \mu_o}{(k \pm 2)} \frac{1}{h^2}$$

$$c \rightarrow \frac{-j}{(k \pm 2)} \frac{1}{h} \quad . \qquad d \rightarrow \omega \mu_o \left(\frac{k \pm 1}{k \pm 2}\right) \frac{1}{h^2}$$

$$f \rightarrow \mp g \rightarrow \frac{1}{\omega \mu_o (k \pm 2)} \tag{III-6}$$

The longitudinal fields remain coupled until resonance is reached and coefficient c vanishes. Neglecting terms of the order 1/h and smaller in equations II-10 and II-11 leaves

$$H_z = 0 \tag{III-7a}$$

$$\nabla_t^2 E_z + \omega^2 \mu_o \epsilon_3 (k \pm 2) E_z = 0 \quad . \tag{III-7b}$$

Apparently the resonant fields are TM (transverse magnetic) with

$$E_z = E_o J_n(Tr) e^{-jn\theta} \tag{III-8a}$$

and

$$T^2 = \omega^2 \mu_o \epsilon_3 (k \pm 2) \quad . \tag{III-8b}$$

Solving equation III-8b for k and equating it to expression III-4 yields the dispersion relation

$$-h^2 = -\frac{\epsilon_2}{\epsilon_3} T^2 \pm 2\omega^2 \mu_o \epsilon_2 = \omega^2 \mu_o (\epsilon_1 \pm \epsilon_2) - \frac{\epsilon_2}{\epsilon_3} T^2 \quad . \tag{III-9}$$

Retaining only the lowest power of $1/h$ the transverse field relations II-8 and II-9 reduce to

$$\underline{E}_t = \frac{-1}{(k \pm 2)h} \left[(k \pm 1) \nabla_t E_z + j \underline{e}_z \times \nabla_t E_z \right] \tag{III-10}$$

$$\underline{H}_t = \frac{1}{j\omega\mu_o (k \pm 2)} \left[j \nabla_t E_z \pm \underline{e}_z \times \nabla_t E_z \right] \quad . \tag{III-11}$$

All three boundary requirements, $E_z\big|_{r_o} = E_\theta\big|_{r_o} = H_r\big|_{r_o} = 0$, cannot be satisfied unless $E_o = 0$, in which case the entire wave vanishes; or else $E_z \to 0$ as $k \to \mp 2$. For the latter situation, the transverse fields remain non-zero and finite as E_z vanishes. Using several familiar recursion relations for the Bessel function and its derivative

$$\frac{\nabla_t E_z}{(k \pm 2)} = \frac{E_o T}{2(k \pm 2)} \left[(J_{n-1} - J_{n+1}) \underline{e}_r - j(J_{n-1} + J_{n+1}) \underline{e}_\theta \right] e^{-jn\theta} \quad .$$

Since equation III-8 shows that $T \to 0$ as $k \to \mp 2$, and because $J_{n\pm1}(0) = \delta_{n,\mp1}$, it follows that

$$\lim_{k \to \mp 2} \left[\frac{\nabla_t E_z}{(k \pm 2)} \right] = \frac{A}{2} \left[(\underline{e}_r - j\underline{e}_\theta)\delta_{n,+1} - (\underline{e}_r + j\underline{e}_\theta)\delta_{n,-1} \right] e^{-jn\theta}$$

$$= \frac{A}{2} \left[(\underline{e}_x - j\underline{e}_y)\delta_{n,+1} - (\underline{e}_x + j\underline{e}_y)\delta_{n,-1} \right] e^{-jn\theta} \tag{III-12}$$

where $A = \lim_{k \to \mp 2} \left[\frac{E_o T}{(k \pm 2)} \right]$. Accordingly, III-10 and III-11 become

$$\underline{E}_t = - \frac{j\omega \mu_o}{h} (\underline{e}_z \times \underline{H}_t) = \frac{A}{h} (\underline{e}_x \mp j \underline{e}_y) \qquad \text{(III-13a)}$$

for $n = \pm 1$ respectively. Meanwhile, for $T \to 0$, dispersion relation III-9 becomes

$$-h^2 = \omega^2 \mu_o (\epsilon_1 \pm \epsilon_2) \qquad \text{(III-13b)}$$

Locally, the waveguide fields at cyclotron resonance resemble the circularly polarized TEM waves that propagate along $\underline{B}_o$ in an unbounded plasma. If T and h are regarded as the transverse and longitudinal components of a propagation vector, then at cyclotron resonance where T is negligible compared to h , the waveguide propagation vector parallels the magnetostatic field and the waveguide fields have the same dispersion and structure as the plane waves of equation I-29b.

Plasma resonance. The conditions at plasma resonance are obtained by allowing h to increase without bound while restraining all other quantities to finite magnitudes. Again the limiting behavior of the coefficients in equation II-4 must be examined as $|h| \to \infty$. This leads to

$$a \to \frac{-1}{jh} \qquad\qquad b \to \frac{\omega \mu_o \gamma_2}{-h^4}$$

$$c \rightarrow \frac{-\gamma_2}{jh^3} \qquad d \rightarrow \frac{\omega\mu_o}{h^2}$$

$$f \rightarrow \frac{\omega\epsilon_2}{-h^2} \qquad g \rightarrow \frac{\omega\epsilon_1}{-h^2} \quad . \tag{III-14}$$

Although only the third and higher powers of $1/h$ need be discarded to decouple the longitudinal fields, a consistent picture of plasma resonance is obtained if just the lowest power of $1/h$, i.e., coefficient a, is retained. In that case differential equations II-10 and II-11 reduce to

$$j\omega\,\mu_o\,H_z = 0 \tag{III-15a}$$

$$j\omega\,\epsilon_3\,E_z = 0 \tag{III-15b}$$

while the resonant transverse fields approach

$$\underline{E}_t = ja\,\nabla_t\,E_z = -\frac{1}{h}\nabla_t\,E_z \tag{III-16a}$$

$$\underline{H}_t = ja\,\nabla_t\,H_z = -\frac{1}{h}\nabla_t\,H_z \quad . \tag{III-16b}$$

Since H_z and $\underline{H}_t$ are already zero according to equations III-15a and III-16b, the entire electromagnetic field vanishes unless $\epsilon_3 = 0$ in equation III-15b. This resonance occurs at $\omega = \Omega_p$, the plasma frequency.

To describe this resonant wave as TM would be a misnomer because at the plasma frequency the entire magnetic field vanishes. In fact, since $\underline{E}$ has an e^{-hz} axial dependence, equation III-16a

can be written in an alternate form

$$(\nabla \times \underline{E}) = 0 \qquad \text{(III-17)}$$

which demonstrates that the electric field at plasma resonance may be derived from a scalar potential. It is for this reason that the quasi-static approximation (described in the appendix) correctly predicts wave solutions near the plasma frequency.

To obtain the asymptotic dispersion relation it is necessary to retain the next larger power of $1/h$ as it appears in the coefficient g of equation II-11. A TM wave equation is then obtained with

$$\nabla_t^2 E_z + T^2 E_z = 0 \qquad \text{and} \qquad T^2 \equiv -\frac{\omega\epsilon_3}{g} = \frac{\epsilon_3}{\epsilon_1} h^2 \quad . \qquad \text{(III-18)}$$

The boundary conditions $E_z\Big|_{r_o} = E_\theta\Big|_{r_o} = 0$, applied to the solution $E_z = E_o J_n(Tr) e^{-jn\theta}$ of this equation, demand

$$J_n(Tr) = 0 \qquad \text{with} \qquad h^2 = \frac{\epsilon_1}{\epsilon_3} T^2 \quad . \qquad \text{(III-19)}$$

Exactly the same dispersion relation is obtained by the quasi-static approach.

Resonance takes place whenever the fields excite one of the natural modes of the plasma. In the absence of the signal, the electrons and ions gyrate at their respective cyclotron frequencies in small circular orbits about the magnetostatic lines of force. The plasma also entertains a longitudinal mode of oscillation in which the particles vibrate along $\underline{B}_o$ at the rate Ω_p. If the local transverse field of an incident wave is resolved into two equal-amplitude, counter-rotating,

circularly polarized waves, then the effect of each circular component is to excite one of the transverse normal modes of the plasma. When the signal frequency and the sense of rotation agree with the motion of the particles, the interaction between the field and the charge is strongest and cyclotron resonance results. The electromagnetic energy of the wave then converts into the kinetic energy of the particles and propagation ceases. Plasma resonance occurs when the longitudinal component of the local electric vector excites an electrostatic oscillation of the plasma by rhythmically displacing each particle from its equilibrium position in synchronism with the plasma frequency.

The Cut-Off Frequencies

The signal frequencies at which propagation halts and $h = 0$ are referred to as the cut-off frequencies. A knowledge of the cut-off frequencies and their dependence upon the magnetostatic field strength and plasma density includes valuable information about the mode spectrum. Primarily it reveals which modes propagate for a particular condition; indeed this is essential if numerical calculations of the phase constant are to be performed efficiently. Then again, the cut-off frequency is physically observable and therefore a useful diagnostic for the experimentalist.

At cut-off the propagation constant h is zero and the coefficients a, c, and f of the field expressions vanish. The remaining coefficients become

$$b = \frac{\epsilon_2}{\omega(\epsilon_1^2 - \epsilon_2^2)} \qquad d = \frac{\epsilon_1}{\omega(\epsilon_1^2 - \epsilon_2^2)} \qquad g = \frac{-1}{\omega \mu_o} \quad . \qquad \text{(III-20)}$$

With these substitutions equations II-8 and II-9 for the transverse

fields reduce to

$$\underline{E}_t = \frac{1}{\omega(\epsilon_1^2 - \epsilon_2^2)} \left[\epsilon_2 \nabla_t H_z + j\epsilon_1 \underline{e}_z \times \nabla_t H_z \right] \qquad \text{(III-21)}$$

$$\underline{H}_t = \frac{1}{j\omega\mu_o} \underline{e}_z \times \nabla_t E_z \quad . \qquad \text{(III-22)}$$

Furthermore, because the coupling coefficient c vanishes at cut off, the longitudinal field equations II-10 and II-11 separate and reduce to wave equations in H_z and E_z .

$$\nabla_t^2 H_z + S^2 H_z = 0 \qquad S^2 \equiv \omega^2 \mu_o (\epsilon_1^2 - \epsilon_2^2)/\epsilon_1 \qquad \text{(III-23)}$$

$$\nabla_t^2 E_z + T^2 E_z = 0 \qquad T^2 \equiv \omega^2 \mu_o \epsilon_3 = (\omega^2 - \Omega_p^2)/V_c^2 \; . \qquad \text{(III-24)}$$

The solutions to these equations in cylindrical coordinates are respectively

$$H_z = H_o J_n(Sr) e^{-jn\theta} \qquad \text{and} \qquad E_z = E_o J_n(Tr) e^{-jn\theta} \qquad \text{(III-25)}$$

where H_o and E_o are arbitrary constants determined by the field sources.

The eigenvalues T and S are determined by the boundary conditions at the perfectly conducting waveguide wall. There at $r = r_o$,

$$E_z = E_\theta = H_r = 0 \quad .$$

Substituting III-25 into III-21 and III-22 and applying these boundary conditions gives

$$E_z\Big|_{r_o} = E_o J_n(Tr_o) = 0$$

$$E_\theta\Big|_{r_o} = \frac{-j\epsilon_2 H_o}{\omega(\epsilon_1^2 - \epsilon_2^2)} \left[\frac{n}{r_o} \epsilon_2 J_n(Sr_o) - \epsilon_1 S J_n'(Sr_o) \right] = 0$$

$$H_r\Big|_{r_o} = \frac{1}{\omega\mu_o} \frac{n}{r_o} E_o J_n(Tr_o) = 0 \quad .$$

Obviously S and T satisfy independent relations. Since neither the boundary conditions nor the wave equations couple E_z to H_z the fields at cut off are characterized as TE (transverse electric) and TM (transverse magnetic) modes.

The TM modes have $H_z = 0$; due to equation III-21 the transverse electric field also vanishes. Nevertheless, the transverse magnetic field remains and it has a radial component which is proportional to E_z ,

$$H_r = \frac{1}{\omega\mu_o} \frac{n}{r} E_z \quad .$$

If T is selected to satisfy the electric boundary condition $E_z\Big|_{r_o} = 0$, the magnetic boundary condition is immediately insured. The characteristic cut-off relation is therefore

$$J_n(Tr_o) = 0 \qquad \text{with} \qquad \omega_{4,n} = \sqrt{(TV_c)^2 + \Omega_p^2} \quad . \qquad \text{(III-26)}$$

The subscript distinguishes ω from the three TE cut-off frequencies which follow. Two observations regarding $\omega_{4,n}$ can be made at once:

1) The TM cut-off frequency for the empty waveguide has been increased by the plasma frequency but is unaffected by the magnetostatic field because the electric vector and the particle motion are both parallel to $\underline{B}_o$.

2) Unlike the TE cut-offs which follow, the positive and negative angular dependent TM modes have the same cut-off frequency since $J_{-n}(Tr_o) = (-1)^n J_n(Tr_o) = 0$.

Next consider those modes with TE cut-offs. Taking $E_z = 0$ guarantees that the transverse magnetic intensity is identically zero; in particular that H_r vanishes at the boundary. The only remaining condition is that E_θ must likewise have a null at the conducting wall. This condition determines the eigenvalues for S and the TE cut-off frequencies:

$$\left[\epsilon_2 n\, J_n(Sr_o) - \epsilon_1 (Sr_o)\, J_n'(Sr_o)\right] = 0 \qquad \text{(III-27)}$$

where according to equation III-23

$$S^2 = \omega^2 \mu_o (\epsilon_1^2 - \epsilon_2^2)/\epsilon_1 \quad . \qquad \text{(III-28)}$$

The behavior of the TE cut-off frequencies is obscured by the transcendental nature and algebraic complexity of these cut-off relations. An obvious solution to this set of equations is $\omega = 0$, but to understand the character of the other cut-off frequencies it is helpful to inspect the asymptotic form of these equations. For a neutral two-component plasma the number of independent variables are diminished twofold, once because $\Omega_i^2 = \frac{\omega_i}{\omega_e} \Omega_e^2$ (charge neutrality) and then because ω_i/ω_e is fixed by the electron to ion mass ratio. Even for a hydrogen plasma $\frac{\omega_i}{\omega_e} = \frac{m_e}{m_i} = \frac{1}{1836}$ is exceedingly small. When the permittivities involved in equation III-28 and explicitly defined by equations I-18 are simplified by the neutrality assumption, one obtains

$$\epsilon_1 = \epsilon_o \frac{(\omega^2 - \omega_a^2)(\omega^2 - \omega_b^2)}{(\omega^2 - \omega_i^2)(\omega^2 - \omega_e^2)} \tag{III-29}$$

$$= \frac{\epsilon_o}{(\omega^2 - \omega_i^2)(\omega^2 - \omega_e^2)} \left\{\omega^4 - (\omega_e^2 + \omega_i^2 + \Omega_p^2)\omega^2 + \omega_e\omega_i(\omega_e\omega_i + \Omega_p^2\right\}$$

$$\epsilon_2 = \epsilon_o \frac{\omega(\omega_i\Omega_i^2 - \omega_e\Omega_e^2)}{(\omega^2 - \omega_i^2)(\omega^2 - \omega_e^2)} \tag{III-30}$$

$$(\epsilon_1 \pm \epsilon_2) = \epsilon_o \frac{(\omega \pm \omega_L)(\omega \mp \omega_R)}{(\omega \pm \omega_i)(\omega \mp \omega_e)}$$

$$= \frac{\epsilon_o}{(\omega \pm \omega_i)(\omega \mp \omega_e)} \left\{\omega^2 \mp (\omega_e - \omega_i)\omega - (\omega_e\omega_i + \Omega_p^2)\right\} \tag{III-31}$$

and

$$(\epsilon_1^2 - \epsilon_2^2) = \epsilon_o \frac{(\omega^2 - \omega_L^2)(\omega^2 - \omega_R^2)}{(\omega^2 - \omega_i^2)(\omega^2 - \omega_e^2)} \tag{III-32}$$

$$= \frac{\epsilon_o}{(\omega^2 - \omega_i^2)(\omega^2 - \omega_e^2)} \left\{\omega^4 - (\omega_e^2 + \omega_i^2 + 2\Omega_p^2)\omega^2 + (\omega_e\omega_i + \Omega_p^2)^2\right\}$$

where

$$\omega_a = \left\{\frac{1}{2}(\omega_e^2 + \omega_i^2 + \Omega_p^2) - \frac{1}{2}\sqrt{(\omega_e^2 - \omega_i^2 + \Omega_e^2 - \Omega_i^2)^2 + 4\Omega_e^2\,\Omega_i^2}\right\} \tag{III-33a}$$

$$\omega_b = \left\{\frac{1}{2}(\omega_e^2 + \omega_i^2 + \Omega_p^2) + \frac{1}{2}\sqrt{(\omega_e^2 - \omega_i^2 + \Omega_e^2 - \Omega_i^2)^2 + 4\Omega_e^2\,\Omega_i^2}\right\} \tag{III-33b}$$

$$\omega_L = -\left(\frac{\omega_e - \omega_i}{2}\right) + \sqrt{\left(\frac{\omega_e + \omega_i}{2}\right)^2 + \Omega_p^2}\,. \tag{III-34a}$$

$$\omega_R = + \left(\frac{\omega_e - \omega_i}{2}\right) + \sqrt{\left(\frac{\omega_e + \omega_i}{2}\right)^2 + \Omega_p^2} \qquad \text{(III-34b)}$$

$$\Omega_p = \sqrt{\Omega_e^2 + \Omega_i^2} \quad . \qquad \text{(III-35)}$$

The zeros of ϵ_1 are the cut-off frequencies ω_a and ω_b which later appear in the quasi-static and narrow waveguide approximations. It will also be shown that ω_a and ω_b are the upper bounds for the cut-off frequencies in the first two passbands of the exact solution. ω_L and ω_R describe the lower bound to the second and third passbands. Physically they are the cut-off frequencies of the left and right circularly polarized plane waves which propagate parallel to $\underline{B}_o$ in an infinite medium.

Substituting for ϵ_1 and ϵ_2, equation III-28 becomes:

$$\left\{\omega^6 - (S^2V_c^2 + \omega_e^2 + \omega_i^2 + 2\Omega_p^2)\omega^4 + \left[S^2V_c^2(\omega_e^2 + \omega_i^2 + \Omega_p^2) + (\omega_e\omega_i + \Omega_p^2)^2\right]\omega^2 - \omega_e\omega_i S^2V_c^2(\omega_e\omega_i + \Omega_p^2)\right\} = 0 \quad . \qquad \text{(III-36)}$$

Equation III-27 is repeated here for reference

$$\left[\epsilon_2 n\, J_n(Sr_o) - \epsilon_1 (Sr_o)\, J_n'(Sr_o)\right] = 0 \quad . \qquad \text{(III-37)}$$

The limiting properties of these cut-off relations are studied in the next six cases.

For an empty waveguide $\Omega_e^2 = \frac{\omega_e}{\omega_i}\Omega_i^2 \to 0$. As the plasma becomes increasingly tenuous $\epsilon_1 \to \epsilon_o$, $\epsilon_2 \to 0$, and the above expressions reduce to

$$(\omega^2 - \omega_i^2)(\omega^2 - \omega_e^2)(\omega^2 - S^2V_c^2) = 0 \quad , \quad J_n'(Sr_o) = 0 \quad . \qquad \text{(III-38)}$$

Thus while the first two cut-off frequencies approach and cancel the cyclotron resonances at ω_i and ω_e, the third factor describes the usual TE cut-off condition for an empty waveguide.

In the magnetohydrodynamic (MHD) limit the plasma frequency Ω_p is so very much larger than either cyclotron frequency that equation III-36 becomes

$$\omega^6 - (S^2V_c^2 + 2\Omega_p^2)\omega^4 + \Omega_p^2(S^2V_c^2 + \Omega_p^2)\omega^2 - \omega_e\omega_i\Omega_p^2S^2V_c^2 = 0 \quad . \qquad \text{(III-39)}$$

When, as here, two of the cubic roots are much larger than the third, the smallest root may be obtained by neglecting the first two terms of the cubic equation. Therefore the lowest TE cut-off frequency of the MHD limit is very nearly

$$\omega = SV_c\sqrt{\frac{\omega_e\omega_i}{(S^2V_c^2 + \Omega_p^2)}} \approx SV_c\sqrt{\frac{\omega_e\omega_i}{\Omega_e^2}} = \frac{\omega_i}{\omega_e}\, SV_c \quad . \qquad \text{(III-40a)}$$

The two larger roots are obtained by neglecting the last term of equation III-39, thus yielding the factors

$$(\omega^2 - \Omega_p^2)\left[\omega^2 - (S^2V_c^2 + \Omega_p^2)\right] = 0 \quad . \qquad \text{(III-40b)}$$

The first factor cancels the plasma resonance, while the last factor yields the modified TE waveguide cut-off. The transcendental equation for S does not simplify unless the mode is circularly symmetric ($n = 0$).

If the static magnetic field is reduced, the plasmaguide becomes isotropic and the cyclotron resonances fall to zero frequency. As a result $\epsilon_1 \to \epsilon_3$, $\epsilon_2 \to 0$ whereas equations III-36 and III-37 reduce to

$$\omega^2(\omega^2 - \Omega_p^2)\left[\omega^2 - (S^2 V_c^2 + \Omega_p^2)\right] = 0 \quad \text{and} \quad J_n'(Sr_o) = 0 \ . \quad \text{(III-41)}$$

Note that the lowest TE cut off joins the TEM cut-off frequency at $\omega = 0$ to cancel the two cyclotron resonances at the origin. The second factor has a zero at Ω_p to cancel the plasma resonance. The final root indicates how the presence of an isotropic plasma raises the TE cut-off frequency of an empty waveguide.

In an intense magnetostatic field the plasma is extremely anisotropic and the shifted cut-off frequencies are obtained by neglecting Ω_p relative to ω_i and ω_e . Again $\epsilon_1 \to \epsilon_o$ and $\epsilon_2 \to 0$, leaving

$$(\omega^2 - \omega_i^2)(\omega^2 - \omega_e^2)(\omega^2 - S^2 V_c^2) = 0 \quad \text{and} \quad J_n'(Sr_o) = 0 \ . \quad \text{(III-42)}$$

The first two cut-off frequencies cancel the cyclotron resonances at infinity. The remaining TE cut-off frequency is exactly the same as for an empty waveguide, because in the presence of an infinite longitudinal magnetic bias the particles are unable to respond to a transverse electric force.

The remaining two limits deal exclusively with how the radial extent of the waveguide affects the cut-off frequencies. In the limit for which both T and S approach zero, the TM and TE cut-off relations, equations III-26, III-27 and III-28, become respectively

(TM) $$\omega^2 = \Omega_p^2 \qquad \text{(III-43a)}$$

and

(TE) $$\omega^2(\epsilon_1^2 - \epsilon_2^2) = 0 \qquad \text{or} \qquad \omega^2(\omega^2 - \omega_L^2)(\omega^2 - \omega_R^2) = 0 \quad \text{(III-43b)}$$

Thus the TM cut-off cancels the plasma resonance at Ω_p and the TE cut-offs become the plane wave cut-off frequencies $\omega = 0$, ω_L and ω_R. The transcendental relations are identically satisfied by $S = T = 0$. This implies that the plane wave limit, corresponding to an infinite waveguide radius, is equivalent to letting S and T go to zero.

Letting S become infinite reduces dispersion relation III-28 or III-36 to

$$\frac{1}{\omega^2}\epsilon_1 = 0 \quad \text{i.e.} \quad (\omega^2 - \omega_a^2)(\omega^2 - \omega_b^2) = 0 \quad \text{and} \quad \omega = \infty \; . \qquad \text{(III-44)}$$

Transcendental equation III-37 is also satisfied because Bessel functions of infinite real arguments are vanishingly small. Since ω_a and ω_b are the narrow waveguide cut-off frequencies, this indicates that letting S become very large has the same effect as reducing the guide radius.

<u>The circularly symmetric cut-off frequencies.</u> In this section the cut-off frequencies of the circularly symmetric modes are investigated qualitatively and numerically for intermediate values of the plasma parameters. The number of independent variables is kept to a minimum by introducing the following normalizations:

$$\lambda = \frac{\omega r_o}{V_c} = \omega\sqrt{\mu_o \epsilon_o}\, r_o \quad , \qquad \Lambda = \frac{\Omega r_o}{V_c} = \Omega\sqrt{\mu_o \epsilon_o}\, r_o \quad ,$$

$$\text{and} \quad \bar{S} = S r_o \quad . \tag{III-45}$$

The character λ should not be confused with the conventional symbol for the wavelength which never appears here. Cut-off relations III-36 and III-37 for $n = 0$ therefore become

$$\left\{ \lambda^6 - (\bar{S}^2 + \lambda_e^2 + \lambda_i^2 + 2\Lambda_p^2)\lambda^4 + \left[\bar{S}^2(\lambda_e^2 + \lambda_i^2 + \Lambda_p^2) + (\lambda_e\lambda_i + \Lambda_p^2)^2 \right] \lambda^2 \right.$$
$$\left. - \lambda_e\lambda_i \bar{S}^2(\lambda_e\lambda_i + \Lambda_p^2) \right\} = 0 \tag{III-46}$$

where

$$J_1(\bar{S}) = 0 \quad . \tag{III-47}$$

To facilitate the evaluation of the two larger roots of equation III-46, it is argued that for oscillations much faster than the ion cyclotron frequency, the ions may be treated as a <u>stationary</u> background charge which provides neutrality to the plasma. The validity of this assumption is based on the large ion to electron mass ratio which in practice always exceeds 1,836. Taking $\lambda_i = 0$ and $\Lambda_p^2 \equiv \Lambda_e^2 (1 + \frac{\lambda_i}{\lambda_e}) \approx \Lambda_e^2$, bicubic equation III-46 acquires the form

$$\lambda^2 \left\{ \lambda^4 - (\bar{S}^2 + \lambda_e^2 + 2\Lambda_e^2)\lambda^2 + \left[\bar{S}^2(\lambda_e^2 + \Lambda_e^2) + \Lambda_e^4 \right] \right\} = 0 \quad . \tag{III-48}$$

The two larger TE cut-off frequencies are therefore approximately

$$\lambda_{2,0} = \left\{ \frac{1}{2} (\bar{S}^2 + \lambda_e^2 + 2\Lambda_e^2) - \frac{1}{2} \sqrt{(\bar{S}^2 - \lambda_e^2)^2 + 4\lambda_e^2 \Lambda_e^2} \right\}^{1/2} \qquad \text{(III-49)}$$

$$\lambda_{3,0} = \left\{ \frac{1}{2} (\bar{S}^2 + \lambda_e^2 + 2\Lambda_e^2) + \frac{1}{2} \sqrt{(\bar{S}^2 - \lambda_e^2)^2 + 4\lambda_e^2 \Lambda_e^2} \right\}^{1/2} . \qquad \text{(III-50)}$$

The first subscript distinguishes the cut-off frequency, the second numeral denotes the angular dependence. A third subscript could also be used to indicate the order of the radial dependence.

The lowest TE cut-off frequency can be determined approximately if the two leading terms in equation III-46 are neglected. When terms of the order λ_i/λ_e are discarded relative to unity, we obtain

$$\lambda_{1,0} = \bar{S} \sqrt{\frac{\lambda_e \lambda_i (\lambda_e \lambda_i + \Lambda_e^2)}{\bar{S}^2(\lambda_e^2 + \Lambda_e^2) + (\lambda_e \lambda_i + \Lambda_e^2)^2}} . \qquad \text{(III-51)}$$

To check the validity of the foregoing approximations, some representative values of λ_e, Λ_e and $\bar{S}$ were chosen, and the above expressions were compared to the exact solutions of the bicubic equation. The Table III-1 summarizes the calculations and demonstrates that formulas III-49, III-50 and III-51 may be used with complete confidence.

On the following pages the lowest circularly symmetric TE and TM cut-off frequencies are illustrated as functions of the electron density for various fixed values of the static magnetic field. The plasma under examination is a completely ionized hydrogen gas.

Two transitions exist: the first occurs when $\lambda_e = \bar{S}$, at which time $\lambda_{2,0}$ (Fig.III-2) and $\lambda_{3,0}$ (Fig.III-3) interchange roles; the second transition occurs at a much larger magnetic field $\lambda_i = \bar{S}$; here

λ_e	Λ_e	Approximate $\lambda_{3,0}$	Exact $\lambda_{3,0}$	Approximate $\lambda_{4,0}$	Exact $\lambda_{4,0}$	Approximate $\lambda_{5,0}$	Exact $\lambda_{5,0}$
1	10^{-1}	2.3845×10^{-3}	2.3852×10^{-3}	1.0046	1.0046	3.8331	3.8331
	1	1.6231×10^{-2}	1.6272×10^{-2}	1.3883	1.3917	3.9692	3.9706
	10	8.3447×10^{-3}	8.3397×10^{-3}	9.7840	9.7917	1.0952×10^{1}	1.0960×10^{1}
	10^{2}	8.9417×10^{-4}	8.9269×10^{-4}	9.9537×10^{1}	9.9564×10^{1}	1.0054×10^{2}	1.0056×10^{2}
50	10^{-1}	2.7333×10^{-2}	2.7333×10^{-2}	3.8327	3.8317	5.0000×10^{1}	5.000×10^{1}
	1	3.5856×10^{-2}	3.5861×10^{-2}	3.8322	3.8311	5.0020×10^{1}	5.0020×10^{1}
	10	2.0452×10^{-1}	2.0479×10^{-1}	4.2266	4.2340	5.1931×10^{1}	5.1931×10^{1}
	10^{2}	4.4709×10^{-2}	4.4656×10^{-2}	7.8137×10^{1}	7.8179×10^{1}	1.2811×10^{2}	1.2812×10^{2}

Table III-1. A Comparison of formulas III-49, III-50 and III-51 with the exact solution of equation III-46 for $\overline{S} = 3.8317$

$\lambda_{1,0}$ and $\lambda_{2,0}$ switch parts. At these points the waveguide geometry and the plasma variables are of equal prominence; in other areas one factor or the other dominates.

Note how the curves (Fig. III-1) for $\lambda_{1,0}$ rise, crowd together, and tend to flatten with increasing magnetic field λ_e. First the asymptote $\lambda_{1,0} = \lambda_i$ is sought, but eventually λ_i exceeds $\bar{S}$ and the traces saturate near $\lambda_{1,0} = \bar{S}$ for infinite magnetic fields. For intermediate magnetic fields and decreasing plasma densities, the loci of $\lambda_{1,0}$ run into and cancel the ion cyclotron frequency. At large values of Λ_e, $\lambda_{1,0}$ becomes the MHD cut-off frequency $\frac{\lambda_i}{\Lambda_i}\bar{S}$.

Quite unlike the other cut-off frequencies, $\frac{\partial\lambda_{2,0}}{\partial\lambda_e}$ is negative when $\lambda_e > \bar{S}$ (Fig. III-2). As observed earlier, $\lambda_e = \bar{S}$ marks the spot where $\lambda_{2,0}$ and $\lambda_{3,0}$ interchange roles. For λ_e much less than $\bar{S}$, the loci of $\lambda_{2,0}$ and $\lambda_{3,0}$ approach Λ_p and $\sqrt{\bar{S}^2 + \Lambda_p^2}$ respectively. For large magnetic fields ($\lambda_e >> \bar{S}$), $\lambda_{2,0}$ first levels off at $\bar{S}$ but then, as B_o is increased beyond the transition $\lambda_i = \bar{S}$, these curves crowd toward λ_i. Meanwhile $\lambda_{3,0}$ approaches λ_e without incident. In the MHD limit (large Λ_e), the $\lambda_{2,0}$ traces converge upon Λ_p whereas the $\lambda_{3,0}$ curves have $\sqrt{\bar{S}^2 + \Lambda_p^2}$ as an asymptote. In a tenuous plasma $\lambda_{2,0}$ and $\lambda_{3,0}$ respectively approach either $\bar{S}$ and λ_e, or λ_e and $\bar{S}$ depending on whether λ_e is greater or less than $\bar{S}$. In the empty waveguide one of these cut-off frequencies cancels the electron cyclotron resonance, the other becomes the TE waveguide cut-off.

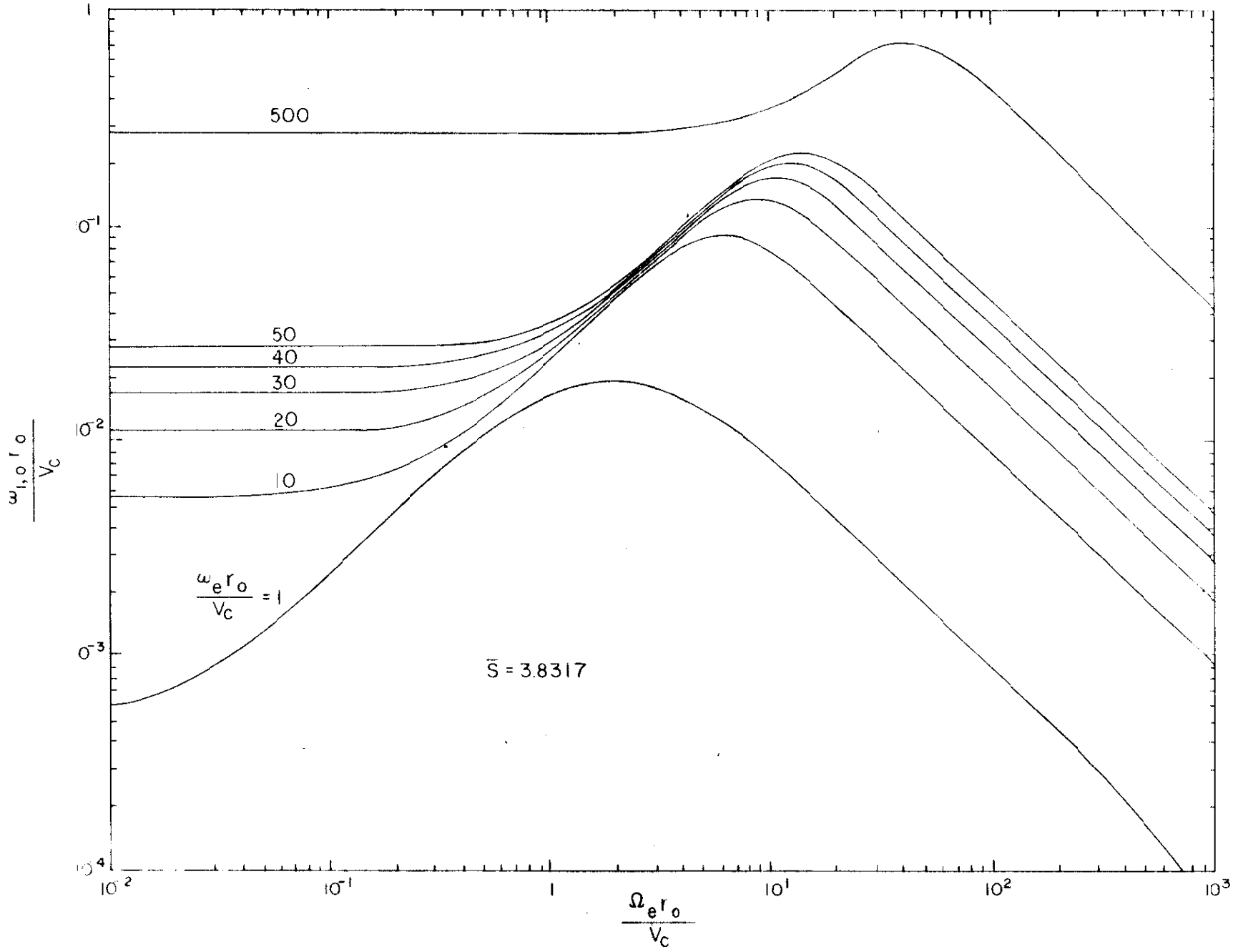

Figure III.1. The first TE cut-off frequency for the lowest radial order, circularly symmetric (n = 0) mode as a function of the plasma density, for successive values of the magnetostatic field.

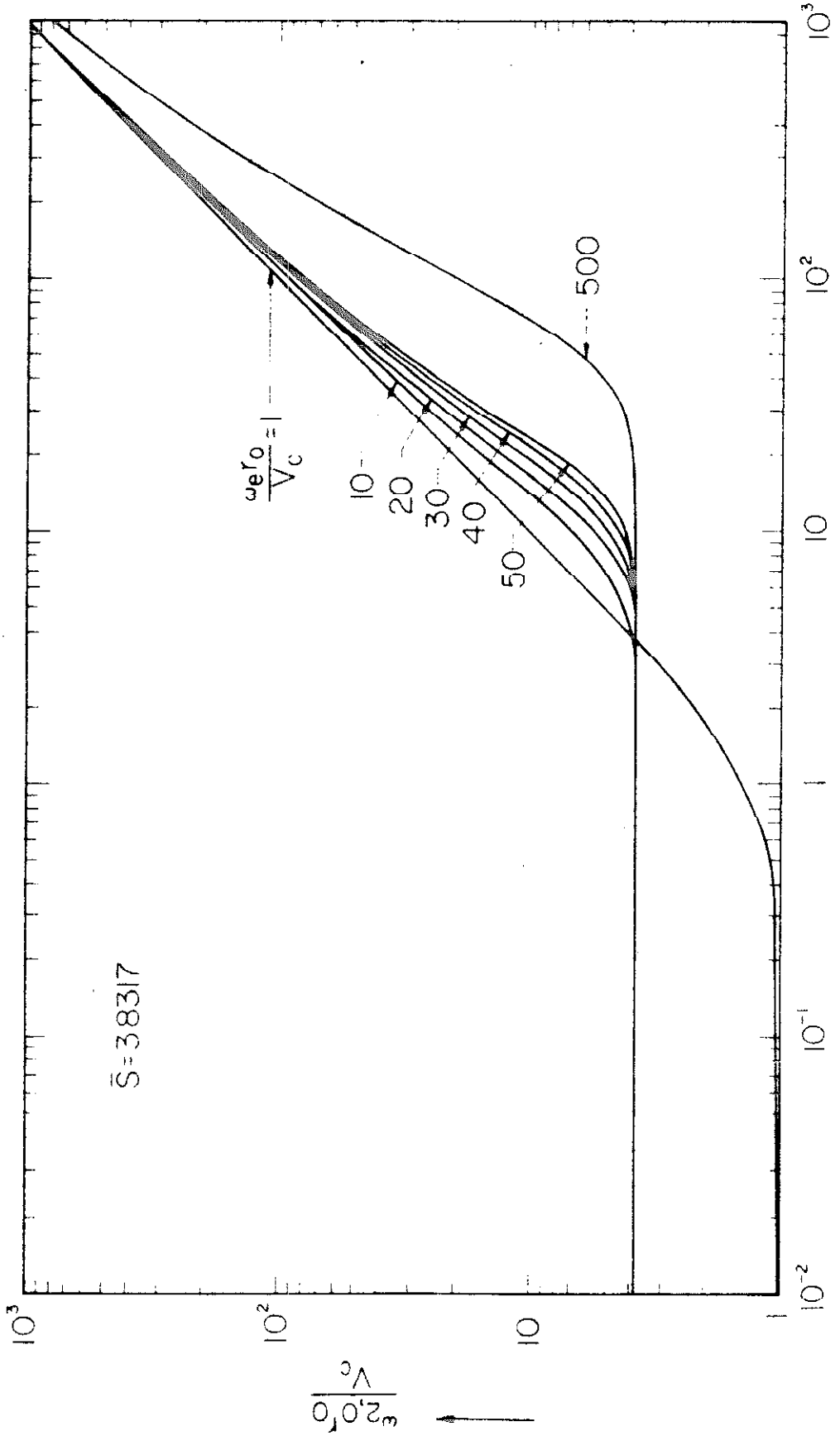

Figure III-2. The second TE cut-off frequency for the lowest radial order, circularly symmetric (n = 0) mode as a function of the plasma density, for successive values of the magnetostatic field.

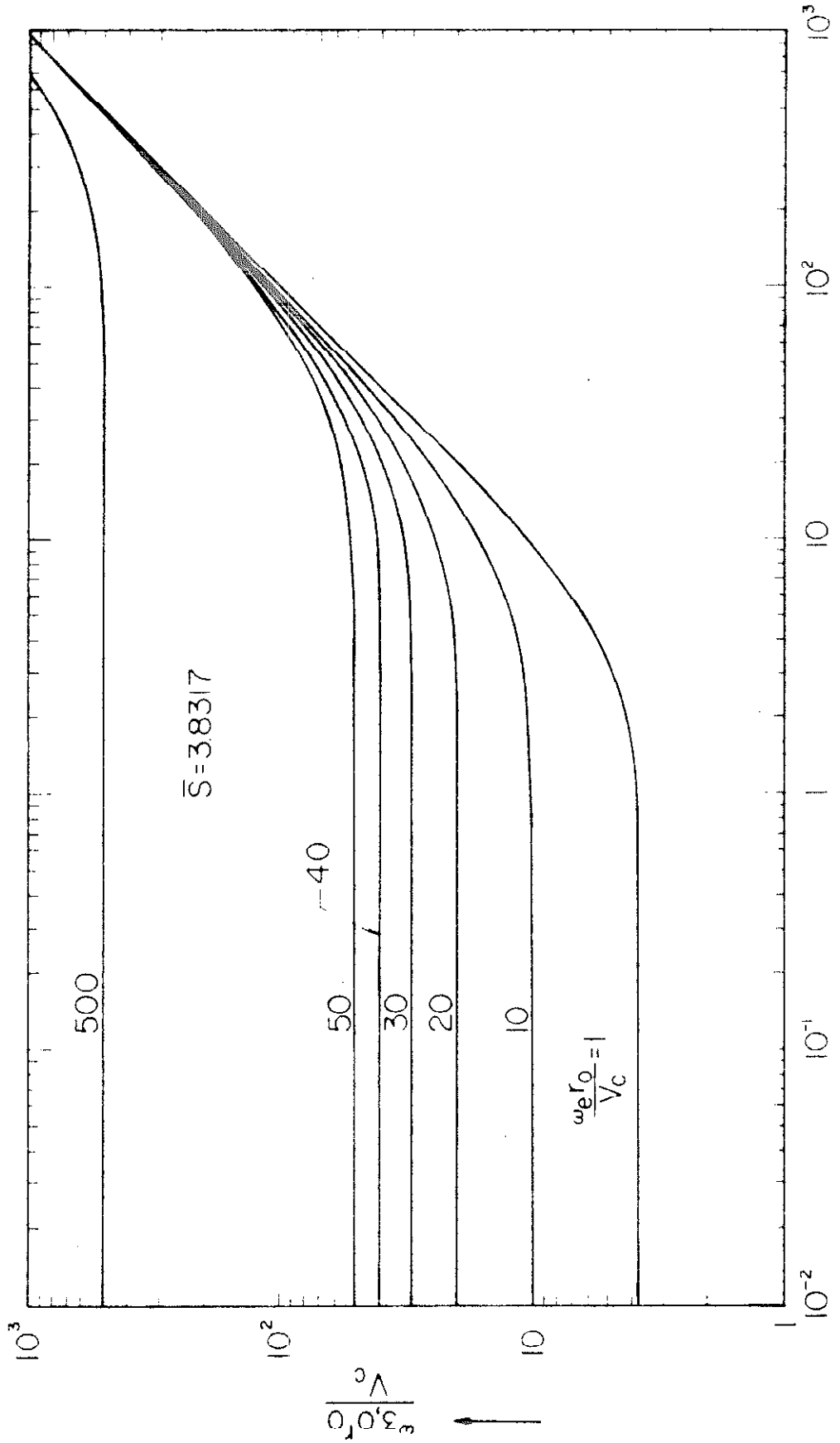

Figure III-3. The third TE cut-off frequency for the lowest radial order, circularly symmetric (n = 0) mode as a function of the plasma density, for successive values of the magnetostatic field.

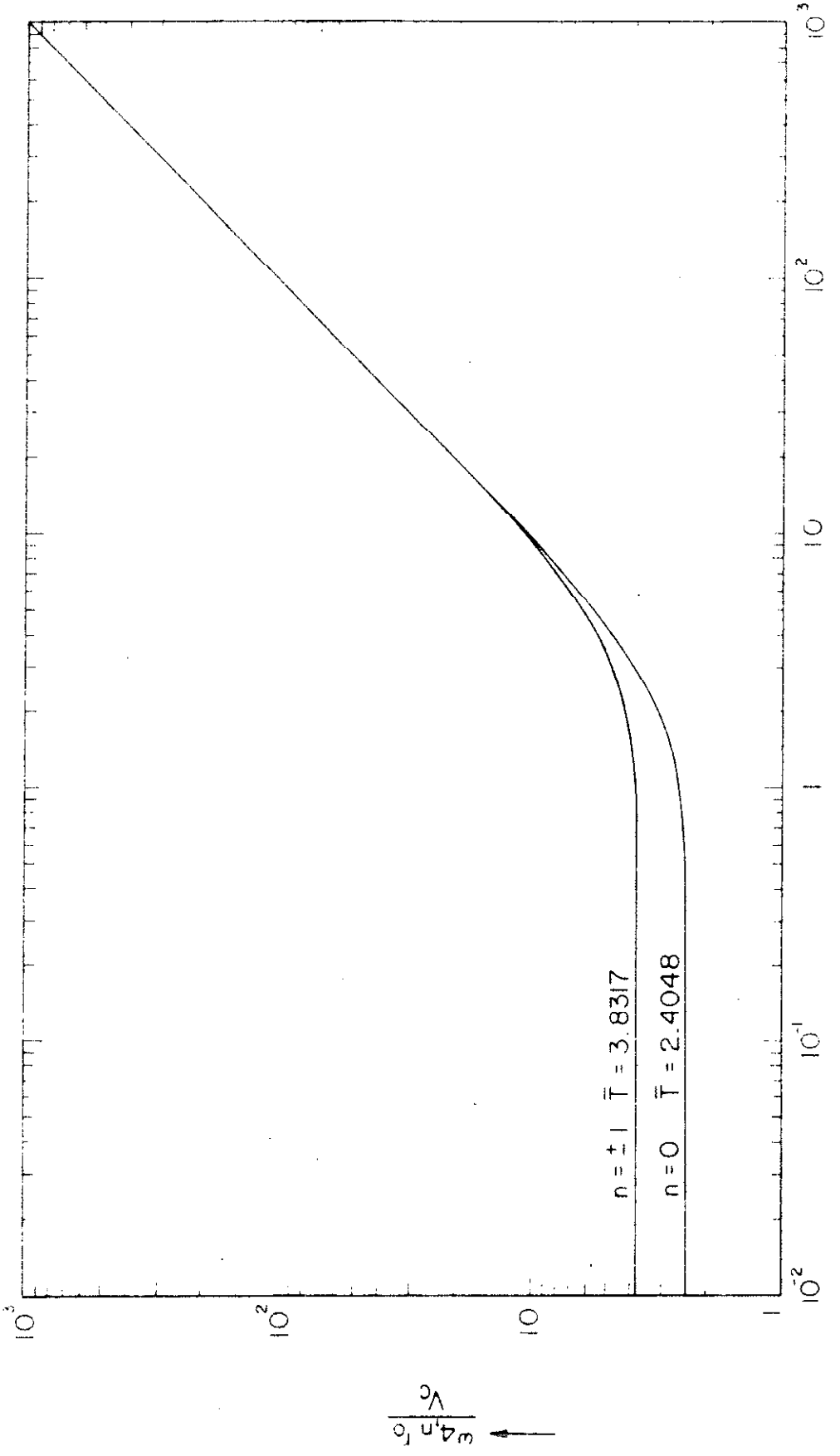

Figure III-4. The lowest radial order, TM cut-off frequency for the n = 0 , ±1 angularly dependent modes as a function of the plasma density

The behavior of the TM cut-off frequencies is not as involved because they are independent of the magnetic field strength. However, in certain respects the $\lambda_{4,n}$ cut-offs are similar to $\lambda_{2,0}$ or $\lambda_{3,0}$.

A sinusoidal signal propagating through a relaxing plasma can produce a very peculiar output at the far end of the waveguide. The continual reduction of the plasma density by recombination causes some of the cut-off frequencies to pass (perhaps twice in the case of $\lambda_{1,0}$) through the signal frequency. With each pass the output signal is turned off or on. The existence of several propagating modes would account for the partial extinction of the wave. The occurrence of higher order modes only complicates the situation.

The effect of the field's radial dependence upon the TE cut-off frequencies is illustrated in Figures III-5 and III-6 for the range $\lambda_i < \bar{S} < \lambda_e = 50$. In all cases the cut-off frequencies are raised as $\bar{S}$ is increased. $\bar{S}$ affects each of the three TE cut offs in a different range of plasma density. For instance, $\lambda_{1,0}$ varies like λ_i/Λ_i $\bar{S}$ in the MHD limit, but equals λ_i in an empty waveguide where $\lambda_{2,0} = \bar{S}$. At larger plasma densities $\lambda_{2,0}$ becomes independent of $\bar{S}$ and tangent to the line $\lambda = \Lambda_p$. As a result the radial dependence does not influence $\lambda_{1,0}$ at small plasma densities nor $\lambda_{2,0}$ at large densities.

Cut-off frequency $\lambda_{3,0}$ is bounded by the asymptotes λ_e and $\sqrt{\Lambda_p^2 + \bar{S}^2}$. For $\lambda_e \gg \bar{S}$, the intersection of the asymptotes occurs at approximately $\Lambda_p = \lambda_e \gg \bar{S}$. Consequently the asymptotic dependence of $\lambda_{3,0}$ upon $\bar{S}$ is masked by the much larger values of Λ_p. Calculations show that the maximum change in $\lambda_{3,0}$ between successive

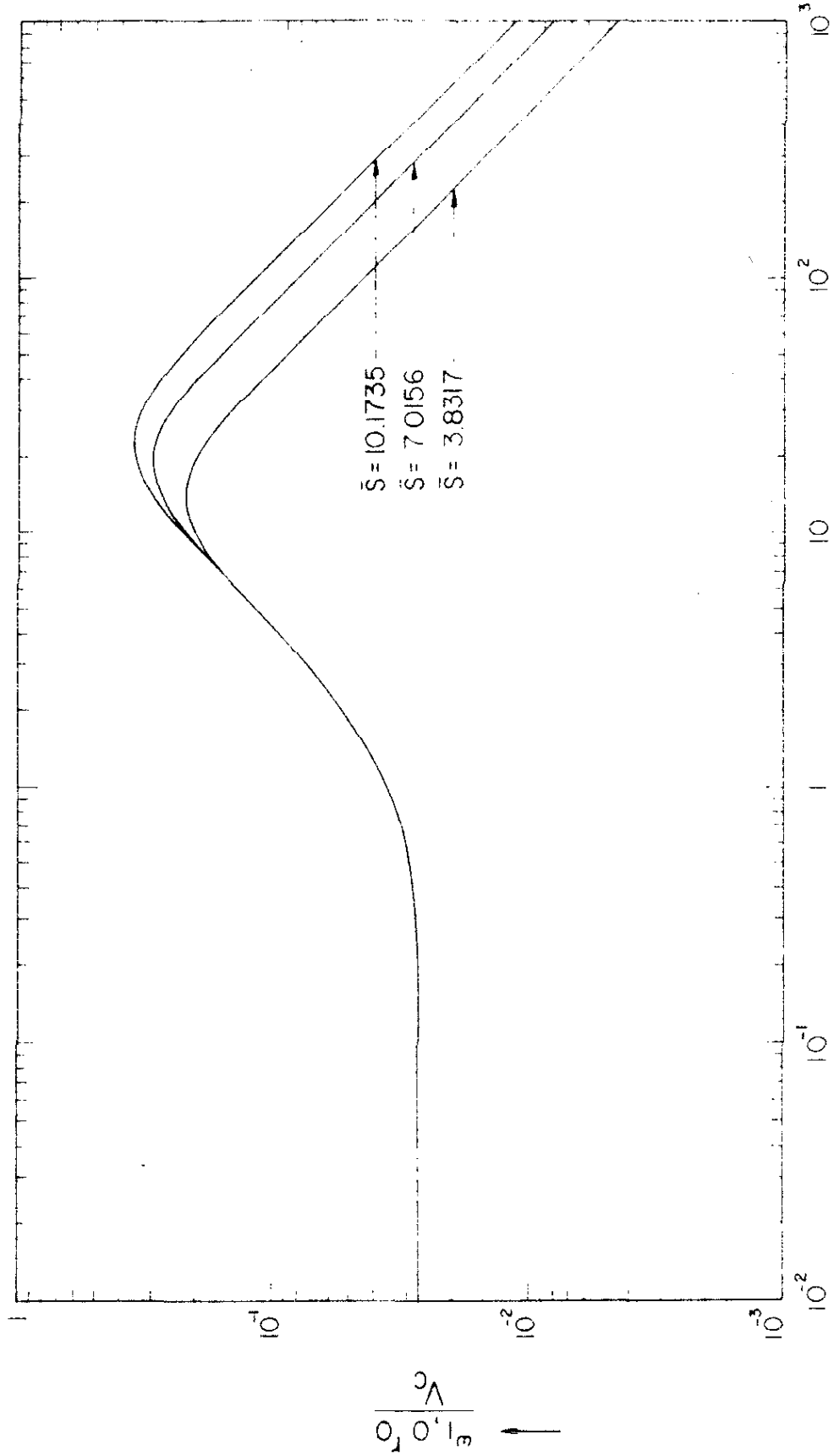

Figure III-5. The first TE cut-off frequency of the circularly symmetric (n = 0) mode as a function of the plasma density for consecutively higher radial wave orders and $\lambda_e = 50$.

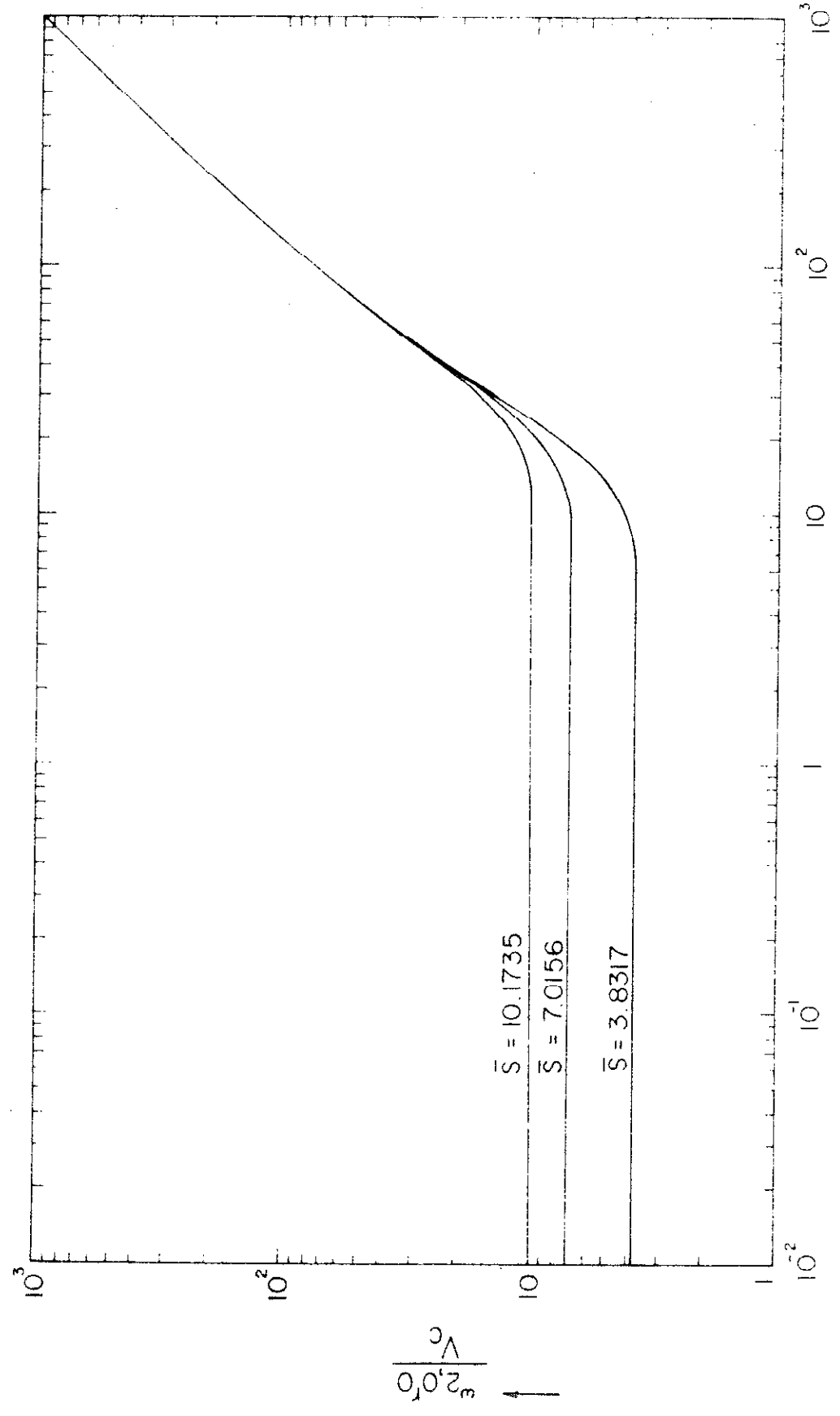

Figure III-6. The second TE cut-off frequency of the circularly symmetric (n = 0) mode as a function of the plasma density for consecutively higher radial wave orders and $\lambda_e = 50$.

radial orders occurs at about $\Lambda_p = \bar{S}$, but that this difference is always less than 0.1% of $\lambda_{3,0}$.

The angularly dependent cut-off frequencies. The critical frequencies λ_a, λ_b, λ_L, λ_R influence the values of the cut-off frequencies and the latter--together with the resonant frequencies λ_i, λ_e and Λ_p --determine the wave behavior and the stop bands of the dispersion diagram. It is therefore useful to have some notion as to the relative sizes of the system's critical frequencies. Observe that for all λ_e and Λ_e the following inequalities are always obeyed in a neutral plasma

$$\boxed{\infty > \lambda_R > \lambda_b > \lambda_L > \lambda_a > \lambda_i > 0} \quad . \tag{III-52}$$

The behavior of the angularly dependent cut-off frequencies is predicted by equations III-27 and III-28, viz.

$$\frac{nJ_n(\bar{S})}{\bar{S}\,J_n'(\bar{S})} = \frac{\epsilon_1}{\epsilon_2} \tag{III-53a}$$

where, according to III-29 and III-32

$$\bar{S} = \lambda \sqrt{\frac{\epsilon_1^2 - \epsilon_2^2}{\epsilon_1}} = \lambda \sqrt{\frac{(\lambda^2 - \lambda_L^2)(\lambda^2 - \lambda_R^2)}{(\lambda^2 - \lambda_a^2)(\lambda^2 - \lambda_b^2)}} \quad . \tag{III-53b}$$

Expressed in this manner, whether $\bar{S}$ is positive real or imaginary, the left hand side of the first equation is always real. Furthermore, the transcendental and algebraic terms are separated.

The wave number of the hybrid transverse-longitudinal wave (summarized in Figure I-2d) which propagates perpendicular to the magnetic field is

$$\beta = \omega\mu_o \sqrt{\frac{\epsilon_1^2 - \epsilon_2^2}{\epsilon_1}} \quad .$$

By writing $\bar{S} = \beta r_o$ we obtain the auxiliary cut-off equation III-53b. This indicates that as cut-off is approached, the propagation vector within the guide becomes increasingly inclined to the static magnetization $\underline{B}_o$ until at cut-off it is normal to the z axis.

Taking heed of the inequalities which exist between the system's critical frequencies, the variation of $\bar{S}^2$ with λ^2 is readily sketched in Figure III-7a. Alternatively, $\bar{S}$ may be plotted against λ as in Figure III-7b. In the second sketch $\bar{S}$ is parabolic in the neighborhood of the zeros, e.g., $\bar{S} \sim \sqrt{(\lambda - \lambda_L)}$ about $\lambda \approx \lambda_L$; and $\bar{S}$ has a hyperbolic dependence at the poles, e.g., $\bar{S} \sim \frac{1}{\sqrt{(\lambda - \lambda_a)}}$ neat λ_a . Note that $\bar{S}$ is alternately real and imaginary with intervals:

$0 < \lambda < \lambda_a$ where $\bar{S}$ is real

$\lambda_a < \lambda < \lambda_L$ where $\bar{S}$ is imaginary

$\lambda_L < \lambda < \lambda_b$ where $\bar{S}$ is real

$\lambda_b < \lambda < \lambda_R$ where $\bar{S}$ is imaginary

$\lambda_R < \lambda < \infty$ where $\bar{S}$ is real.

On the other hand, the function $f_1(\bar{S}) = \frac{n\, J_n(\bar{S})}{\bar{S}\, J_n'(\bar{S})}$ has the following behavior:

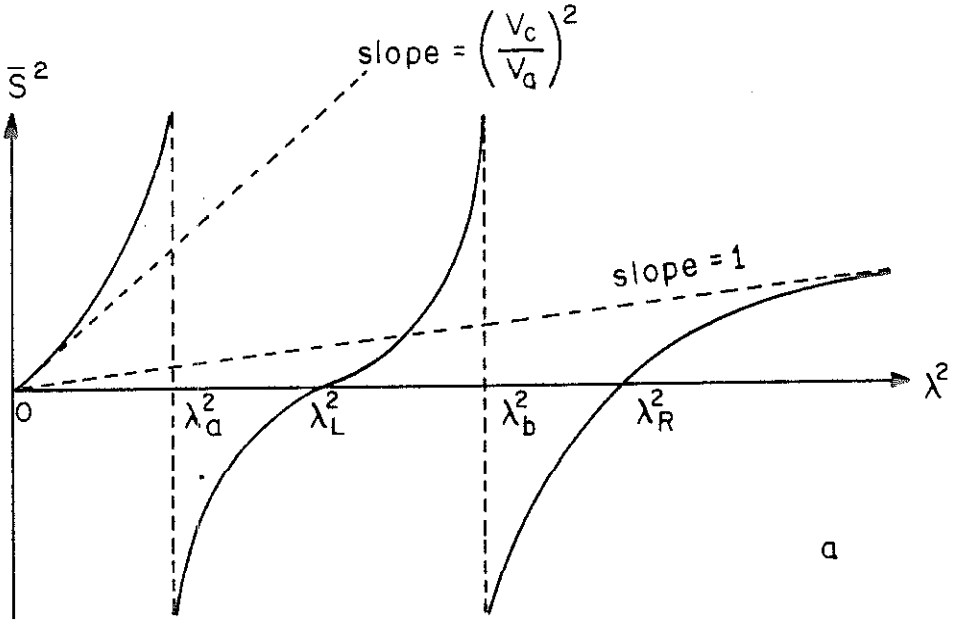

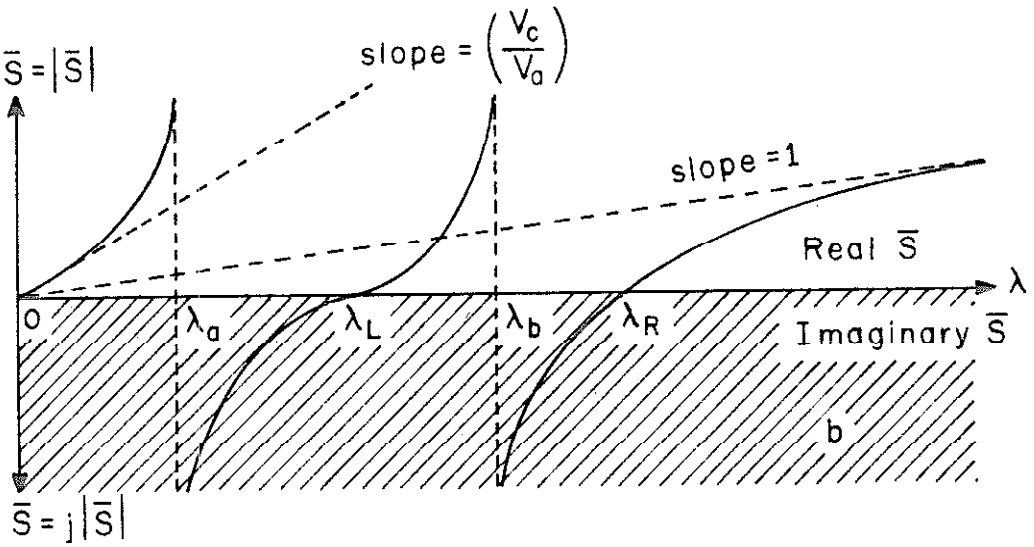

$$\bar{S} = \lambda \sqrt{\frac{(\lambda-\lambda_L)(\lambda+\lambda_L)(\lambda-\lambda_R)(\lambda+\lambda_R)}{(\lambda-\lambda_a)(\lambda+\lambda_a)(\lambda-\lambda_b)(\lambda+\lambda_b)}}$$

Figures III-7a,b. The normalized radial wave number $\bar{S}$ versus the normalized frequency λ .

As $\bar{S} \to 0$, $J_n(\bar{S}) \to \frac{\bar{S}^n}{2^n\, n!}$ and $f_1(\bar{S}) \to 1$; whereas, if $\bar{S} \to \infty$, then

$$J_n(\bar{S}) \to \left(\frac{2}{\pi \bar{S}}\right)^{1/2} \cos\left(\bar{S} - \frac{(2n+1)\pi}{4}\right)$$

and $$f_1(\bar{S}) \to \frac{n}{\bar{S}} \tan\left(\bar{S} - \frac{(2n-1)\pi}{4}\right) \quad .$$

At finite real arguments $f_1(\bar{S})$ continues to resemble the trigonometric tangent function because the zeros of $J_n(\bar{S})$ and the zeros of $J_n'(\bar{S})$ (i.e., the maxima and minima of $J_n(\bar{S})$) are interlaced. The relative amplitudes and phases of $J_n(\bar{S})$ and $J_n'(\bar{S})$ change as $\bar{S}$ is decreased, causing deviations from an actual trigonometric behavior.

$\bar{S}$ can also become purely imaginary, but never complex. In such a region where $\bar{S} = j\,|\bar{S}| = js$, the ordinary Bessel function $J_n(\bar{S})$ is replaced by the modified Bessel function $I_n(s)$ according to the following rules:

$$J_n(js) = j^n\, I_n(s) \qquad \text{also} \qquad J_n'(\bar{S}) = j^{n-1}\, I_n'(s) \quad .$$

Recall that for large arguments, i.e., $s \to \infty$, all orders n of the modified Bessel function approach the same limit, namely:

$$In(s) \to \left(\frac{1}{2\pi s}\right)^{1/2} e^s \qquad \text{hence} \qquad I_n'(s) \to \left(\frac{1}{2\pi s}\right)^{1/2} e^s \quad .$$

Thus the transcendental function $f_1(s)$ for large imaginary arguments becomes

$$f_1(\bar{S}) = \frac{nJ_n(js)}{jsJ_n'(js)} = \frac{nI_n(s)}{sI_n'(s)} \to \frac{n}{s} = \frac{n}{|\bar{S}|} \quad .$$

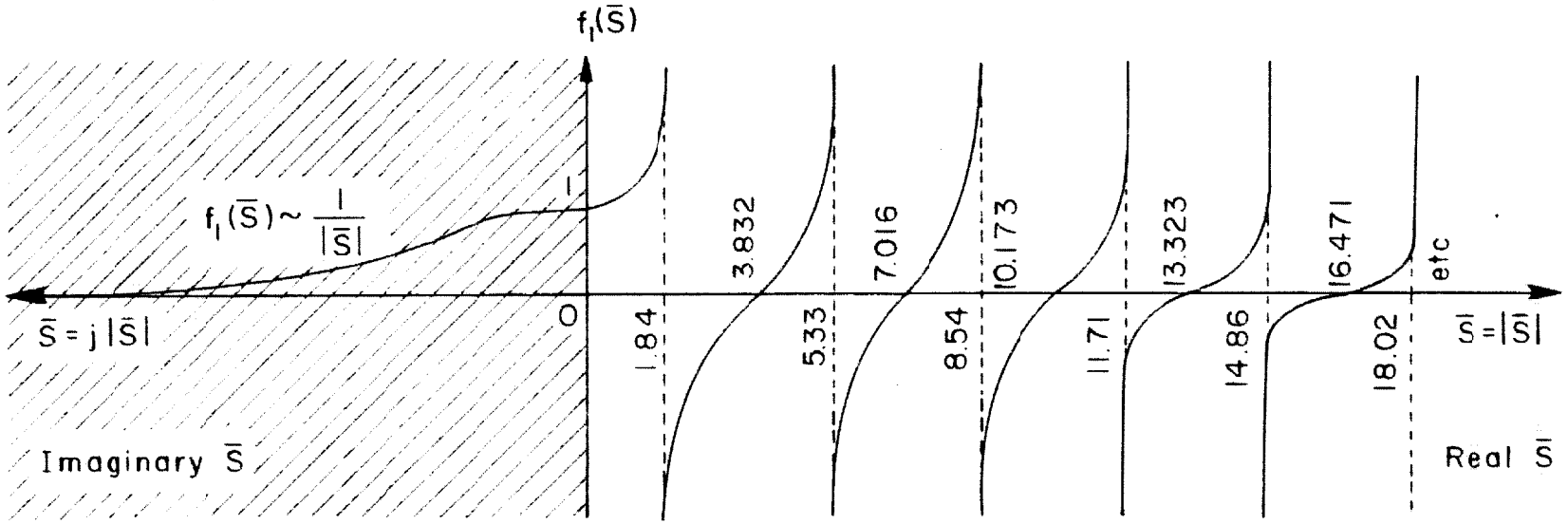

Figure III-8. $r_1(\bar{S}) = \dfrac{n\, J_n(\bar{S})}{\bar{S}\, J_n'(\bar{S})}$ versus $\bar{S}$

For very small arguments the modified Bessel function exhibits the same behavior as does the ordinary Bessel function. It is readily demonstrated that $f_1(\bar{S})$ has zero slope in the vicinity of $\bar{S} = 0$ and that the function monotonically decreases with increasing imaginary values of $\bar{S}$. The function $f_1(\bar{S})$ therefore has the character illustrated in Figure III-8. The indicated singularities are for the case $n = +1$.

The right side of cut-off relation III-53a contains the function

$$f_2(\lambda) \equiv \frac{\epsilon_1}{\epsilon_2} = \frac{-(\lambda^2 - \lambda_a^2)(\lambda^2 - \lambda_b^2)}{\lambda\left[\Lambda_e^2 \lambda_e (1 - \frac{\lambda_i^2}{\lambda_e^2})\right]} \qquad \text{(III-54)}$$

now to be examined. $f_2(\lambda)$ obviously has zeros at λ_a and λ_b, and poles at $\lambda = 0$ and ∞. Several other points are easily located. Thus at λ_L and at λ_e, $f_2(\lambda) = +1$; while λ_i and λ_R are positions where $f_2(\lambda) = -1$. The curve of $f_2(\lambda)$ is traced in Figure III-9.

To construct the graphical solution for the cut-off frequencies, it remains necessary to exhibit $f_1(\bar{S})$ as a function of λ on the same coordinate axes as $f_2(\lambda)$. This is readily accomplished by evaluating $\bar{S}$ at each frequency λ according to Figure III-7b and then determining $f_1(\bar{S})$ from Figure III-8. The resulting function, labeled $f_1(\lambda)$, is then superimposed upon Figure III-9. The equality $f_1(\lambda) = f_2(\lambda)$ defines the cut-off condition for the waveguide structure. Those frequencies for which the two functions are equal, i.e., the points at which their respective curves intersect, denote the

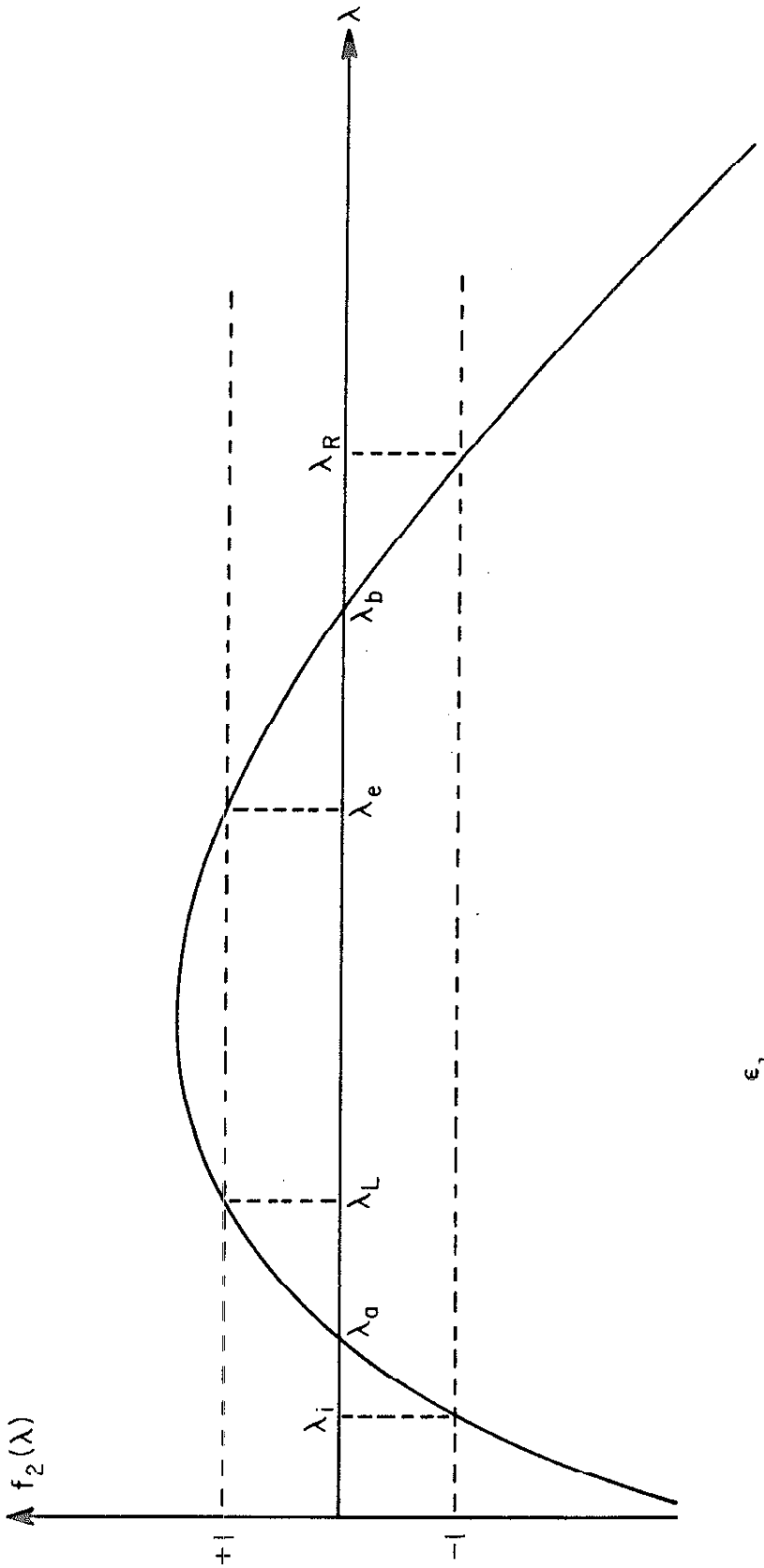

Figure III-9. $f_2(\lambda) = \frac{\epsilon_1}{\epsilon_2}$ versus λ

cut-off frequencies. The graphical solution of the transcendental cut-off relation is illustrated in Figures III-10a,b.

The solutions occur in three distinct bands, each in a range where $\bar{S}$ is real. As λ approaches λ_a, λ_b or infinity, the argument $\bar{S}$ of the Bessel function becomes boundless (Figure III-7b) and the frequency of $f_1(\lambda)$ (Figure III-8) becomes increasingly rapid. The density of solutions also increases (Figure III-10) until at λ_a, λ_b and ∞ the highest modes of each band result. The intersections at λ_L and λ_R, where $\bar{S} = 0$, are the plane wave cut-off frequencies for a magnetized plasma of infinite transverse extent (c.f., Figure IV-4) and are to be discarded as extraneous. The solutions just above λ_L and λ_R are, however, waveguide solutions and indicate the effect of the waveguide wall on the plane waves. The lowest $n = +1$ and $n = -1$ modes of each passband have field configurations that most nearly resemble the left and right circularly polarized plane waves, respectively. Consequently the cut-off frequencies of these modes may be expected to occur closer to $\lambda = 0$ and, respectively, λ_L or λ_R than the cut-off frequencies of any other mode.

When $n = +1$ the lowest mode of the $0, \lambda_a$ band or the λ_R, ∞ band is situated between the root of $J_1'(\bar{S})$ at $\bar{S} = 1.84$ and the zero of $J_1(\bar{S})$ at $\bar{S} = 3.83$. The next series of modal cut-offs occurring in these bands falls between the pole of $f_1(\bar{S})$ at $\bar{S} = 5.33$ and the zero at $\bar{S} = 7.01$. This information is essential if a digital computer program is to converge upon a particular solution. For large positive n, the location of the lowest modal cut-off for the first

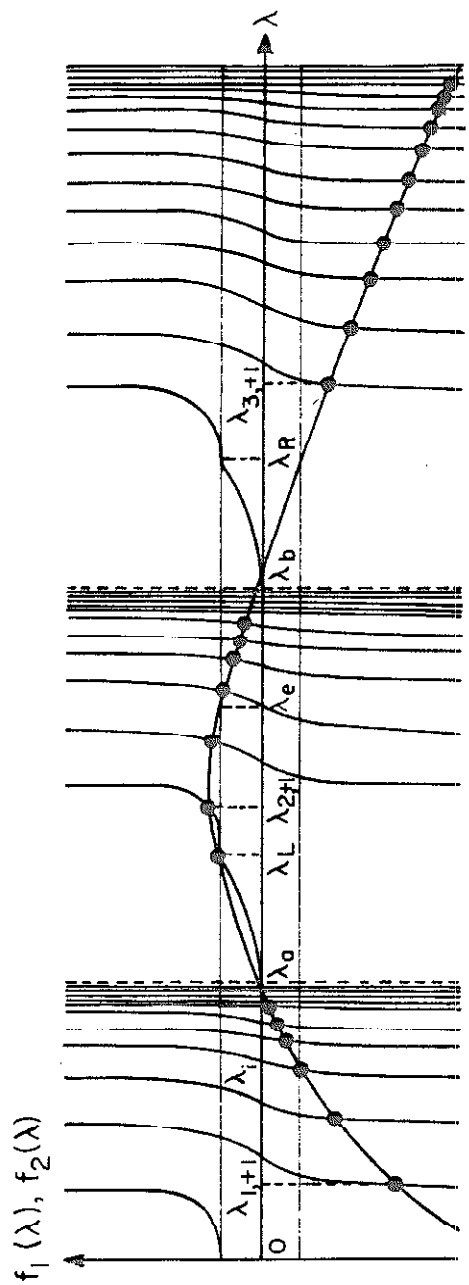

a) Positive angular dependent modes (n = +1)

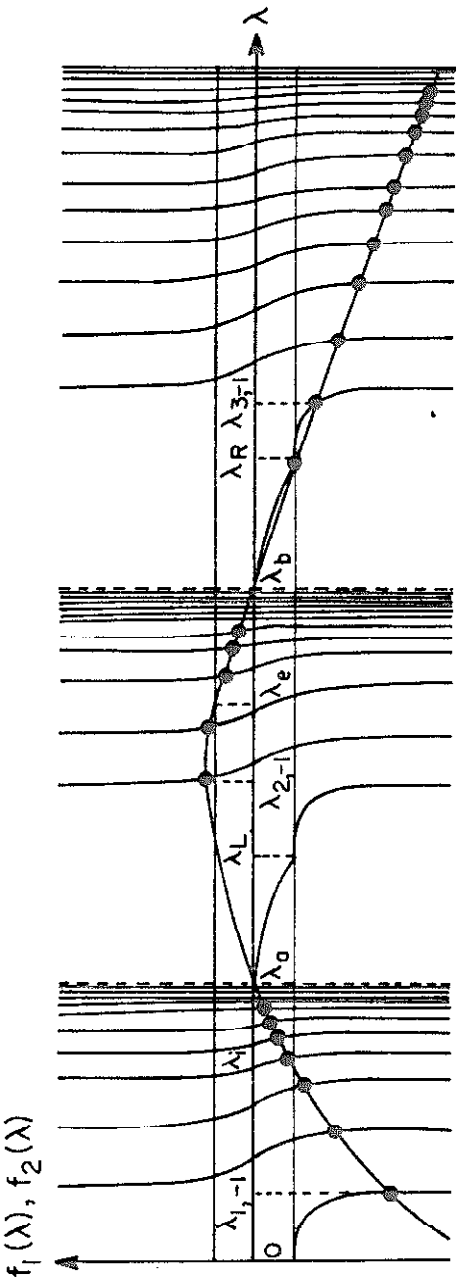

b) Negative angular dependent modes (n = -1)

Figure III-10. Graphical solution of the TE cut-off relation III-53.

and third bands (23) is defined by

$$(n + 0.808\sqrt[3]{n} + \cdots) \leq \bar{S} \leq (n + 1.855\sqrt[3]{n} + \cdots) \quad . \quad \text{(III-55)}$$

The left side of the inequality characterizes the first root of $J_n'(\bar{S})$ and the right side of the inequality specifies the first non-zero root of $J_n(\bar{S})$.

The first mode in the λ_L, λ_b band occurs between the zero of $J_1(\bar{S})$ at $\bar{S} = 0$ and the root of $J_1'(\bar{S})$ at $\bar{S} = 1.84$. The next mode lies between $\bar{S} = 3.83$ and 5.33. For large positive n the lowest mode is always to be found in the range

$$0 < \bar{S} \leq (n + 0.808\sqrt[3]{n} + \cdots) \quad . \quad \text{(III-56)}$$

Evidently as the mode number n is increased the first solution of each band recedes from the plane wave cut-off frequency at $\lambda = 0$, λ_L or λ_R , and advances toward the quasi-static and narrow waveguide cut-off frequencies at λ_a , λ_b or ∞ .

For a negative angular dependence $(n < 0)$, $f_1(\bar{S}) = \dfrac{nJ_n(\bar{S})}{\bar{S}\, J_n'(\bar{S})}$ must be replaced by $- f_1(\bar{S})$ because for integral n

$$J_{-n}(\bar{S}) = (-1)^n J_n(\bar{S}) \quad \text{and} \quad J'_{-n}(\bar{S}) = (-1)^n J_n'(\bar{S}) \quad ;$$

likewise,

$$I_{-n}(s) = I_n(s) \qquad \text{and} \qquad I'_{-n}(s) = I_n'(s) \quad .$$

This inverts the transcendental curve as in Figure III-10b. The intersections of the inverted curve with $f_2(\lambda) = \epsilon_1/\epsilon_2$ are the $n = -1$

cut-off frequencies. The lowest mode of the $0,\lambda_a$ or λ_R,∞ band is positioned between $\bar{S} = 0$ and the first root of $J_1'(\bar{S})$ at $\bar{S} = 1.84$. The primary mode of the λ_b,λ_L band occurs in the range $1.84 \leq \bar{S} \leq 3.83$. For large negative n the corresponding values of $\bar{S}$ fall in the range

$$0 < \bar{S} \leq (|n| + 0.808\ \sqrt[3]{|n|} + \cdots) \qquad \text{(III-57)}$$

for the first and third bands, and between

$$(|n| + 0.808\ \sqrt[3]{|n|} + \cdots) \leq \bar{S} \leq (|n| + 1.855\ \sqrt[3]{|n|} + \cdots) \qquad \text{(III-58)}$$

for the central band. As with the positive angular-dependent modes, an increase in the mode number n is characterized by an attendant departure of the waveguide cut-off frequencies from those of the plane wave.

The cut-off frequencies of each band correspond to different modes, all of the same character, but shifted in their respective frequencies. Special attention should be devoted to the solutions closest to $\lambda = 0$, λ_L and λ_R as these cut-off frequencies display the greatest latitude of variation. The solutions toward the upper end of each band are increasingly cramped and therefore exhibit less drastic variations.

It is of interest to investigate the relative positions of $\lambda_{1,n}$ and λ_i . Since $\lambda = 0$ is known to be a cut-off frequency, the occurrence of $\lambda_{1,n}$ below the wave resonance at λ_i would imply that the dispersion is double valued. Double-valued dispersion is

reminiscent of plane waves propagating along $\underline{B}_o$ (cf., Figure IV-4), but not of quasi-static fields which in all instances have a single-valued dispersion relation (cf., Appendix). Let us examine the $n = +1$ case first. A glance at Figure III-11a convinces us that $\lambda_{1,+1}$ may lie above or below λ_i subject to the relative values of the plasma density and the magnetostatic field strength. However, Figure III-11b illustrates that λ_i always exceeds $\lambda_{1,-1}$. Hence dispersion in the lowest frequency range may be double or single valued, depending upon the mode number and the plasma condition. The variation of $\lambda_{1,-1}$ and $\lambda_{1,+1}$ with plasma density, for fixed values of the magnetic field, appears in Figures III-12 and III-13. Cut-off frequency $\lambda_{1,-1}$ always remains less than λ_i and tends toward the plane wave cut-off at $\lambda = 0$, while $\lambda_{1,+1}$ assumes a character which typifies the higher positive and negative angular dependent modes. Note the resemblance of Figure III-13 for $\lambda_{1,+1}$ to Figure III-1 for the circularly symmetric cut-off frequency $\lambda_{1,0}$.

Consider next the cut-off frequencies near λ_L. According to Figure III-10, $\lambda_{2,+1}$ is always smaller than $\lambda_{2,-1}$. Thus, while $\lambda_{2,-1}$ has its minimum value at $\bar{S} = 1.84$, $\lambda_{2,+1}$ is free to descend from $\bar{S} = 1.84$ to λ_L where $\bar{S} = 0$. At $\bar{S} = 0$ the waveguide mode has the same cut-off frequency as the left circular plane wave. However, according to equations III-21, III-22 and III-25, all components of the cut-off TE field disappear.

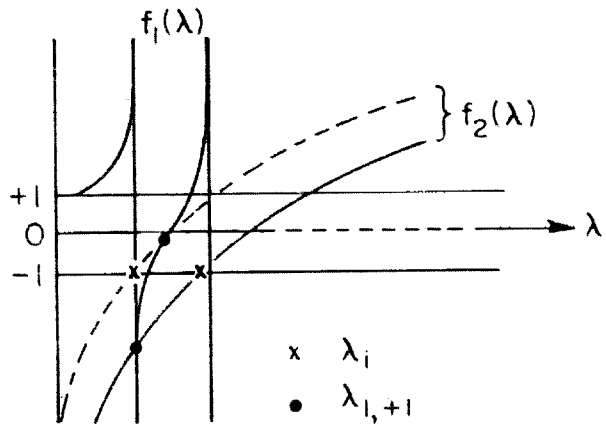

a) $n > 0$

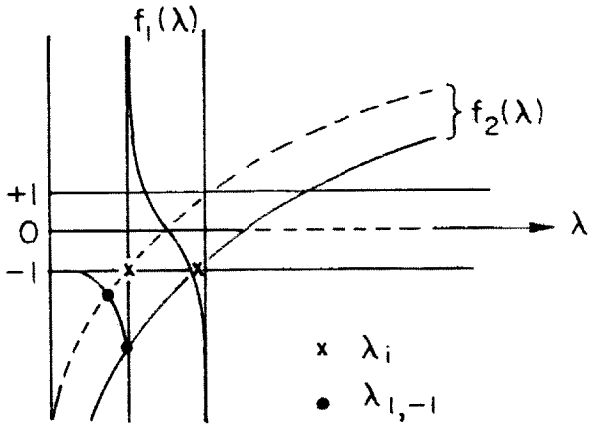

b) $n < 0$

Figure III-11. Graphical solution of $\lambda_{l,\pm 1}$ for two positions of $f_2(\lambda)$

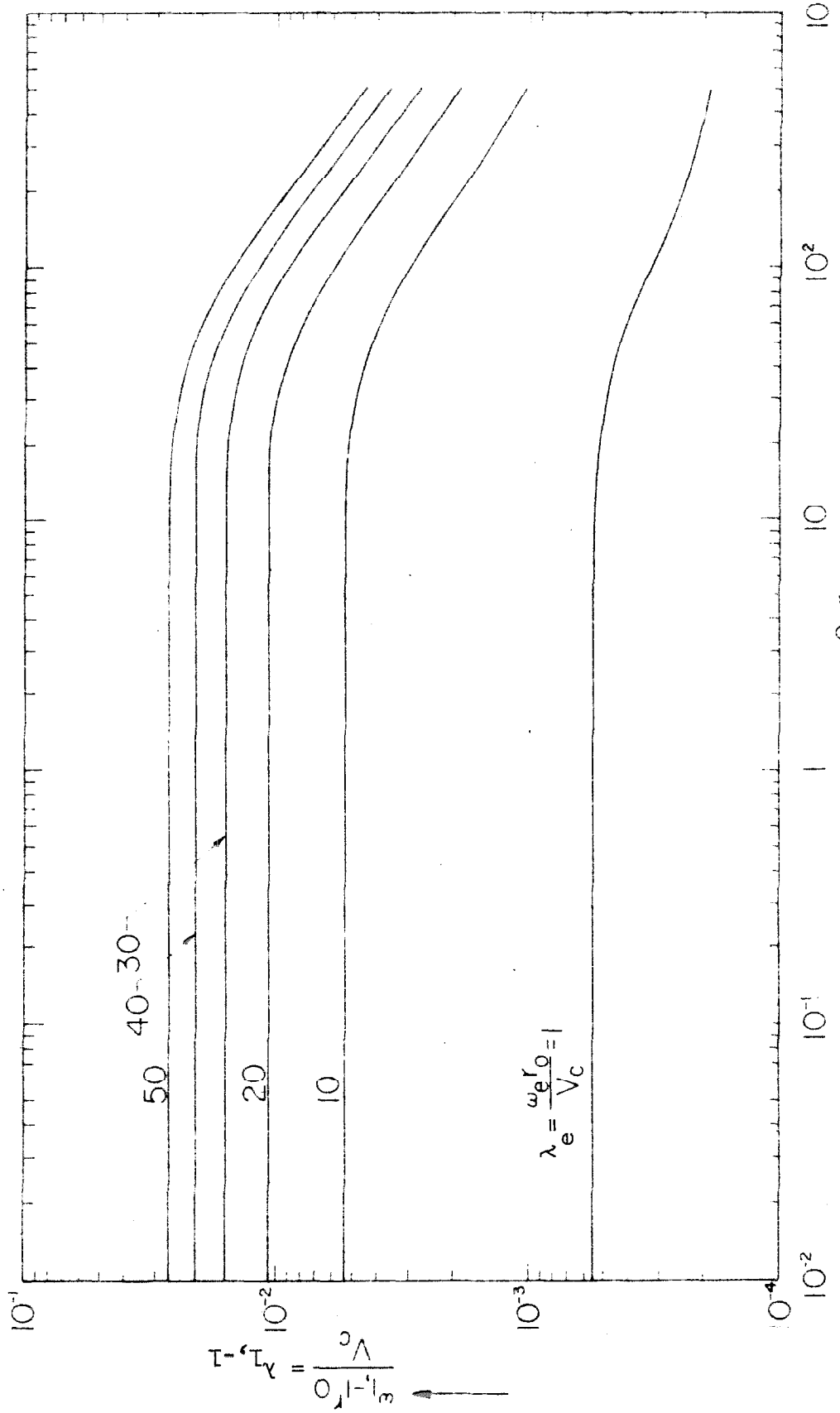

Figure III-12. The first TE cut-off frequency for the lowest radial order, n = -1 mode as a function of the plasma density, for successive values of the magnetostatic field

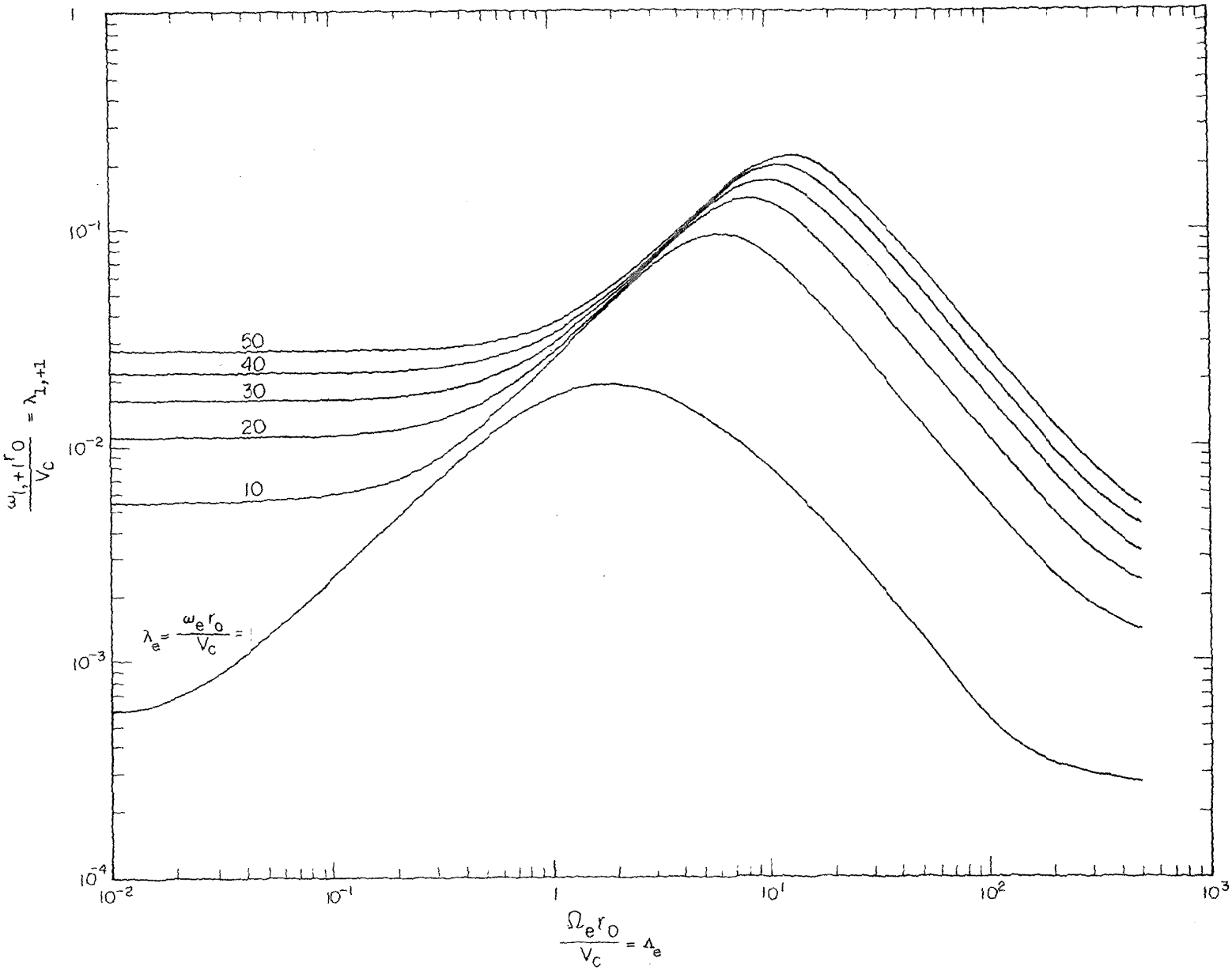

Figure III-14. The first TE cut-off frequency for the lowest radial order, n = +1 mode as a function of the plasma density, for successive values of the magnetostatic field.

To follow the variation of $\lambda_{2,+1}$ note that $f_2(\lambda) = \epsilon_1/\epsilon_2$ is equal to unity at λ_L and λ_e with a maximum between. If $\lambda_e > \lambda_L$, the root $\lambda_{2,+1}$ appears within the interval $0 > \bar{S} \leq 1.84$ as in Figure III-14a. As λ_L and λ_e approach one another, the maximum of $f_2(\lambda)$ decreases and the root $\lambda_{2,+1}$ moves closer to λ_L. When the slopes of $f_1(\lambda)$ and $f_2(\lambda)$ at λ_L are equal, $\lambda_{2,+1}$ and λ_L will have coalesced. The condition for $\lambda_{2,+1}$ to equal λ_L is therefore

$$\left.\frac{\partial f_2(\lambda)}{\partial \lambda}\right|_{\lambda_L} = \left[\frac{\partial f_1(\bar{S})}{\partial \bar{S}} \quad \frac{\partial \bar{S}}{\partial \lambda}\right]_{\lambda_L} \quad \text{or equivalently, } \lambda_L = \lambda_e \, .$$

Since $\left.\frac{\partial f_1(\bar{S})}{\partial \bar{S}}\right|_{\lambda_L} = 0$, the condition for $\lambda_{2,+1} = \lambda_L$ reduces to

$$\left.\frac{\partial f_2(\lambda)}{\partial \lambda}\right|_{\lambda_L} = 0 \quad \text{or equivalently} \quad \lambda_L = \lambda_e \, . \tag{III-59}$$

When terms of the order λ_i/λ_e or smaller are neglected relative to unity, either of expressions III-59 give $\Lambda_e = \sqrt{2}\ \lambda_e$. Thus for $\Lambda_e < \sqrt{2}\ \lambda_e$, $\bar{S} > 0$ and $\lambda_{2,+1}$ is larger than λ_L; for $\Lambda_e = \sqrt{2}\lambda_e$, $S = 0$ and the fields of this mode vanish.

The numerical solutions to the cut-off relations III-53 for $\lambda_{2,\pm 1}$ are plotted in Figures III-15 and III-16. The family of curves depicting $\lambda_{2,+1}$ are asymptotic to the plane wave limit λ_L, while the curves for $\lambda_{2,-1}$ resemble the circularly symmetric cut-off frequency $\lambda_{2,0}$ of Figure III-2. The behavior of $\lambda_{2,-1}$ is

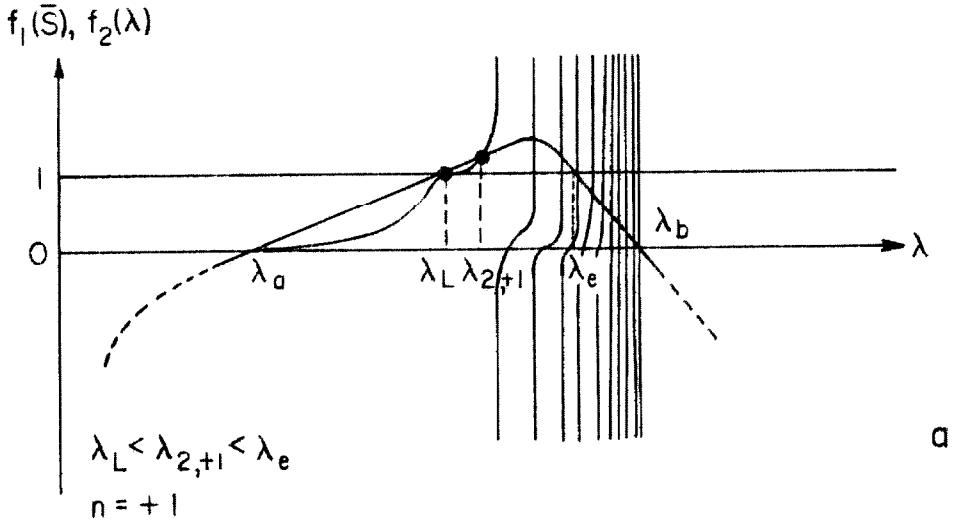

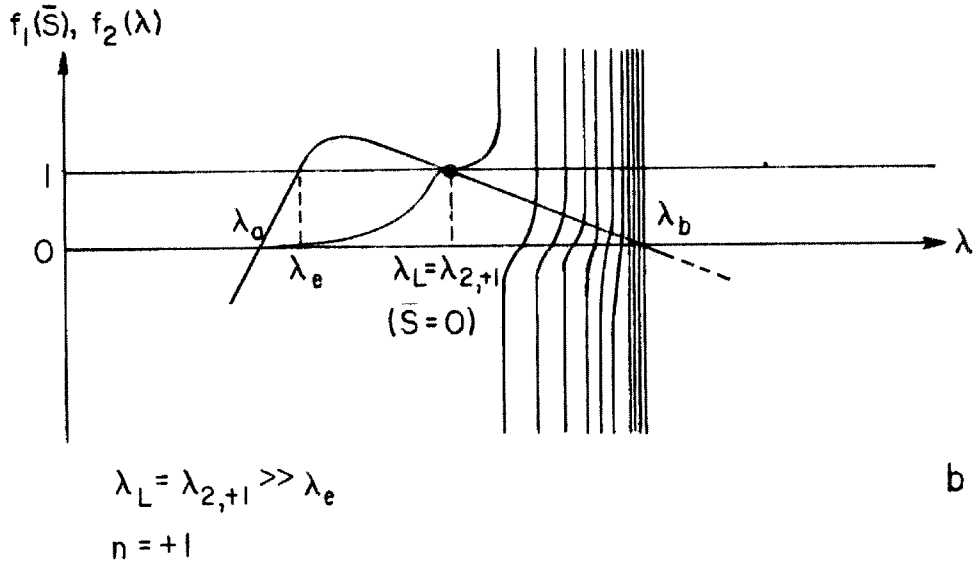

Figure III-14a,b. Graphical solution of $\lambda_{2,+1}$

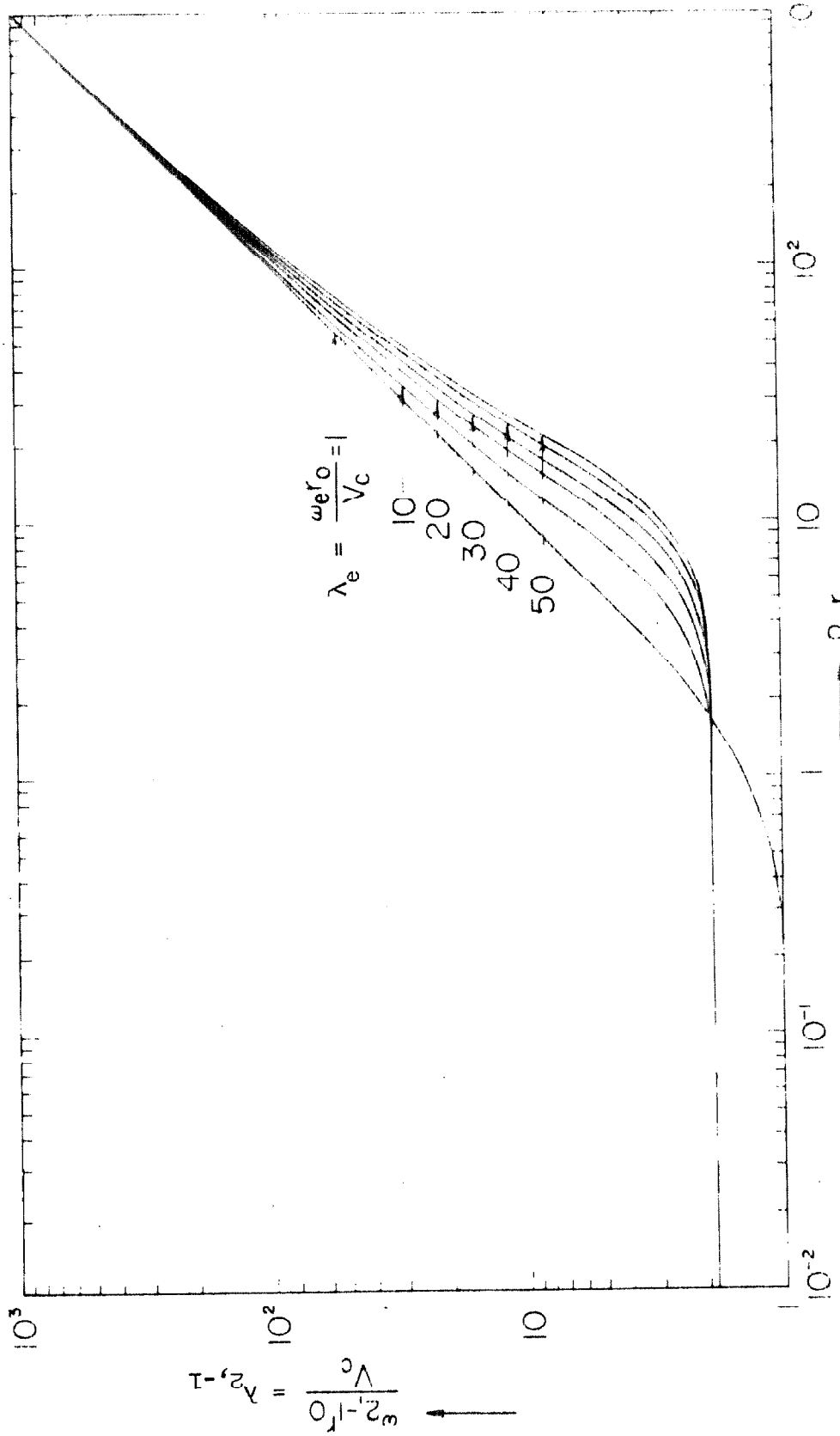

Figure III-15. The second TE cut-off frequency for the lowest radial order, n = -1 mode as a function of the plasma density, for successive values of the magnetostatic field.

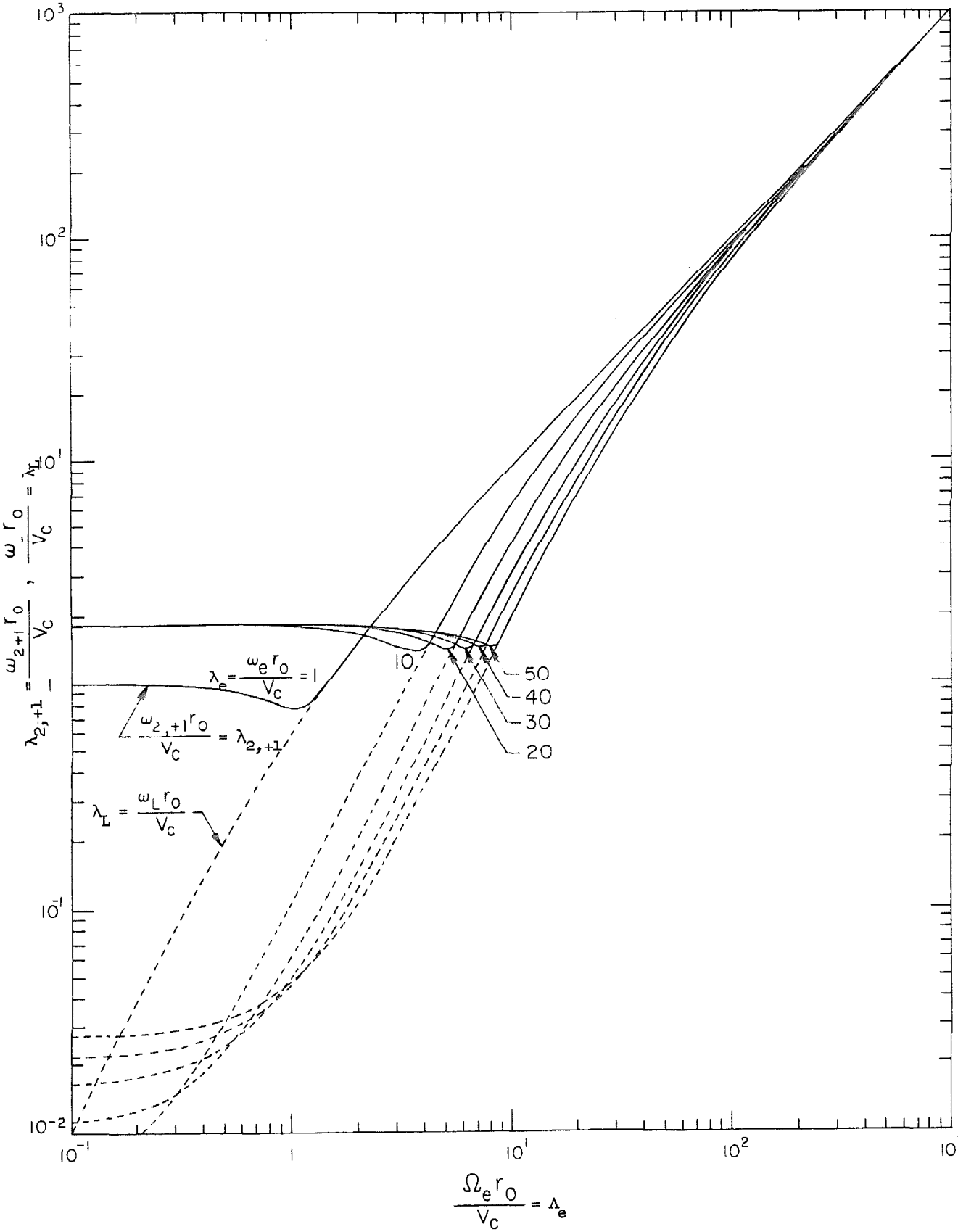

Figure III-16. The second TE cut-off frequency for the lowest radial order, n = +1 mode as a function of the plasma density, for successive values of the magnetostatic field

representative of all higher modal cut-off frequencies for positive or negative n in the λ_L, λ_b band.

The situation at λ_R for $n = -1$ is much simpler; cf. Figure III-10b. The slope of $f_1(\lambda)$ at λ_R, where $\bar{S} = 0$, is zero, but becomes negative at larger $\bar{S}$. The slope of $f_2(\lambda)$ is negative everywhere in this band and consequently $f_1(\lambda)$ and $f_2(\lambda)$ intersect a second time before the pole of $f_1(\lambda)$ at $\bar{S} = 1.84$ is reached. This root, designated $\lambda_{3,-1}$ in Figure III-10b, always exceeds λ_R. The loci of $\lambda_{3,-1}$ and $\lambda_{3,+1}$ are illustrated in Figures III-17 and III-18. They deviate only slightly from one another and from the circularly symmetric cut-off $\lambda_{3,0}$ of Figure III-3. Furthermore, since equation III-53b is insensitive to $\bar{S}$ at large λ, both curves are asymptotic to the plane wave cut-off λ_R.

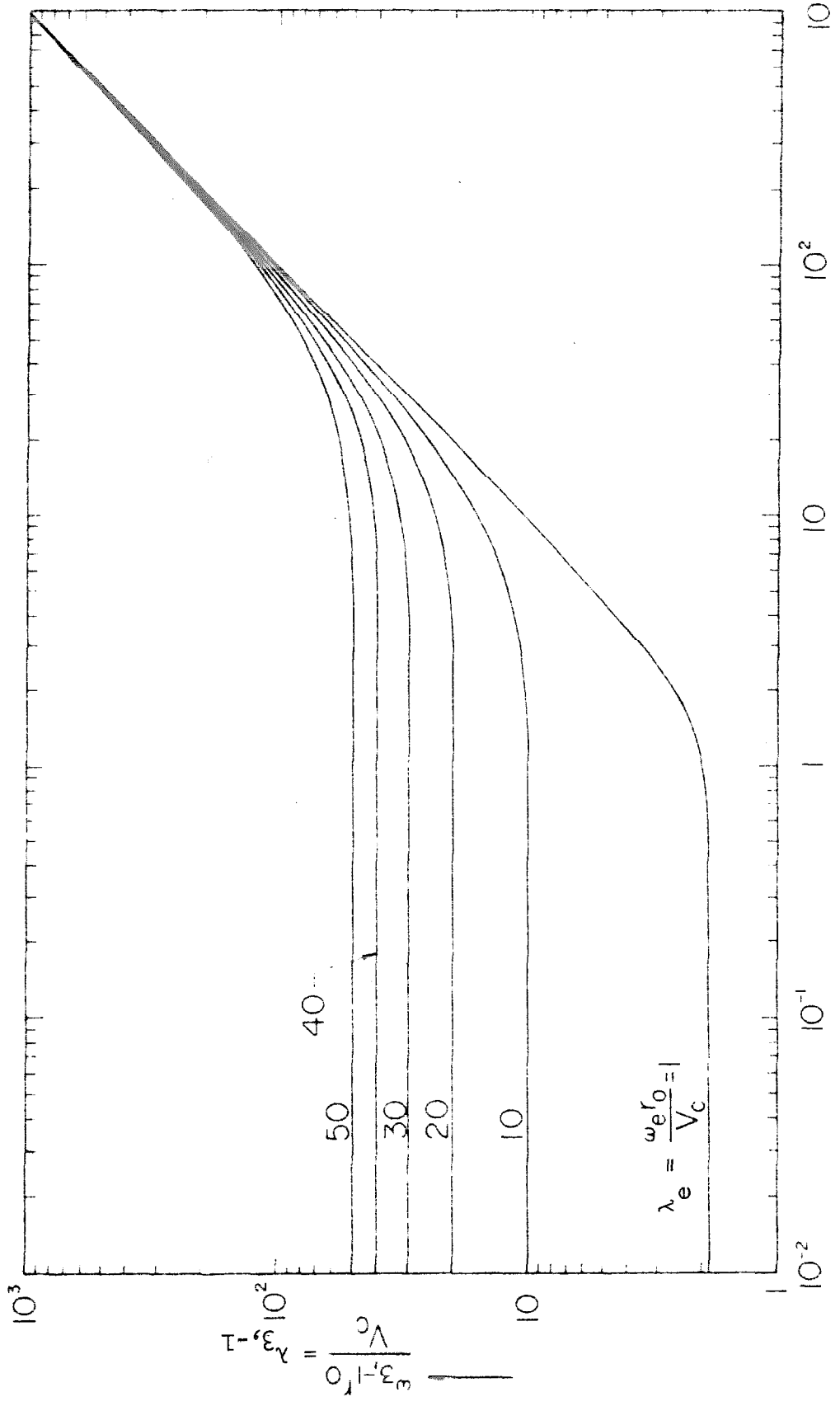

Figure III-17. The third TE cut-off frequency for the lowest radial order, n = -1 mode as a function of the plasma density, for successive values of the magnetostatic field.

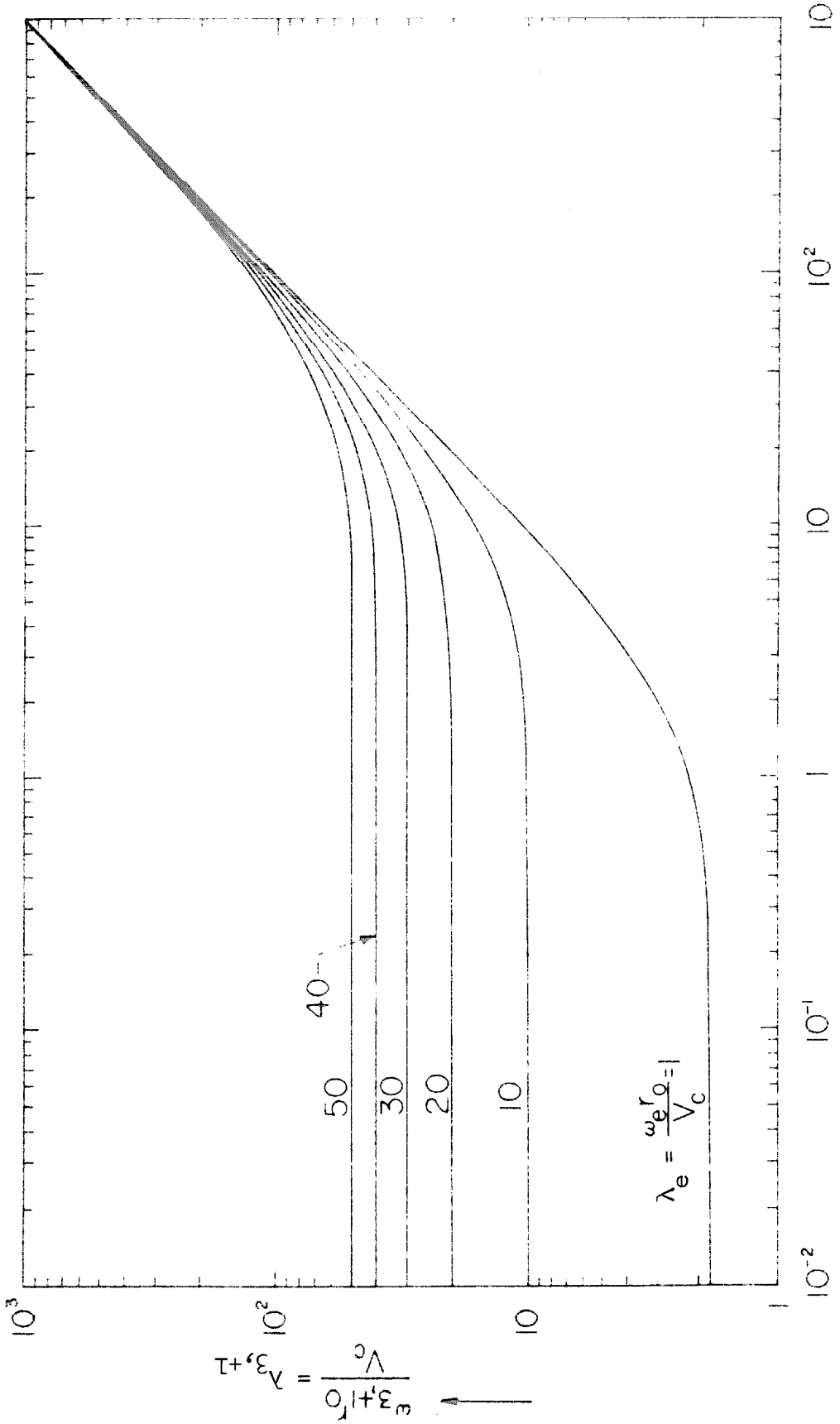

Figure III-18. The third TE cut-off frequency for the lowest radial order, n = +1 mode as a function of the plasma density, for successive values of the magnetostatic field.

CHAPTER IV. LIMITING FORMS OF WAVE PROPAGATION IN THE CIRCULAR PLASMAGUIDE

The modes that propagate in the anisotropic waveguide are usually of a mixed variety, being neither TE nor TM. As demonstrated in the previous chapter, the longitudinal fields E_z and H_z decouple in the vicinity of resonance and cut off, and thereby submit to conventional waveguide descriptions. Before pursuing the complications of coupled wave phenomena, it is well to inquire whether other limits exist for which simple propagation can occur.

The coefficient c of equation II-4, which is responsible for coupling E_z and H_z through equations II-10 and II-11, vanishes whenever the Hall permittivity ϵ_2 can be made zero. Thus for zero or infinite magnetostatic fields the waveguide supports simple TE and TM waves. The same occurs for arbitrary magnetostatic intensities at the lowest frequencies of the MHD limit, or else when microwave frequencies are involved. The physical width of the waveguide is another factor that governs wave coupling. The very slender waveguide supports, in addition to TE fields, a TM wave which is related to the quasi-static approximation. In the opposite extreme the mixed waveguide fields develop, with increasing guide radius, into circularly polarized plane waves.

Each of these situations is subsequently investigated with regard to wave character, configuration and dispersion. Wherever possible, the mathematics is supplemented with physical insight.

Limiting Magnetostatic Fields

No magnetic bias ($\underline{B}_o = 0$). The gyroelectric properties of the plasma result from the transfer of charge across the magnetic flux. If the transverse particle motion or the magnetostatic field is eliminated, the conductivity and permittivity tensors are replaced by diagonal matrices. The electrostatic plasma oscillations are an example of a degenerate wave for which the particles vibrate parallel to $\underline{B}_o$. An infinite magnetostatic field (next section) is also capable of restraining the transverse motion. The Hall effect also vanishes ($\sigma_2 = \epsilon_2 = 0$) if the magnetostatic field is removed entirely. For $\underline{B}_o = 0$ equations I-11, I-12, I-17 and I-18 show that the plasma is isotropic with

$$\underline{\underline{\sigma}} \to \frac{1}{j\omega}\left(\frac{n_e q_e^2}{m_e} + \frac{n_i q_i^2}{m_i}\right) = \sigma_3 \qquad \text{(IV-1)}$$

$$\underline{\underline{\epsilon}} \to \epsilon_o\left(1 - \frac{\Omega_p^2}{\omega^2}\right) = \epsilon_3 \quad . \qquad \text{(IV-2)}$$

The conductivity of the plasma is a reactive scalar because the current is impeded only by the inertia of the charge.

In this same limit ($\underline{B}_o = 0$) the auxiliary parameters of equations II-3 and II-4 approach

$$\gamma_1 = -(h^2 + \omega^2\mu_o\epsilon_3) \quad ; \quad \gamma_2 = 0 \quad \text{and} \qquad \text{(IV-3)}$$

$$b = c = f = 0 \quad ; \quad a = \frac{+jh}{h^2 + \omega^2\mu_o\epsilon_3} \quad ; \quad d = \frac{\omega\mu_o}{h^2 + \omega^2\mu_o\epsilon_3} \quad ;$$

$$g = \frac{-\omega\epsilon_3}{h^2 + \omega^2\mu_o\epsilon_3} \quad . \qquad \text{(IV-4)}$$

By defining

$$S^2 - T^2 = (h^2 + \omega^2 \mu_o \epsilon_3) \tag{IV-5}$$

equations II-10 and II-11 become

$$\frac{j\omega \mu_o}{h^2 + \omega^2 \mu_o \epsilon_3} (\nabla_t^2 H_z + S^2 H_z) = 0 \tag{IV-6}$$

$$\frac{-j\omega \epsilon_3}{h^2 + \omega^2 \mu_o \epsilon_3} (\nabla_t^2 E_z + T^2 E_z) = 0 \quad . \tag{IV-7}$$

A consequence of removing the magnetic bias has been to diagonalize the dielectric tensor and to decouple the wave equations. As within a conventional waveguide, E_z and H_z satisfy independent equations and any given field may be resolved into a superposition of dissociated TE and TM partial waves.

For $\omega \neq 0$, equation IV-6 has a solution

$$H_z = H_o J_n(Sr) e^{-jn\theta} \tag{IV-8}$$

and for $\epsilon_3 \neq 0$, a solution of equation IV-7 is

$$E_z = E_o J_n(Tr)\, e^{-jn\theta} \quad . \tag{IV-9}$$

As shown in equation III-41, the factor $\omega = 0$ is a remnant of the cyclotron wave which, when the magnetostatic field was present, had a cut off at $\omega_{1,n}$ and a resonance at ω_e . Likewise the factor $\epsilon_3 = 0$, once the resonance of an electromagnetic wave, has in the absence of $\underline{B}_o$ degenerated into an electrostatic oscillation at the plasma frequency; (refer to dispersion diagram IV-1).

In view of relation IV-4, equations II-8 and II-9 for the transverse fields become

$$\underline{E}_t = \frac{1}{h^2 + \omega^2 \mu_o \epsilon_3} \left[-h \nabla_t E_z + j\omega \mu_o \underline{e}_z \times \nabla_t H_z \right] \qquad \text{(IV-10)}$$

$$\underline{H}_t = \frac{1}{h^2 + \omega^2 \mu_o \epsilon_3} \left[-h \nabla_t H_z - j\omega \epsilon_3 \underline{e}_z \times \nabla_t E_z \right] . \qquad \text{(IV-11)}$$

For the TE modes, which already have $E_z = 0$, the boundary conditions at the conducting cylinder r_o require

$$E_\theta \Big|_{r_o} = \frac{j\omega \mu_o}{-h} H_r \Big|_{r_o} = \frac{j\omega \mu_o}{h^2 + \omega^2 \mu_o \epsilon_3} \left. \frac{\partial H_z}{\partial r} \right|_{r_o} = 0 .$$

Therefore according to IV-5 and IV-8, $S = \sqrt{h^2 + \omega^2 \mu_o \epsilon_3}$ is a root of $J_n'(Sr_o) = 0$. Replacing ϵ_3 by expression IV-2 reduces this dispersion relation to

$$h = \pm j \frac{1}{V_c} \sqrt{\omega^2 - \omega_{3,n}^2} \quad \text{with} \quad \omega_{3,n} = \sqrt{\Omega_p^2 + (SV_c)^2}$$

$$\text{and} \quad J_n'(Sr_o) = 0 . \qquad \text{(IV-12)}$$

It is evident from equation III-41 that $\omega_{3,n}$ is the limiting behavior of the cut-off frequency discussed in Chapter III. Since $h = \alpha + j\beta$, the propagating wave has a phase velocity

$$\frac{\omega}{\beta} = \frac{V_c}{\sqrt{1 - \left(\frac{\omega_{3,n}}{\omega}\right)^2}} . \qquad \text{(IV-13)}$$

For transmission the operating frequency ω must exceed the cut-off frequency, $\omega_{3,n}$, hence the phase velocity of each TE mode always exceeds the velocity of light $V_c = \frac{1}{\sqrt{\mu_o \epsilon_o}}$.

Consider next the TM wave solutions, subject to the boundary conditions

$$E_z\Big|_{r_o} = E_\theta\Big|_{r_o} = H_r\Big|_{r_o} = 0 \quad .$$

Because $H_z = 0$ and the fields have an assumed $e^{-jn\theta}$ angular dependence, E_z, E_θ and H_r are proportional to one another, and it suffices to require $J_n(Tr_o) = 0$. Since $T = \sqrt{h^2 + \omega^2 \mu_o \epsilon_3}$ the TM dispersion relation resembles equation IV-12 for the TE modes; whence

$$h = \pm j \frac{1}{V_c} \sqrt{\omega^2 - \omega_{4,n}^2} \quad \text{with} \quad \omega_{4,n} = \sqrt{\Omega_p^2 + (TV_c)^2}$$

$$\text{and} \quad J_n(Tr_o) = 0 \quad . \qquad \text{(IV-14)}$$

The phase velocity of the TM waves

$$\frac{\omega}{\beta} = \frac{V_c}{\sqrt{1 - \left(\frac{\omega_{4,n}}{\omega}\right)^2}} \qquad \text{(IV-15)}$$

also exceeds the speed of light in vacuum.

The dispersive behavior of these waves is conveniently summarized in the ω-β diagram of Figure IV-1. In addition to illustrating equations IV-12 and IV-14, this diagram displays the normalized phase velocity $\frac{1}{V_c} \frac{\omega}{\beta}$ and the normalized group velocity $\frac{1}{V_c} \frac{d\omega}{d\beta}$ of each

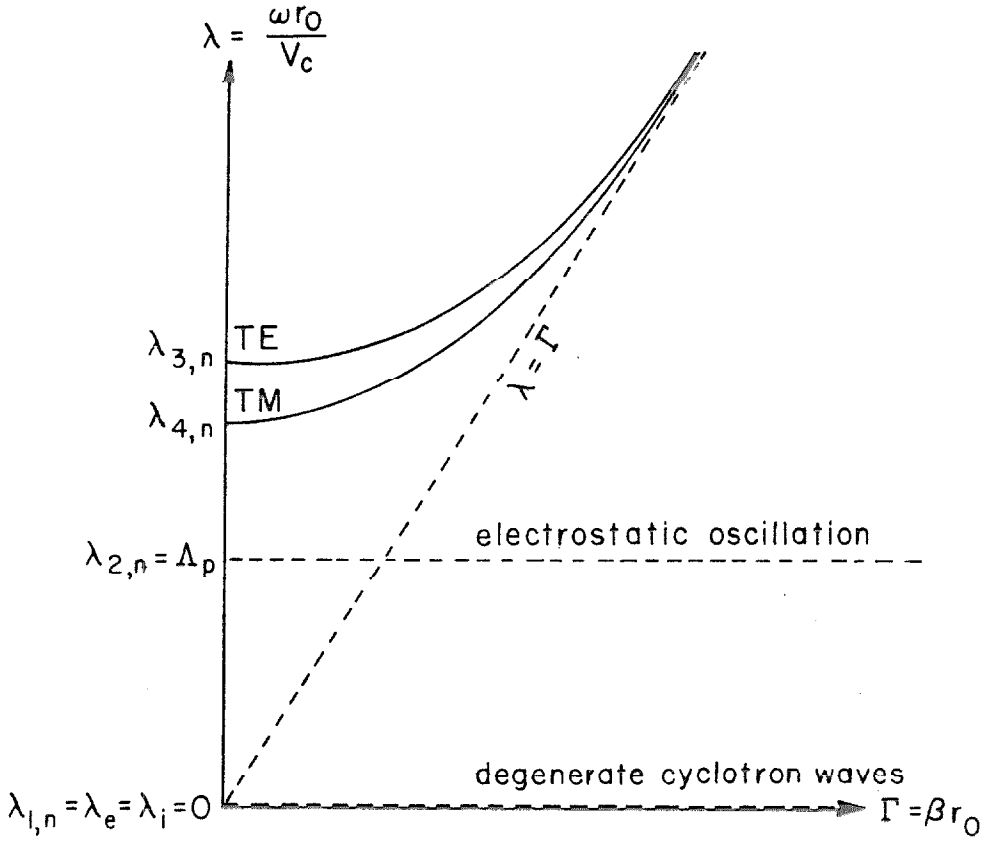

Figure IV-1. Dispersion equations IV-12 and IV-14 for the isotropic plasma-filled waveguide

wave. The normalized phase velocity equals the slope of the line drawn from the origin to the point of interest on the curve; the normalized group velocity is the actual slope of the curve at that point.

The isotropic plasma decreases the effective permittivity of the waveguide, and consequently raises the cut-off frequency and phase velocity of every mode. However, because the product of the phase and group velocities is a constant, viz., $\frac{\omega}{\beta}\frac{d\omega}{d\beta} = V_c^2$, the group velocity is reduced. Aside from an inconsequential resonance at Ω_p, the dispersion is essentially the same as in an empty waveguide. As a result no slow waves propagate in either the plasma-filled or the empty waveguide structures.

Infinite magnetic bias $(\underline{B}_o \to \infty)$. As the axial magnetostatic field is made infinite, the transverse motion of the particles becomes increasingly constrained and all the elements of the conductivity tensor except σ_3 vanish. As a result $\underline{\underline{\epsilon}} = \epsilon_o(\underline{\underline{1}} + \frac{\underline{\underline{\sigma}}}{j\omega\epsilon_o})$ becomes diagonal, although the plasma remains highly anisotropic because $\epsilon_1 \neq \epsilon_3$. Nevertheless, the longitudinal fields are no longer coupled by ϵ_2 .

For an infinite magnetostatic intensity

$$\epsilon_1 \to \epsilon_o \quad , \quad \epsilon_2 \to \epsilon_o\left[\frac{1}{\omega}\left(\frac{\Omega_e^2}{\omega_e} - \frac{\Omega_i^2}{\omega_i}\right)\right] = 0 \quad \text{and} \quad \epsilon_3 = \epsilon_o\left(1 - \frac{\Omega_p^2}{\omega^2}\right) . \tag{IV-16}$$

In an electrically neutral plasma $\Omega_e^2/\omega_e = \Omega_i^2/\omega_i$, so that the rate at which ϵ_2 vanishes is determined by the neutrality of the plasma and the magnitude of $\underline{B}_o$. ϵ_1 reduces to ϵ_o inversely as the square of

B_o , while ϵ_3 is unaffected by the magnetization.

The auxiliary parameters of equations II-3 and II-4 are relatively simple for $\underline{B}_o \to \infty$:

$$\gamma_1 = -(h^2 + \omega^2 \mu_o \epsilon_o) \quad , \qquad \gamma_2 = 0 \tag{IV-17}$$

while $b = c = f = 0$, and

$$a = \frac{\pm jh}{h^2 + \omega^2 \mu_o \epsilon_o} \quad , \qquad d = \frac{\omega \mu_o}{h^2 + \omega^2 \mu_o \epsilon_o} \quad , \qquad g = \frac{-\omega \epsilon_o}{h^2 + \omega^2 \mu_o \epsilon_o} \quad , \tag{IV-18}$$

With these limiting values equations II-10 and II-11 reduce to the Helmholtz equations

$$\nabla_t^2 H_z + S^2 H_z = 0 \qquad S^2 = (h^2 + \omega^2 \mu_o \epsilon_o) \tag{IV-19a,b}$$

$$\nabla_t^2 E_z + T^2 E_z = 0 \qquad T^2 = (h^2 + \omega^2 \mu_o \epsilon_o)\left(1 - \frac{\Omega_p^2}{\omega^2}\right) . \tag{IV-20a,b}$$

The transverse field expressions II-8 and II-9 are now

$$\underline{E}_t = \frac{1}{h^2 + \omega^2 \mu_o \epsilon_o} \left[-h \nabla_t E_z + j\omega \mu_o \underline{e}_z \times \nabla_t H_z \right] \tag{IV-21}$$

$$\underline{H}_t = \frac{1}{h^2 + \omega^2 \mu_o \epsilon_o} \left[-h \nabla_t H_z - j\omega \epsilon_o \underline{e}_z \times \nabla_t E_z \right] . \tag{IV-22}$$

Differential equation IV-19a for the TE modes has a solution

$$H_z = H_o J_n(Sr) e^{-jn\theta} \quad , \qquad E_z = 0 \quad . \tag{IV-23}$$

Accordingly, the transverse fields are

$$\underline{E}_t = \frac{j\omega\mu_o}{h^2 + \omega^2\mu_o\epsilon_o} H_o \frac{1}{r}\left[jn\, J_n(Sr)\, \underline{e}_r + (Sr)J_n'(Sr)\underline{e}_\theta \right] e^{-jn\theta} \quad \text{(IV-24)}$$

$$\underline{H}_t = \frac{-h}{h^2 + \omega^2\mu_o\epsilon_o} H_o \frac{1}{r}\left[(Sr)J_n'(Sr)\underline{e}_r - jn\, J_n(Sr)\underline{e}_\theta \right] e^{-jn\theta} \quad \text{(IV-25)}$$

If the angular component of the electric field and the radial component of the magnetic field are to have nulls everywhere on the conducting cylinder $r = r_o$, then $J_n'(Sr_o) = 0$. This, and definition IV-19b for S^2, describe TE wave dispersion as

$$h = \pm j \frac{1}{V_c}\sqrt{\omega^2 - \omega_{1,n}^2} \quad . \quad \text{(IV-26)}$$

The wave is cut off at $\omega_{1,n} = SV_c$ and propagates with a phase velocity

$$\frac{\omega}{\beta} = \frac{V_c}{\sqrt{1 - \left(\frac{\omega_{1,n}}{\omega}\right)^2}} \quad \text{(IV-27)}$$

exceeding the speed of light in vacuum, V_c.

The physical effect of the infinite magnetostatic bias is to constrain the particles to longitudinal paths. However, without a longitudinal electric field component to accelerate the charge, the TE mode is unable to interact with the plasma. Consequently, the plasma affects neither the fields nor the dispersion of the TE waves.

The TM solutions to equation IV-20a are even more interesting. The longitudinal fields for the TM wave are

$$E_z = E_o J_n(Tr)e^{-jn\theta} \quad , \qquad H_z = 0 \quad . \quad \text{(IV-28)}$$

Consequently the transverse field components become

$$\underline{E}_t = \frac{-h}{h^2 + \omega^2 \mu_o \epsilon_o} E_o \frac{1}{r} \left[(Sr) J_n'(Sr) \underline{e}_r - jn \, J_n(Sr) \underline{e}_\theta \right] e^{-jn\theta} \quad \text{(IV-29)}$$

$$\underline{E}_t = \frac{-j\omega \epsilon_o}{h^2 + \omega^2 \mu_o \epsilon_o} E_o \frac{1}{r} \left[jn \, J_n(Sr) \underline{e}_r + (Sr) \, J_n'(Sr) \underline{e}_\theta \right] e^{-jn\theta} . \quad \text{(IV-30)}$$

Boundary conditions require the tangential electric field and normal magnetic field components to vanish on the conducting wall $r = r_o$. These conditions are satisfied by taking $J_n(Tr_o) = 0$. This, together with equation VI-20b for T^2, leads to the dispersion relation

$$h = \pm j\left(\frac{\omega}{V_c}\right) \sqrt{\frac{\omega^2 - \omega_{4,n}^2}{\omega^2 - \Omega_p^2}} \quad . \quad \text{(IV-31)}$$

The TM wave has a resonance at the plasma frequency Ω_p and is cut off at $\omega = 0$ and at

$$\omega_{4,n} = \sqrt{\Omega_p^2 + (TV_c)^2} \quad . \quad \text{(IV-32)}$$

These modes have a phase velocity

$$\frac{\omega}{\beta} = V_c \sqrt{\frac{\omega^2 - \Omega_p^2}{\omega^2 - \omega_{4,n}^2}} \quad . \quad \text{(IV-33)}$$

Between cut-off at $\omega = 0$ and the resonance at Ω_p, slow waves propagate whose terminal frequencies are independent of the waveguide dimensions and the mode number. Fast TM waveguide modes are also present; these propagate at frequencies above $\omega_{4,n}$. Figure IV-2 illustrates typical TE and TM dispersion curves obtained from relations IV-26 and IV-31.

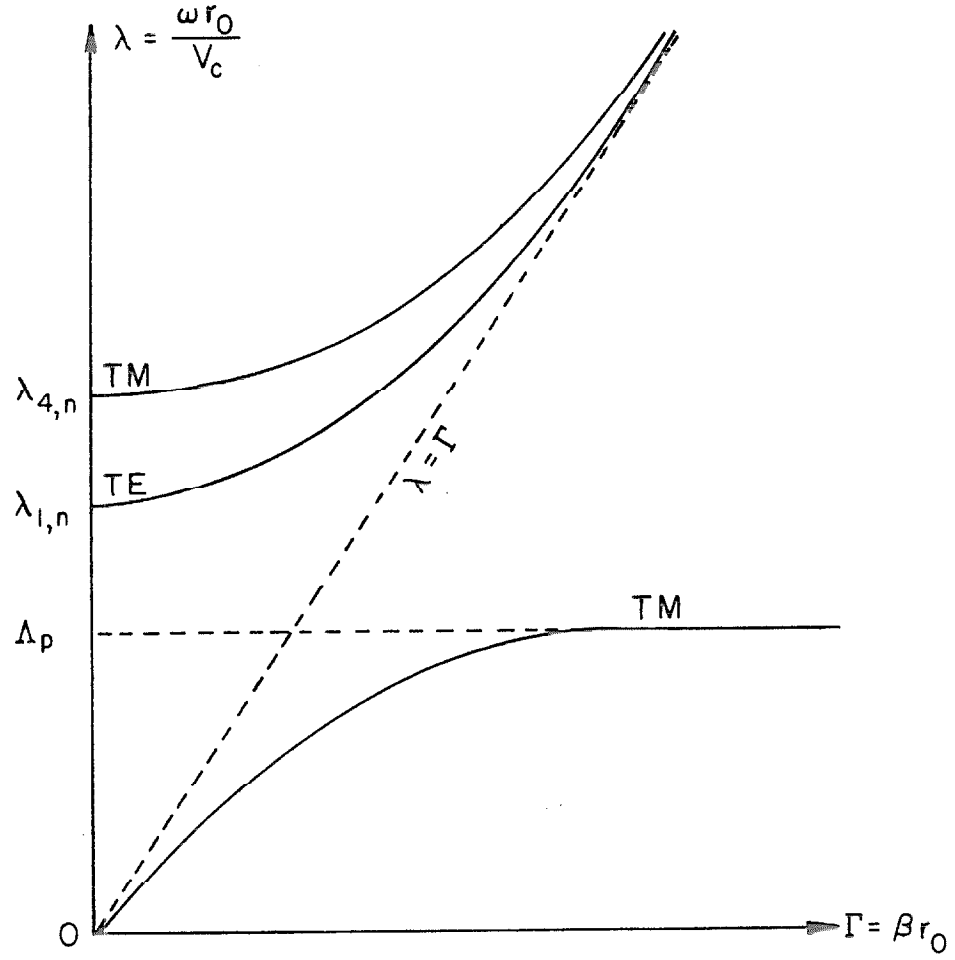

Figure IV-2. Dispersion equations IV-26 and IV-31 for the extremely anisotropic plasma-filled waveguide

The physical origin of the slow TM wave can be traced to the presence of the waveguide wall and the infinite magnetostatic bias. In their absence the unbounded, isotropic plasma has a natural frequency of oscillation Ω_p. If an infinite magnetic field is imposed, the transverse motion of the charge is resisted by an infinite $q\underline{v} \times \underline{B}_o$ force, while motion along $\underline{B}_o$ is unaffected. The plasma now has but one degree of freedom in which it continues to oscillate at frequency Ω_p. However, confining the plasma in a conducting tube coaxial with $\underline{B}_o$, reduces the natural frequency of the oscillation to an extent determined by the plasma reduction factor R. R is a function of $(\frac{r_o}{\lambda_g})$ where r_o is the radius of the metallic boundary or waveguide, and λ_g is the wavelength of the plasma disturbance. The reduction factor is zero for infinitely long disturbances, approaches unity at short wavelengths, and differs from mode to mode. The reduction is caused by the induced image charges present on the conducting wall. At larger wavelengths more of the electrostatic flux from the plasma terminates on the induced wall charge. This diminishes the restoring force experienced by a displaced particle, and hence the natural frequency of its oscillation.

The TM wave possesses an axial component of electric force which is capable of initiating a longitudinal disturbance in the plasma; the TE wave does not. As a result, only the TM wave propagates below Ω_p. Sketches illustrating the plasma reduction factor R, the dispersion relation for an unbounded plasma, and the resultant waveguide dispersion (equal to the product of the two foregoing functions) are drawn on the next page.

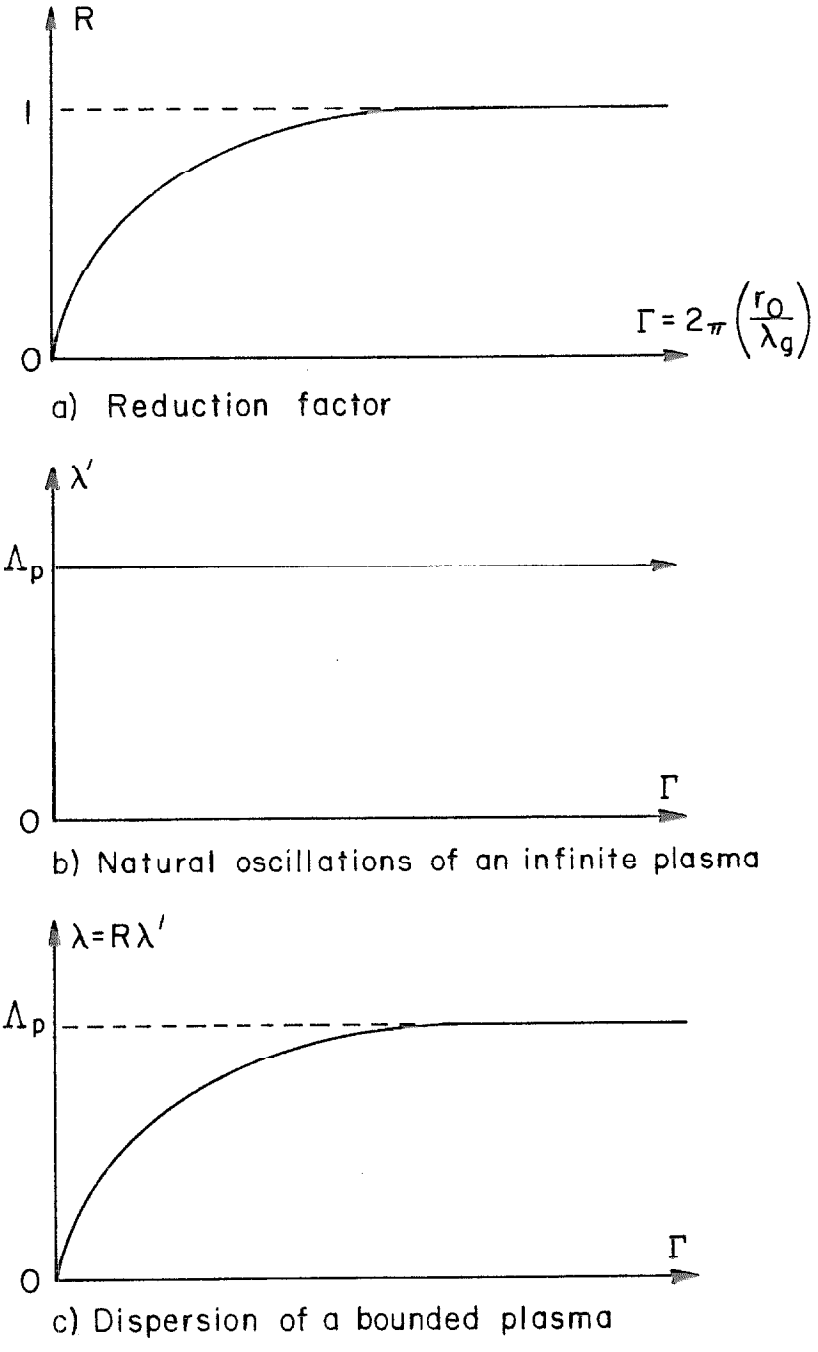

Figure IV-3. An explanation of the TM space charge wave of Figure IV-2.

Fast waveguide modes occur at frequencies considerably higher than the plasma oscillation. At these frequencies the individual particles act as scattering centers to the incident wave. Because of the rapidity of the fields, the particles are unable to follow the field variation and unable to acquire a significant amplitude of oscillation. The particles therefore behave more like polarization charges than free charges. The effective polarization vector, however, is in phase opposition to the electric field, consequently the susceptibility of the material along the infinite axial magnetic field is negative and equal to $-(\frac{\Omega_p}{\omega})^2$. The transverse permittivity ϵ_1 remains equal to the vacuum dielectric constant ϵ_o, and $\epsilon_2 = 0$. A TE wave is therefore unaffected by this plasma. The TM wave has a longitudinal electric field which samples the reduced permittivity which in turn acts to raise the modal dispersion to higher frequencies.

As $\underline{B}_o$ is decreased, transverse motion again becomes possible until at $\underline{B}_o = 0$ the transverse permittivity ϵ_1 has also been reduced by $(\frac{\Omega_p}{\omega})^2 \epsilon_o$ to equal ϵ_3 and the plasma is isotropic. In the isotropic plasma both the TE and the TM wave dispersions are shifted by equal amounts to higher frequencies. The TM space charge wave vanishes as the magnetization is decreased, because with the added transverse degree of freedom, the particles are able to respond to the disruptive force of the induced wall charge.

For an infinite magnetic field the cut-off frequencies $\omega_{2,n}$ and $\omega_{3,n}$ of the coupled wave regime cancel the resonances ω_i and ω_e at $\omega = \infty$. As the magnitude of $\underline{B}_o$ is lessened, the cancelation becomes incomplete and these waves descend to lower frequencies.

A number of involved transitions take place, but eventually $\underline{B}_o$ vanishes and dispersion diagram IV-1 is regained.

Geometric Limits

Plane waves in an unbounded plasma. If one allows the radius of the guide to increase without limit, the plasmaguide's fields and dispersion eventually approach the corresponding plane wave quantities for propagation along $\underline{B}_o$ in an unbounded plasma. The conditions for which the plane wave approximation is valid are investigated using this procedure.

Dispersion in the plasmaguide is dictated by the simultaneous solution of equations II-16 and II-36. If equation II-36 is rewritten as

$$\frac{bn}{r_o^2}\left[(T_1 r_o)^2 - (T_2 r_o)^2\right] + \left[\omega\mu_o - \frac{d}{r_o^2}(T_1 r_o)^2\right]\frac{(T_2 r_o)J_n'(T_2 r_o)}{J_n(T_2 r_o)} +$$

$$- \left[\omega\mu_o - \frac{d}{r_o^2}(T_2 r_o)^2\right]\frac{(T_1 r_o)J_n'(T_1 r_o)}{J_n(T_1 r_o)} = 0$$

and it is assumed that $T_1 r_o$ and $T_2 r_o$ remain finite as the radius r_o becomes infinite, then correct to order $1/r_o$ this expression reduces to

$$\frac{(T_1 r_o)J_n'(T_1 r_o)}{J_n(T_1 r_o)} = \frac{(T_2 r_o)J_n'(T_2 r_o)}{J_n(T_2 r_o)} \quad .$$

The only solution of this equation consistent with the requirement that $T_1 r_o$ and $T_2 r_o$ be finite as $r_o \to \infty$ is $T_1 = T_2 = 0$. Setting $T = 0$ in equation II-16 gives

$$\gamma_1^2 - \gamma_2^2 = (\gamma_1 - \gamma_2)(\gamma_1 + \gamma_2) = 0 \quad . \qquad \text{(IV-34)}$$

Equation II-3 for γ_1 and γ_2 converts these factors into the dispersion relations of equation I-29b, viz.

$$h^2 = -\omega^2\mu_o(\epsilon_1 \pm \epsilon_2) \quad . \tag{IV-35}$$

Since the postulated behavior of $T_1 r_o$ and $T_2 r_o$ properly results in the plane wave dispersion relations, the same assumptions are used to expand the waveguide fields.

For $T_1 = T_2$ it follows from II-17 that $\tau_1 = \tau_2$ and that $\Phi_1 = \Phi_2$. The field components of equations II-29, II-31, and II-32 therefore become

$$H_z = \Phi \qquad \text{and} \qquad E_z = \tau\Phi \quad . \tag{IV-36}$$

For future convenience, the following notation is adopted:

$$\Phi = -\left(\frac{E_o T}{\omega\mu_o}\right) J_n(Tr)e^{-jn\theta} \quad , \tag{IV-37}$$

the exponential dependence $e^{j\omega t - hz}$ is implicitly contained in $E_o(z,t)$. Equations II-30, II-33 and II-34 for the transverse fields are consequently

$$\underline{E}_t = \frac{-E_o T}{\omega\mu_o r}\left\{\left[(ja\tau + b)(Tr)J_n'(Tr) + jn(c\tau + jd)J_n(Tr)\right]\underline{e}_r + \left[-jn(ja\tau + b)J_n(Tr) + (c\tau + jd)(Tr)J_n'(Tr)\right]\underline{e}_\theta\right\} e^{-jn\theta} \tag{IV-38a}$$

$$\underline{H}_t = \frac{-E_o T}{\omega\mu_o r}\left\{\left[(f\tau + ja)(Tr)J_n'(Tr) + jn(jg\tau + c)J_n(Tr)\right]\underline{e}_r + \left[-jn(f\tau + ja)J_n(Tr) + (jg\tau + c)(Tr)J_n'(Tr)\right]\underline{e}_\theta\right\} e^{-jn\theta} \tag{IV-38b}$$

The well-known recursion formulas for the Bessel functions

$$J'_n = \frac{1}{2}(J_{n-1} - J_{n+1}) \qquad \text{and} \qquad nJ_n = \frac{Tr}{2}(J_{n-1} + J_{n+1})$$

permit us to rewrite IV-38 as

$$\underline{E}_t = \frac{-E_o T^2}{2\omega\mu_o}\left\{\left[j(a+c)\tau + (b-d)\right](\underline{e}_r - j\underline{e}_\theta)\,J_{n-1}(Tr) + \right.$$

$$\left. - \left[j(a-c)\tau + (b+d)\right](\underline{e}_r + j\underline{e}_\theta)\,J_{n+1}(Tr)\right\}e^{-jn\theta} \qquad \text{(IV-39a)}$$

$$\underline{H}_t = \frac{-E_o T^2}{2\omega\mu_o}\left\{\left[(f-g)\tau + j(a+c)\right](\underline{e}_r - j\underline{e}_\theta)\,J_{n-1}(Tr) + \right.$$

$$\left. -\left[(f+g)\tau + j(a-c)\right](\underline{e}_r + j\underline{e}_\theta)\,J_{n+1}(Tr)\right\}e^{-jn\theta}\,. \qquad \text{(IV-39b)}$$

Substituting II-4 for coefficients a to g and placing $T^2 = \dfrac{\omega\mu_o}{d - j\tau c}$ according to equation II-17a, after some labor, yields surprisingly simple expressions for the transverse fields.

$$\underline{E}_t = \frac{E_o}{2\gamma_2}\left\{(T^2 + \gamma_1 + \gamma_2)J_{n-1}(Tr)(\underline{e}_r - j\underline{e}_\theta) - (T^2 + \gamma_1 - \gamma_2)J_{n+1}(Tr)\right.$$

$$\left. \times (\underline{e}_r + j\underline{e}_\theta)\right\}e^{-jn\theta} \qquad \text{(IV-40a)}$$

$$\underline{H}_t = \frac{\omega\mu_o E_o}{2h\gamma_2}\left\{\left[(\gamma_1 - \gamma_2 + h^2)(\gamma_1 + \gamma_2) + (\gamma_1 + h^2)T^2\right]J_{n-1}(Tr)(\underline{e}_r - j\underline{e}_\theta) + \right.$$

$$\left. + \left[(\gamma_1 + \gamma_2 + h^2)(\gamma_1 - \gamma_2) + (\gamma_1 + h^2)T^2\right]J_{n+1}(Tr)(\underline{e}_r + j\underline{e}_\theta)\right\}\,e^{-jn\theta}\,. \qquad \text{(IV-40b)}$$

The lowest order fields result when $T = 0$. $J_{n\mp1}(Tr)$ then has unit magnitude for $n = \pm 1$ respectively, and zero amplitude otherwise. It

is practical to introduce the Kronecker delta abbreviation and write

$$J_{n\mp1}(\mathbb{T}r) = \delta_{n,\pm1} \quad .$$

The limiting transverse fields are thus

$$\underline{E}_t = \frac{E_o}{2\gamma_2}\left\{(\gamma_1+\gamma_2)(\underline{e}_r - j\underline{e}_\theta)\delta_{n,1} - (\gamma_1-\gamma_2)(\underline{e}_r + j\underline{e}_\theta)\delta_{n,-1}\right\} e^{-jn\theta} \tag{IV-41a}$$

$$\underline{H}_t = \frac{-E_o}{2\omega\mu_o h\gamma_2}\left\{(\gamma_1-\gamma_2+h^2)(\gamma_1+\gamma_2)(\underline{e}_r - j\underline{e}_\theta)\delta_{n,1} + (\gamma_1+\gamma_2+h^2)(\gamma_1-\gamma_2)(\underline{e}_r + j\underline{e}_\theta)\delta_{n,-1}\right\} e^{-jn\theta} \tag{IV-41b}$$

Because

$$\delta_{n,\mp1}(\underline{e}_r \mp j\underline{e}_\theta)e^{-jn\theta} = \delta_{n,\pm1}\left[(\underline{e}_r\cos\theta - \underline{e}_\theta\sin\theta) \mp j(\underline{e}_r\sin\theta + \underline{e}_\theta\cos\theta)\right] = \delta_{n,\pm1}(\underline{e}_x \mp j\underline{e}_y) \tag{IV-42}$$

the final expressions for the transverse fields are

$$\underline{E}_t = \frac{E_o}{2\gamma_2}\left[(\gamma_1+\gamma_2)(\underline{e}_x - j\underline{e}_y)\delta_{n,1} - (\gamma_1-\gamma_2)(\underline{e}_x + j\underline{e}_y)\delta_{n,-1}\right] \tag{IV-43a}$$

$$\underline{H}_t = \frac{-E_o}{2\omega\mu_o h\gamma_2}\left[(\gamma_1-\gamma_2+h^2)(\gamma_1+\gamma_2)(\underline{e}_x - j\underline{e}_y)\delta_{n,1} + (\gamma_1+\gamma_2+h^2)(\gamma_1-\gamma_2)(\underline{e}_x + j\underline{e}_y)\delta_{n,-1}\right] \quad . \tag{IV-43b}$$

However, equation IV-34 demonstrates that $T=0$ corresponds to $\gamma_1 = \pm\gamma_2$. Accordingly, for $n=+1$ choose $\gamma_1 = +\gamma_2$, and for $n=-1$ take

$\gamma_1 = -\gamma_2$. Equations IV-43 then reduce to the familiar plane wave fields:

$$\underline{E}_t = \frac{-h_+}{\omega\mu_o}\underline{H}_t = E_o(\underline{e}_x - j\underline{e}_y) \quad \text{with} \quad \gamma_1 = +\gamma_2 \text{ , i.e., } h_+ = \pm j\omega\sqrt{\mu_o(\epsilon_1+\epsilon_2)} \tag{IV-44}$$

$$\underline{E}_t = \frac{+h_-}{\omega\mu_o}\underline{H}_t = E_o(\underline{e}_x + j\underline{e}_y) \quad \text{with} \quad \gamma_1 = -\gamma_2 \text{ , i.e., } h_- = \pm j\omega\sqrt{\mu_o(\epsilon_1-\epsilon_2)} \tag{IV-45}$$

while the longitudinal fields of equations IV-36 and IV-37 vanish with T .

As the waveguide radius is made infinite, two circularly polarized TEM plane waves are found to propagate along $\underline{B}_o$. The right circular wave h_+ corresponds to the lowest $n = +1$ waveguide mode, while the left circular wave h_- corresponds to the $n = -1$ waveguide mode. The waves are occasionally referred to as the extraordinary wave and the ordinary wave, respectively.

The conditions under which the waveguide fields of the lowest $n = \pm 1$ modes may be treated as plane waves are appraised by reviewing the steps leading from IV-40 to IV-41. For small arguments

$$J_o(Tr) \approx 1 - \left(\frac{Tr}{2}\right)^2 + \cdots .$$

Thus it is assumed that $\left|\frac{Tr}{2}\right| \ll 1$ or, equivalently

$$\left(\frac{r}{r_o}\right) \ll \left|\frac{2}{Tr_o}\right| \quad . \tag{IV-46}$$

Equation IV-46 provides a criterion for estimating the radius to which the $n = \pm 1$ waveguide fields approximate plane waves. Since the argument

Tr_o is basically a zero of $J_1'(x)$ or $J_1(x)$, the size of $\frac{2}{Tr_o}$ is slightly less than unity for the lowest mode and becomes progressively smaller for the higher modes. The higher the mode, the poorer the plane wave approximation at any given radius. Because the field configuration of a coupled mode will vary as the frequency and plasma are changed, the plane wave approximations are likely to be more suitable in some frequency ranges than in others. The criteria which determine when the plane wave approximations are appropriate can also be estimated from equations IV-40 and IV-41. These expressions require

$$\left| \frac{\gamma_1 \pm \gamma_2}{T^2} \right| \gg 1 \qquad \text{(IV-47)}$$

for $n = \pm 1$ respectively.

By means of equation III-31 the plane wave propagation factors contained in equations IV-44 and IV-45 may be expressed explicitly in terms of the frequency

$$-h_+^2 = \omega^2 \mu_o (\epsilon_1 + \epsilon_2) = \frac{\omega^2}{V_c^2} \left\{ 1 - \frac{\Omega_e^2}{\omega(\omega-\omega_e)} - \frac{\Omega_i^2}{\omega(\omega+\omega_i)} \right\} = \frac{\omega^2}{V_c^2} \frac{(\omega+\omega_L)(\omega-\omega_R)}{(\omega+\omega_i)(\omega-\omega_e)} \qquad \text{(IV-48a)}$$

$$-h_-^2 = \omega^2 \mu_o (\epsilon_1 - \epsilon_2) = \frac{\omega^2}{V_c^2} \left\{ 1 - \frac{\Omega_e^2}{\omega(\omega+\omega_e)} - \frac{\Omega_i^2}{\omega(\omega-\omega_i)} \right\} = \frac{\omega^2}{V_c^2} \frac{(\omega-\omega_L)(\omega+\omega_R)}{(\omega-\omega_i)(\omega+\omega_e)} . \qquad \text{(IV-48b)}$$

According to III-34

$$\omega_L = -\left(\frac{\omega_e - \omega_i}{2}\right) + \sqrt{\left(\frac{\omega_e + \omega_i}{2}\right)^2 + (\Omega_e^2 + \Omega_i^2)} \qquad \text{(IV-49a)}$$

$$\omega_R = +\left(\frac{\omega_e - \omega_i}{2}\right) + \sqrt{\left(\frac{\omega_e + \omega_i}{2}\right)^2 + (\Omega_e^2 + \Omega_i^2)} \quad . \qquad \text{(IV-49b)}$$

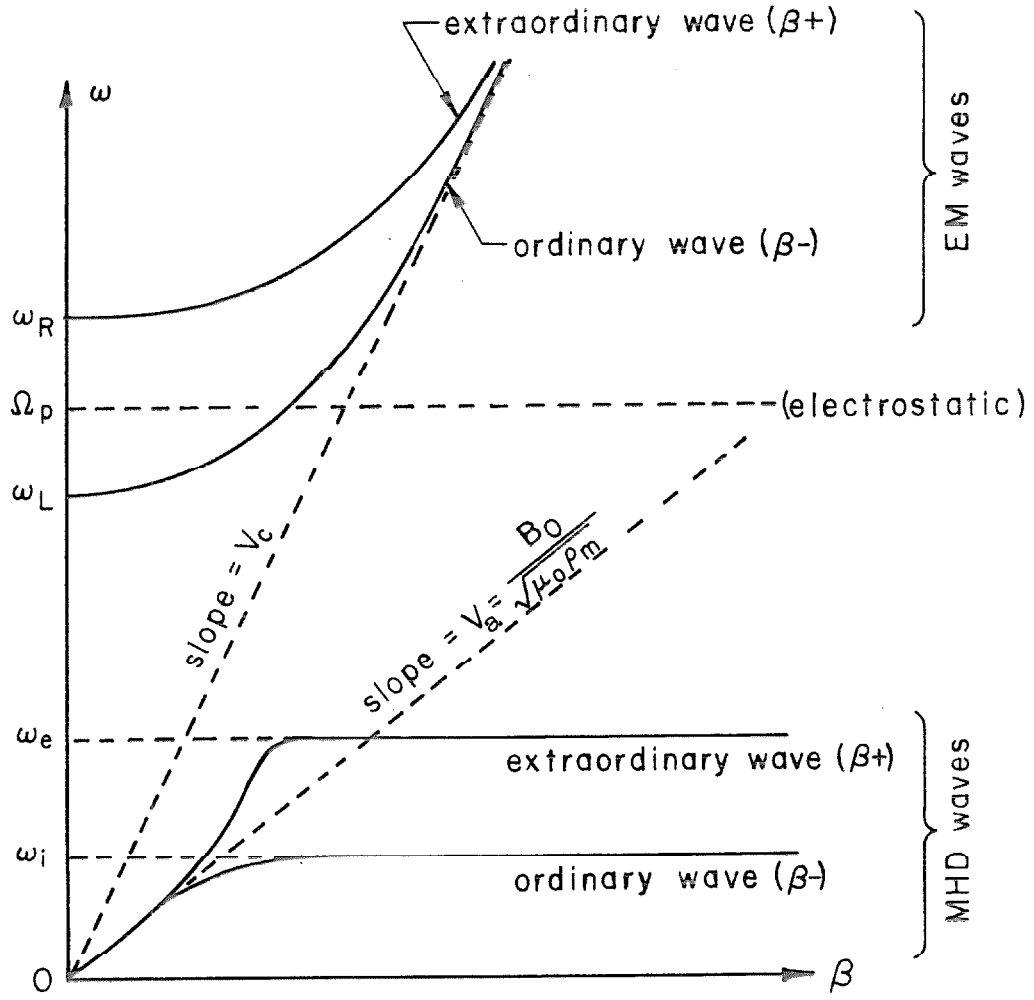

Figure IV-4. Plane wave dispersion for propagation along the magnetostatic field

A sketch of these plane wave dispersion functions appears in Figure IV-4.

Let us briefly examine the transition from waveguide dispersion to plane wave propagation. As the waveguide radius is increased and $T_2 \to T_1 \to 0$, $\omega_{4,n} = \sqrt{(TV_c)^2 + \Omega_p^2} \to \Omega_p$. As $\omega_{4,n}$ drops, it overtakes the $\omega_{2,n}$ cut-off frequency which is also falling. Mode mixing occurs and $\omega_{2,n}$ and $\omega_{4,n}$ interchange roles; $\omega_{4,n}$ eventually characterizes a longitudinal electrostatic oscillation of the plasma at frequency Ω_p. $\omega_{2,n}$ becomes the cut-off frequency of the left circularly polarized plane wave. Meanwhile $\omega_{1,n}$ and $\omega_{3,n}$ also decrease as $r_o \to \infty$, to become the two remaining plane wave cut-off frequencies $\omega = 0$ and ω_R, respectively. The transition and mode mixing are sketched below.

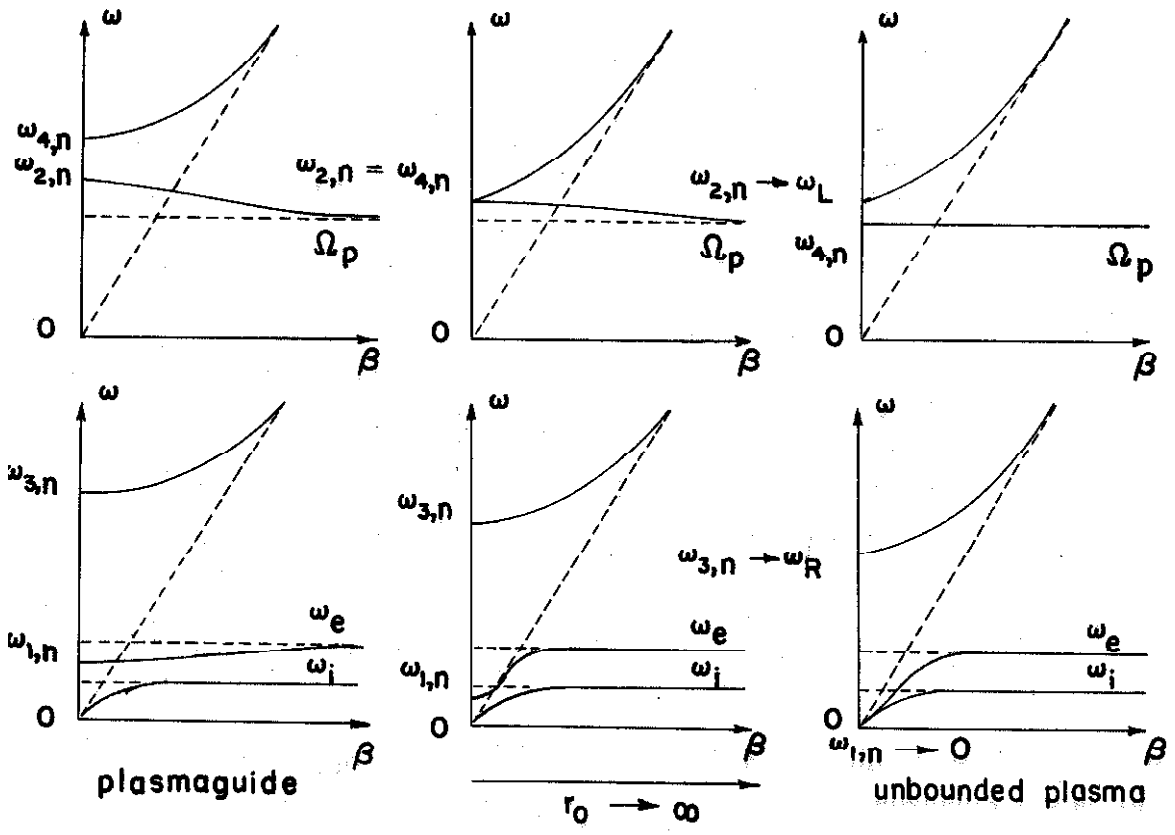

Figure IV-5. Transition from waveguide modes to plane waves

Except near $\omega_{4,n}$ and Ω_p, the fields are TE at cut-off and become TEM as resonance is approached. For intermediate frequencies $T_1 r_o$ remains very nearly equal to a zero of $J_n'(x)$, as if it belonged to a TE mode of an isotropic waveguide. The magnitude of $T_2 r_o$ is usually several orders larger than $T_1 r_o$. If this is due to a large real part, then the Bessel functions of $T_2 r_o$ are very small indeed. In any case the coefficients that multiply $J_n(T_2 r_o)$ are generally much smaller than the corresponding coefficients of $J_n(T_1 r_o)$. As a result the Bessel functions with argument $T_2 r_o$ are of secondary importance. Since the mode having a TM cut-off at $\omega_{4,n}$ and resonating at Ω_p transforms with increasing guide radius into an electrostatic oscillation of no further interest, the TEM plane waves are the outgrowth of coupled waves which are predominantly TE. A sketch of the TE_{11} fields in a circular isotropic waveguide is reproduced in Figure IV-6. Note how the fields in the central portion of the guide resemble a plane TEM wave. It is not surprising then, that the $n = \pm 1$ waveguide modes reduce to plane TEM waves.

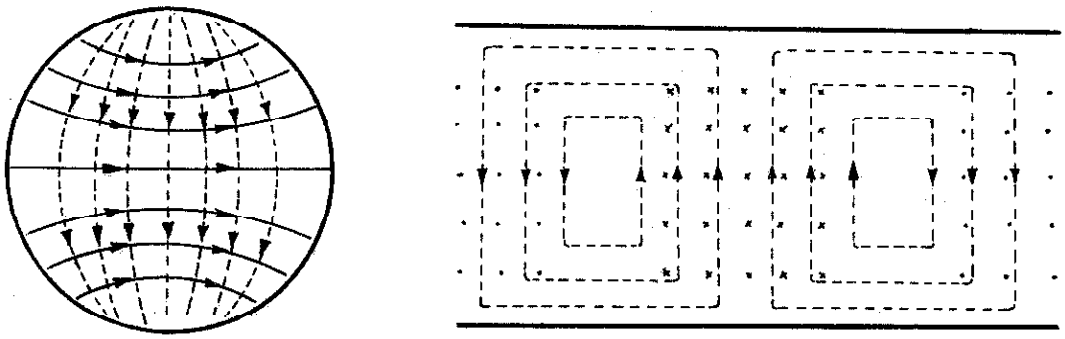

Figure IV-6. The TE_{11} mode of an isotropic circular waveguide. The electric field is shown solid, the magnetic field is indicated by the broken line.

Two regions of diagram IV-4 are of special interest; these are the linear non-dispersive range of the Alfvén wave and the parabolic frequency dependence of the whistler mode. In the Alfvén region near $\omega = 0$, the transverse components of the permittivity tensor as given by equation I-18 reduce to

$$\epsilon_1 = \epsilon_o \left(1 + \frac{\Omega_e^2}{\omega_e^2} + \frac{\Omega_i^2}{\omega_i^2} \right) \quad \text{and} \quad \epsilon_2 = 0 \quad . \tag{IV-50}$$

Meanwhile both plane wave propagation factors of equations IV-44 and IV-45 degenerate into

$$\beta = \pm\omega \sqrt{\mu_o(\epsilon_1 \pm \epsilon_2)} \xrightarrow[\omega \to 0]{} \pm\omega \sqrt{\left(\frac{1}{V_a^2} + \frac{1}{V_c^2}\right)} \approx \pm \left(\frac{\omega}{V_a}\right) \; ; \quad \alpha = 0 \tag{IV-51}$$

where

$$V_a = \left[\mu_o \epsilon_o \left(\frac{\Omega_e^2}{\omega_e^2} + \frac{\Omega_i^2}{\omega_i^2} \right) \right]^{-1/2} = \frac{B_o}{\sqrt{\mu_o(n_e m_e + n_i m_i)}} = \frac{B_o}{\sqrt{\mu_o \rho_m}} \tag{IV-52}$$

is known as the Alfvén velocity, and

$$\rho_m = (n_e m_e + n_i m_i) \tag{IV-53}$$

is the plasma mass density. Thus the plasma supports electromagnetic waves that propagate with equal group and phase velocities, $\frac{d\omega}{d\beta} = \frac{\omega}{\beta} = V_a$, which do not depend upon the frequency until ω nears ω_i. An interesting physical picture of this wave can be found in Alfvén's book (24). By treating the magnetic induction as stressed elastic strings, the wave can be described as an oscillation of these flux lines.

In the frequency range $\omega_i \ll \omega \ll \omega_e$ only the extraordinary wave propagates, and this has a wave number (cf. equation IV-48a)

$$\alpha_+ = 0$$

$$\beta_+ = \frac{\omega}{V_c}\left\{1 + \frac{\Omega_e^2}{\omega\omega_e}\left(1 - \frac{\omega_e}{\omega}\,\frac{\Omega_i^2}{\Omega_e^2}\right)\right\}^{1/2} \approx \frac{\omega}{V_c}\left(1 + \frac{\Omega_e^2}{\omega\omega_e}\right)^{1/2} \qquad \text{(IV-54)}$$

because in a neutral plasma $\frac{\omega_e}{\omega}\,\frac{\Omega_i^2}{\Omega_e^2} = \frac{\omega_i}{\omega} \ll 1$. A frequency component ω , belonging to a group of such waves excited at $t = 0$, reaches the observer at an instant

$$t(\omega) = \int \frac{ds}{V_g(\omega, s)} \qquad . \qquad \text{(IV-55)}$$

The integral is evaluated along the path of propagation of which ds is an element; V_g is the group velocity of the wave as it passes through the position s . Since the wave normal and the magnetization are parallel, it is not necessary to distinguish between the ray direction $(\underline{E} \times \underline{H})$ in which the energy flows, and the direction of the wave normal $(\underline{D} \times \underline{H})$; they are the same.

If it is assumed that the ionization everywhere along the path is sufficiently dense that the condition

$$\frac{\Omega_e^2}{\omega_e^2} > \frac{\Omega_e^2}{\omega\omega_e} \gg 1$$

prevails, then

$$\beta_+ = \frac{\omega}{V_c}\left(1 + \frac{\Omega_e^2}{\omega\omega_e}\right)^{1/2} \approx \frac{\Omega_e}{V_c}\sqrt{\frac{\omega}{\omega_e}} \qquad \text{(IV-56)}$$

and

$$\frac{1}{V_g} = \frac{d\beta_+}{d\omega} = \frac{1}{2V_c} \frac{\Omega_e}{\sqrt{\omega\,\omega_e}} = \frac{1}{2} \frac{\beta_+}{\omega} = \frac{1}{2V_{phase}} \quad . \qquad \text{(IV-57)}$$

The arrival time is therefore

$$t(\omega) = \left\{ \frac{1}{2V_c} \int \frac{\Omega_e(s)ds}{\sqrt{\omega_e(s)}} \right\} \omega^{-1/2} = D\,\omega^{-1/2} \quad . \qquad \text{(IV-58)}$$

The quantity D, defined by the bracket, is called the "dispersion". It is a measure of the spread experienced by a wave packet along a given path of propagation. Equation IV-58 demonstrates that a transmitted audio pulse will appear to the observer as a whistling tone of descending pitch. For this reason the wave is often referred to as the whistler mode. Lightning frequently excites whistlers which enter the ionosphere in the extraordinary MHD mode and propagate dispersively along the earth's magnetic field to the opposite hemisphere (25). Recently attempts have been made to excite the whistler mode in waveguides and shock tubes (26). The results obtained have been superficially explained by a plane wave analysis. A later section of this chapter, devoted to guided MHD waves, provides the theory for adequately explaining the Alfven wave and the whistler mode in a circular guide.

The narrow waveguide limit and the quasi-static approximation.

Wave dispersion is examined next in plasmaguides having extremely small cross-sections. To satisfy the boundary conditions at the waveguide wall, it is necessary for T_1 and T_2 to become very large as the waveguide radius r_o is reduced. It is equally important that h

be large, otherwise the wave would be substantially cut off. Physically, fields are sought whose phase velocities $\frac{\omega}{\beta}$ are very much slower than the velocity of light through the medium. Such waves are usually studied via a quasi-static analysis. However, by examining the limit of a coupled wave in a narrow waveguide, a more versatile dispersion relation is obtained which, for very large values of T, reduces to the quasi-static relation.

A useful approximation based upon these considerations is

$$\left|\gamma_1(\gamma_1 + T^2)\right| \gg \gamma_2^2 \quad . \tag{IV-59}$$

This inequality is fulfilled in the microwave range where $\gamma_2 = 0$, and in the low frequency MHD range where $\gamma_2 \to 0$ faster than either $\gamma_1 \to 0$ (torsional or TM mode) or $(\gamma_1 + T^2) \to 0$ (compressional or TE mode). Inequality IV-59 is also satisfied at plasma resonance where $\gamma_1 \to \infty$ with h, and at cyclotron resonance where $\gamma_1^2 = \gamma_2^2$ so that IV-59 reduces to $\left|\gamma_1 T^2\right| \gg 0$.

When approximation IV-59 is valid, dispersion relation II-16 for the coupled wave becomes

$$(\gamma_1 + T^2)\left[\gamma_1 - \frac{T^2}{\omega^2 \mu_o \epsilon_3}(\gamma_1 + h^2)\right] = 0$$

or, because $\gamma_1 \equiv -h^2 - \omega^2 \mu_o \epsilon_1$, these factors are

$$(\gamma_1 + T^2)(\gamma_1 + \frac{\epsilon_1}{\epsilon_3} T^2) = 0 \quad .$$

Thus in the narrow waveguide limit

$$\text{a)} \quad T_1^2 = -\gamma_1 \quad , \qquad \text{b)} \quad T_2^2 = -\frac{\epsilon_3}{\epsilon_1}\gamma_1 \quad . \qquad \text{(IV-60)}$$

The most appropriate form for equation II-36, relating T and h to the boundary conditions at r_o, is

$$\left[bn(T_1^2 - T_2^2)J_n(T_1 r_o) - (\omega\mu_o - dT_2^2)(T_1 r_o)J_n'(T_1 r_o) \right] J_n(T_2 r_o) +$$

$$+ (\omega\mu_o - dT_1^2)(T_2 r_o)\, J_n'(T_2 r_o)\, J_n(T_1 r_o) = 0 \quad . \qquad \text{(IV-61)}$$

According to IV-59 and IV-60 the coefficients of this equation are

$$b(T_1^2 - T_2^2) = \frac{-\omega\mu_o\gamma_1\gamma_2}{\gamma_1^2 - \gamma_2^2}\left(1 - \frac{\epsilon_3}{\epsilon_1}\right)$$

and

$$(\omega\mu_o - dT^2) = \omega\mu_o \left| \frac{\gamma_1^2 - \gamma_2^2 + \gamma_1 T^2}{\gamma_1^2 - \gamma_2^2} \right| \approx \omega\mu_o \frac{\gamma_1(\gamma_1 + T^2)}{\gamma_1^2 - \gamma_2^2} \quad ,$$

Substituting for T_1 and T_2,

$$(\omega\mu_o - dT_1^2) = 0$$

$$(\omega\mu_o - dT_2^2) = \frac{\omega\mu_o\gamma_1^2}{\gamma_1^2 - \gamma_2^2}\left(1 - \frac{\epsilon_3}{\epsilon_1}\right)$$

whence equation IV-61 reduces to the product of two factors, viz.

$$\text{a)} \quad \left[n\gamma_2 J_n(T_1 r_o) + \gamma_1(T_1 r_o)J_n'(T_1 r_o) \right] = 0 \quad \text{and} \quad \text{b)} \quad J_n(T_2 r_o) = 0 \quad . \qquad \text{(IV-62)}$$

Equations IV-60 and IV-62 completely describe dispersion in the narrow waveguide limit. Note that the limiting process has divided equations

II-16 and II-36 into separate relations for T_1 and T_2.

To understand the field structures to which equations IV-60 and IV-62 apply, these dispersion relations are now derived directly from equations II-8 through II-11 for the waveguide fields. By invoking inequality IV-59, γ_2 is effectively set equal to zero. According to II-4 coefficient c also vanishes; whereupon equations II-10 and II-11 decouple into

$$\nabla_t^2 H_z + S^2 H_z = 0 \qquad S^2 = -\gamma_1 \tag{IV-63a}$$

$$\nabla_t^2 E_z + T^2 E_z = 0 \qquad T^2 = -\frac{\epsilon_3}{\epsilon_1}\gamma_1 \quad . \tag{IV-63b}$$

These equations have solutions

$$H_z = H_o J_n(Sr)\, e^{-jn\theta} \tag{IV-64a}$$

$$E_z = E_o J_n(Tr)\, e^{-jn\theta} \quad . \tag{IV-64b}$$

The transverse fields are specified in terms of E_z and H_z by equations II-8 and II-9. The boundary conditions which require E_z, E_θ, and E_r to vanish at the waveguide radius r_o are therefore

$$E_z\Big|_{r_o} = E_o J_n(Tr_o) = 0 \tag{IV-65a}$$

$$E_\theta\Big|_{r_o} = \frac{E_o}{r_o}\left[na\, J_n(Tr_o) + c(Tr_o)\, J_n'(Tr_o)\right] - j\,\frac{H_o}{r_o}\left[nb\, J_n(Sr_o) - d(Sr_o)\, J_n'(Sr_o)\right] = 0 \tag{IV-65b}$$

$$H_r\Big|_{r_o} = -\frac{E_o}{r_o}\left[ng\, J_n(Tr_o) - f(Tr_o) J_n(Tr_o)\right] + + j\,\frac{H_o}{r_o}\left[nc\, J_n(Sr_o) - a(Sr_o)\, J_n'(Sr_o)\right] = 0 \tag{IV-65c}$$

If E_o and H_o are eliminated between equations IV-65b and IV-65c, then using identity II-5

$$\frac{b}{c} = -\frac{d}{a}$$

the following transcendental equation results:

$$\left\{\frac{c}{b}\left[na\, J_n(Tr_o) + c(Tr_o)J_n'(Tr_o)\right] - \left[ng\, J_n(Tr_o) - f(Tr_o)J_n'(Tr_o)\right]\right\} \times$$

$$\times \left[nb\, J_n(Sr_o) - d(Sr_o)J_n'(Sr_o)\right] = 0 \quad . \qquad \text{(IV-66)}$$

Setting the second factor of equation IV-66 equal to zero satisfies boundary conditions IV-65 only if $E_o = 0$. This corresponds to a TE wave which, according to equations II-8 and II-9, has

$$\underline{E}_t = \frac{j\omega\mu_o}{-h}(\underline{e}_z \times \underline{H}_t) = b\,\nabla_t H_z + jd\,\underline{e}_z \times \nabla_t H_z \qquad \text{(IV-67)}$$

H_z given by equation IV-64a, and $E_z = 0$. The dispersion relation which S, h and ω satisfy is obtained by substituting II-4 for b and d into the second factor of IV-66, yielding

$$\left[n\,\gamma_2 J_n(Sr_o) + \gamma_1(Sr_o)J_n'(Sr_o)\right] = 0 \qquad \text{(IV-68)}$$

where $S^2 = -\gamma_1 = h^2 + \omega^2\mu_o\epsilon_1$.

Comparing IV-68 with IV-60a and IV-62a we conclude that the narrow waveguide limit associated with $T_1 = S$ is transverse electric (TE).

The first factor of equation IV-66 cannot vanish and at the same time be consistent with boundary condition IV-65a unless γ_2 is sufficiently small that c and f may be neglected. Then, if $H_o = 0$ or else equation IV-68 is satisfied, boundary conditions IV-65a,b,c are fulfilled. Consequently for γ_2 essentially zero, the fields

are TM with E_z defined by equation IV-64b , $H_z = 0$, and as a result of II-8 and II-9

$$\underline{E}_t = \frac{-h}{j\omega\epsilon_1} (\underline{e}_z \times \underline{H}_t) = \frac{h}{\gamma_1} \nabla_t E_z \quad . \tag{IV-69}$$

Due to equation IV-65a, the boundary conditions are satisfied by choosing

$$J_n(Tr_o) = 0 \qquad \text{with} \qquad T^2 = -\frac{\epsilon_3}{\epsilon_1}\gamma_1 = \frac{\epsilon_3}{\epsilon_1}(h^2 + \omega^2\mu_o\epsilon_1) \quad . \tag{IV-70}$$

Reviewing equations IV-60b and IV-62b, it is immediately observed that the dispersion relation for T_2 corresponds to the TM fields of equations IV-64b and IV-69.

Referring to the appendix, we note that the TM narrow waveguide limit

$$-h^2 = \omega^2\mu_o\epsilon_1 - \frac{\epsilon_1}{\epsilon_3}T^2 \quad ; \qquad J_n(Tr_o) = 0 \tag{IV-71}$$

and the quasi-static approximation

$$-h^2 = -\frac{\epsilon_1}{\epsilon_3}T^2 \quad ; \qquad J_n(Tr_o) = 0 \tag{IV-72}$$

are identical for $T^2 \gg \omega^2\mu_o|\epsilon_3|$, i.e.,

$$T^2 \gg \frac{1}{V_c^2}\left|\omega^2 - \Omega_p^2\right| \quad . \tag{IV-73}$$

The inequality is satisfied in very slender waveguides where, in order that the roots of $J_n(Tr_o)$ remain different from zero, $T \to \infty$ as $r_o \to 0$. Inequality IV-73 is also fulfilled in the vicinity of the plasma resonance. However, the quasi-static approximation fails at frequencies much lower than Ω_p where the TM narrow waveguide limit

correctly depicts the Alfvén wave. As $\omega \to 0$, equation IV-71 approaches

$$- h^2 \longrightarrow \omega^2 \mu_o \epsilon_1 \Big|_{\omega = 0} = \omega^2 \left(\frac{1}{V_a^2} + \frac{1}{V_c^2}\right) \quad . \tag{IV-74}$$

This dispersion limit should be compared with equations IV-51 through IV-53 for the plane Alfvén wave, and/or equation IV-91 for the guided Alfvén wave. It may be parenthically remarked that as ω and γ_2 approach zero, the TE narrow-guide dispersion relation IV-68 reduces to the dispersion relation

$$- h^2 = \omega^2 \mu_o \epsilon_1 - S^2 \underset{\omega \to 0}{\longrightarrow} \omega^2 \left(\frac{1}{V_a^2} + \frac{1}{V_c^2}\right) - S^2 \qquad \text{with} \quad J_n'(Sr_o) = 0 \tag{IV-75}$$

for the compressional MHD wave (c.f., equation IV-85).

Introducing equations I-18 and III-29 into expressions IV-71 and IV-72 permits us to rewrite the TM narrow-guide dispersion relation as

$$- h^2 = \frac{\omega^2}{V_c^2} \, \frac{(\omega^2 - \omega_a^2)(\omega^2 - \omega_b^2)}{(\omega^2 - \omega_i^2)(\omega^2 - \omega_e^2)} \, \frac{(\omega^2 - \omega_{4,n}^2)}{(\omega^2 - \Omega_p^2)} \tag{IV-76}$$

while the quasi-static dispersion relation becomes

$$- h^2 = - T^2 \omega^2 \, \frac{(\omega^2 - \omega_a^2)(\omega^2 - \omega_b^2)}{(\omega^2 - \omega_i^2)(\omega^2 - \omega_e^2)} \, \frac{1}{(\omega^2 - \Omega_p^2)} \quad . \tag{IV-77}$$

Frequencies ω_a, ω_b and $\omega_{4,n}$ are defined by equations III-33 and III-26. The similarities between equations IV-76 and IV-77 are clear. Certainly if inequality IV-73 is followed, the two relations are identical, for then

$$\frac{1}{V_c^2}(\omega^2 - \omega_{4,n}^2) = \frac{1}{V_c^2}(\omega^2 - \Omega_p^2 - V_c^2 T^2) \approx - T^2 \quad .$$

As already pointed out, the quasi-static approximation incorrectly describes propagation at the lowest frequencies where $\omega^2 \mu_o \epsilon_1$ is of greater importance than $- \frac{\epsilon_1}{\epsilon_3} T^2$. The quasi-static approximation also fails to explain the existence of the fast wave whose cut-off occurs at $\omega_{4,n}$.

Thus each coupled mode is resolved in the narrow-guide limit into a TE mode and a TM mode. Although neither the TE nor the TM narrow waveguide descriptions are valid near cut-off, it should be remarked that the cut-off frequencies $(\lambda_{1,n}, \lambda_{2,n}, \lambda_{3,n})$ of the coupled wave approach, with increasing mode number S, the TM narrow-guide cut-off frequencies $(\lambda_a, \lambda_b, \infty)$ as upper bounds (cf., Figure III-10). The simplicity of the TM dispersion relation, its significance to the quasi-static solution, and the nature of its cut-off frequencies, suggest that this limit may provide a useful foundation for understanding the exact dispersion relation.

As is easily confirmed, the critical frequencies of the TM narrow-guide limit can be arranged in the following sense

$$\infty > \lambda_b > \lambda_e > \lambda_a > \lambda_i > 0 \qquad \text{also} \qquad \lambda_b, \lambda_{4,n} > \Lambda_p \quad . \qquad \text{(IV-78)}$$

Since both $\lambda_{4,n}$ and Λ_p are independent of the magnetostatic field, the full range of dispersion characteristics can be observed by varying the plasma density. At first the density is assumed so large that λ_b and $\lambda_{4,n}$ become the highest critical frequencies of the plasmaguide. Subsequently the density is decreased until finally only

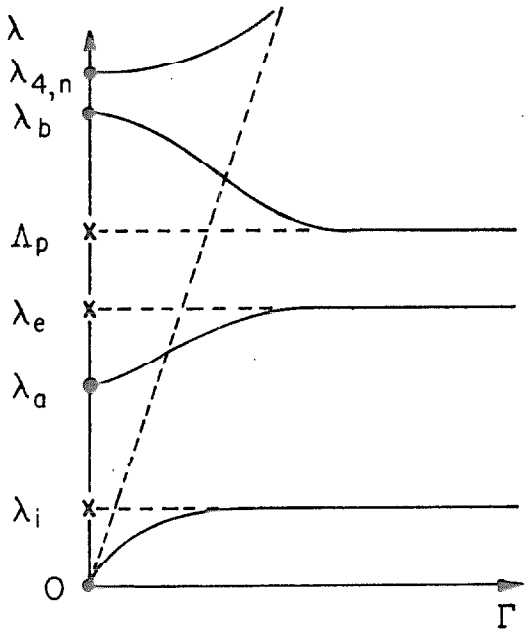

Ⅳ-7(1a) $\lambda_{4,n} > \lambda_b$

$\Lambda_p > \lambda_e$

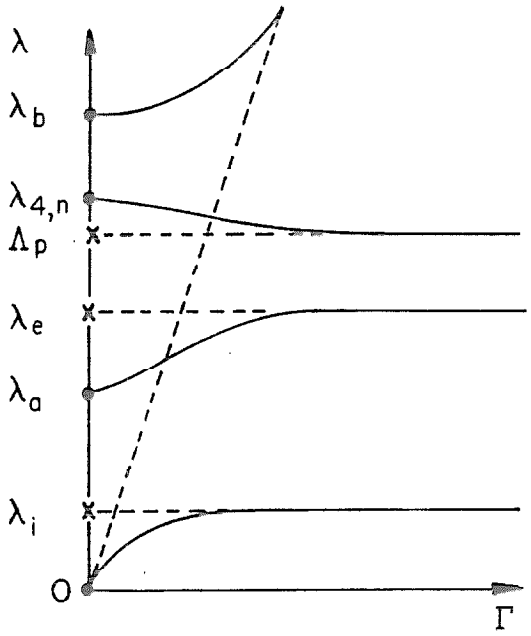

Ⅳ-7(1b) $\lambda_b > \lambda_{4,n}$

$\Lambda_p > \lambda_e$

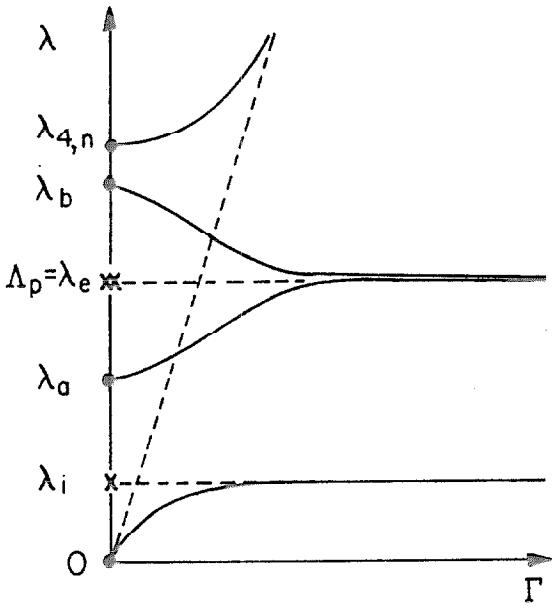

Ⅳ-7(2a) $\lambda_{4,n} > \lambda_b$

$\Lambda_p = \lambda_e$

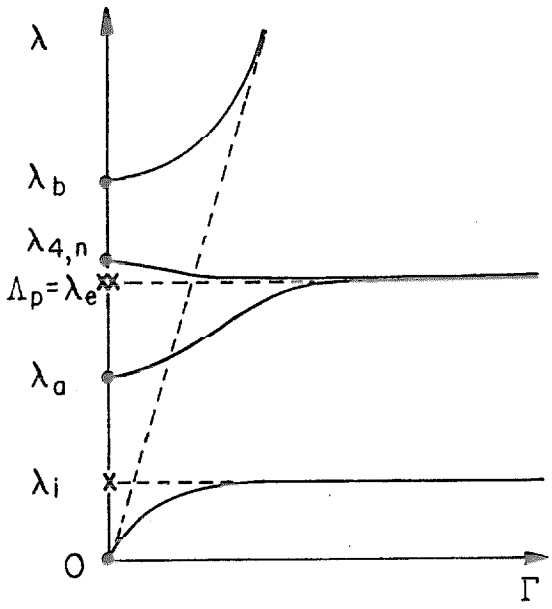

Ⅳ-7(2b) $\lambda_b > \lambda_{4,n}$

$\Lambda_p = \lambda_e$

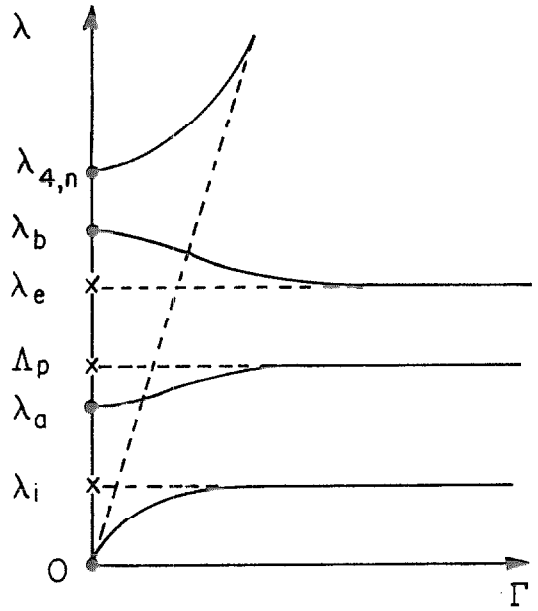

IV-7(3a) $\lambda_{4,n} > \lambda_b$

$\lambda_e > \Lambda_p > \lambda_a$

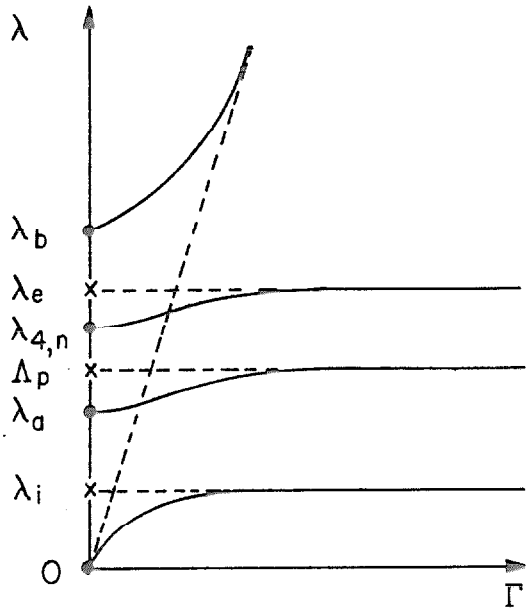

IV-7(3b) $\lambda_b > \lambda_e > \lambda_{4,n}$

$\lambda_{4,n} > \Lambda_p > \lambda_a$

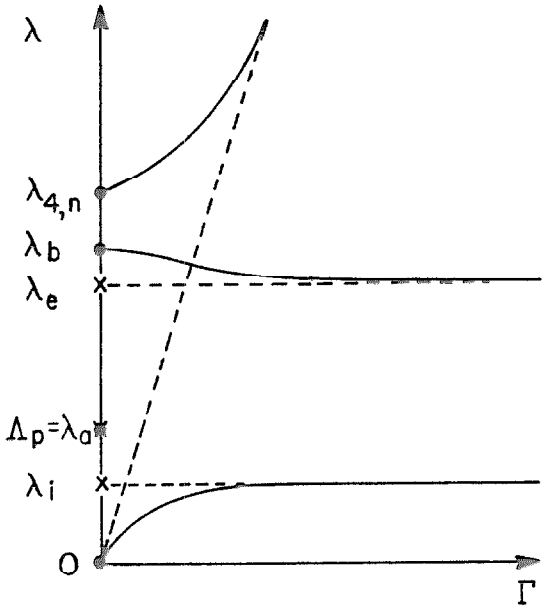

IV-7(4b) $\lambda_{4,n} > \lambda_b$

$\Lambda_p = \lambda_a$

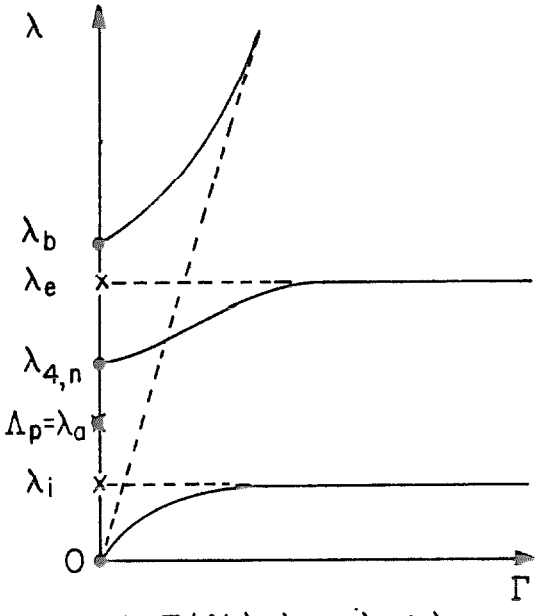

IV-7(4b) $\lambda_b > \lambda_e > \lambda_{4,n}$

$\Lambda_p = \lambda_a$

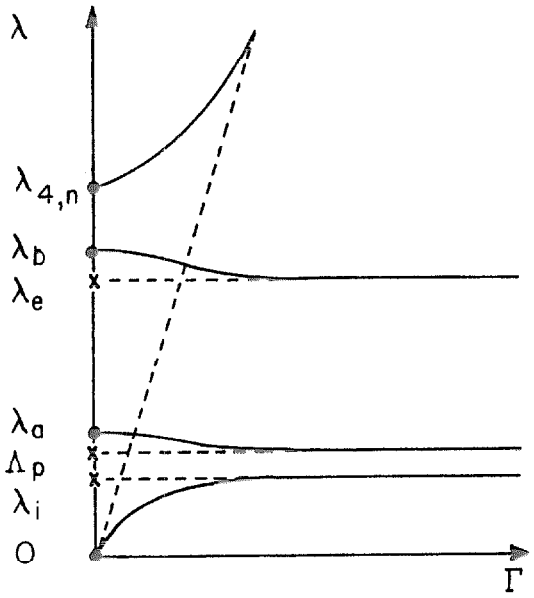

IV-7(5a) $\lambda_{4,n} > \lambda_b$

$\lambda_a > \Lambda_p > \lambda_i$

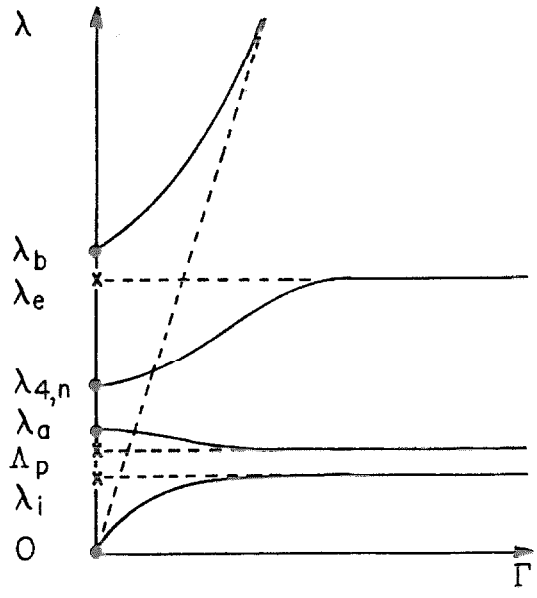

IV-7(5b) $\lambda_b > \lambda_e > \lambda_{4,n}$

$\lambda_a > \Lambda_p > \lambda_i$

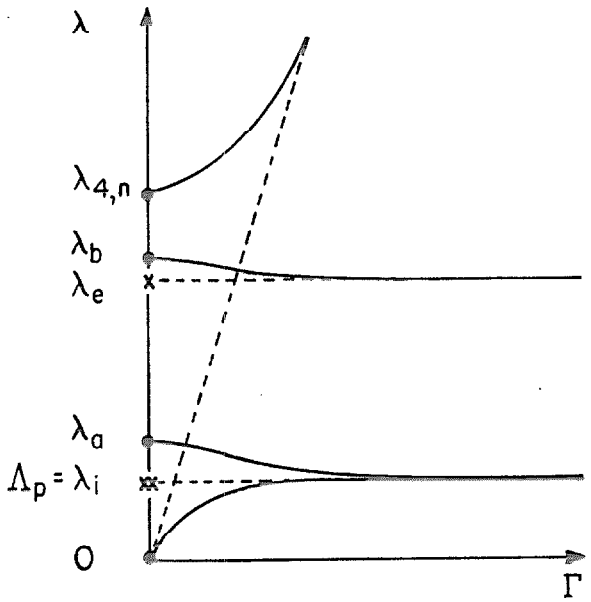

IV-7(6a) $\lambda_{4,n} > \lambda_b$

$\Lambda_p = \lambda_i$

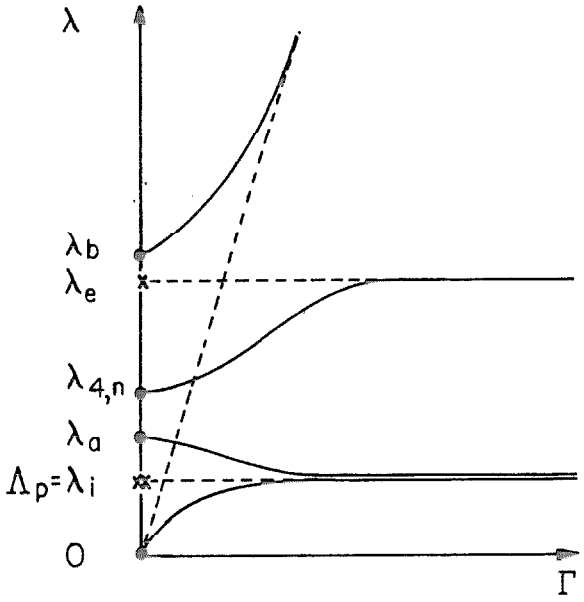

IV-7(6b) $\lambda_b > \lambda_e > \lambda_{4,n}$

$\Lambda_p = \lambda_i$

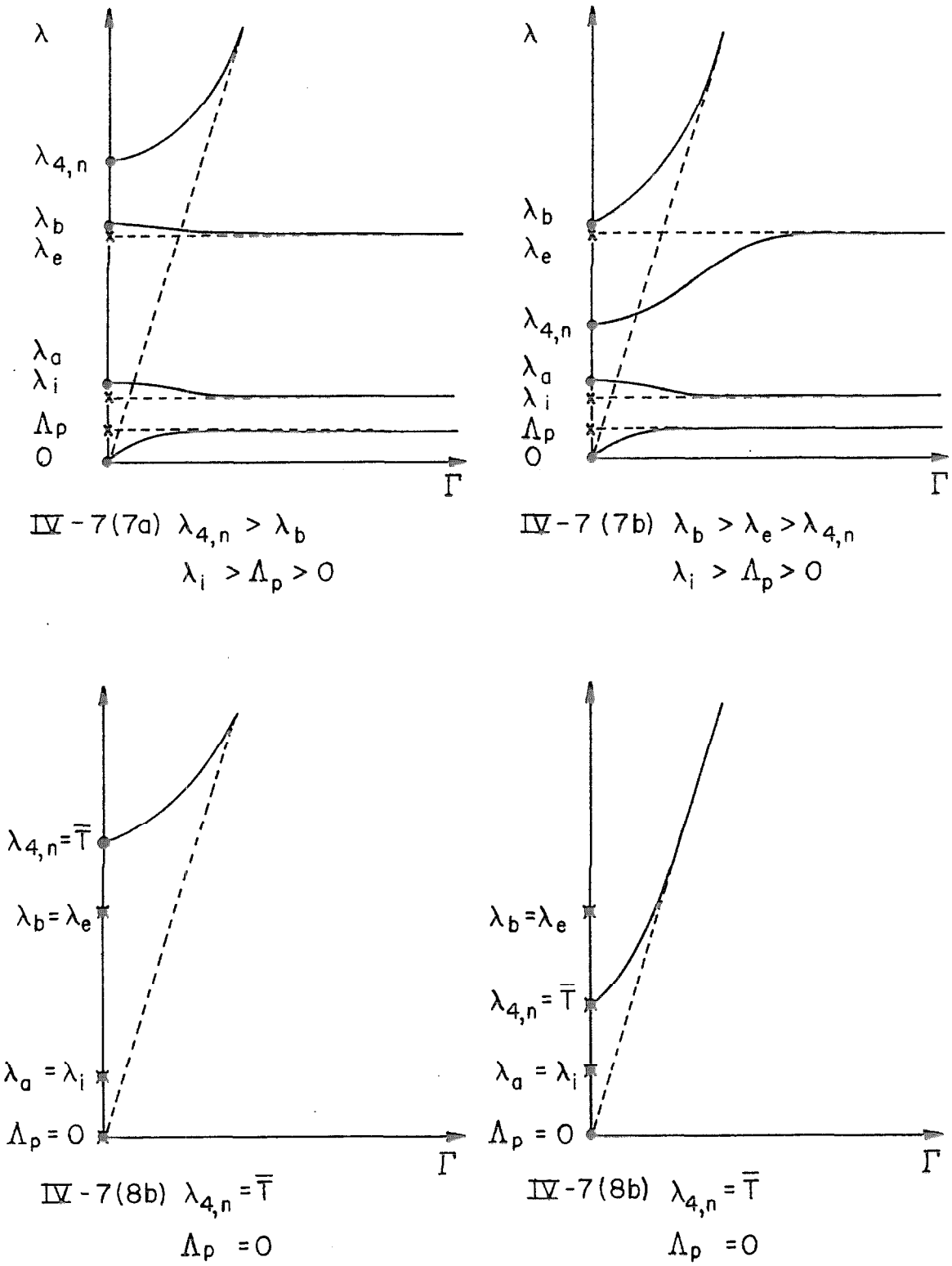

Figure IV-7. Wave dispersion in the TM narrow waveguide limit

the empty waveguide structure remains. The possible dispersion curves which result are sketched in Figure IV-7.

In drawing these sketches the inequality $\lambda_{4,n} > \lambda_a$ was employed. The validity of this inequality rests upon the assumption that $(Tr_o)^2 > (\lambda_i^2 - \Lambda_e^2)$. Suppose that $\Lambda_e = 0$, the lowest value Tr_o assumes is 2.4048, consequently a value of λ_i equal to 2.4000 still satisfies the assumption and, in a hydrogen plasma, corresponds to $\lambda_e = 1846\,\lambda_i = 4400$. Since this value of λ_e is difficult to attain in the laboratory, $\lambda_{4,n}$ is almost certainly greater than λ_a. Secondly, for a fixed magnetic field λ_e and a given mode Tr_o, $\lambda_{4,n}$ is either always larger or smaller than λ_b, independent of the plasma density.

In the next section the MHD limit and the narrow waveguide limit are found to agree at low frequencies where both approximations involve slow wave propagation.

Guided Magnetohydrodynamic Waves

At frequencies far below plasma resonance the plasma behaves like an incompressible conducting fluid. Distinctive of this domain, known as the magnetohydrodynamic (MHD) limit, are the Alfven and whistler modes of propagation. The principles of MHD transmission have already been introduced in connection with the plane waves of an unbounded magnetoactive plasma. The effect of the waveguide structure will now be investigated.

The analysis is divided into three parts; in each division suitable limiting expressions are chosen for the elements of the permittivity tensor. The Alfvén waves are the lowest frequency MHD modes to propagate. They occur in the range $0 \leq \omega \ll \omega_i$ where equations I-18a,b

for a neutral plasma $\left(\frac{\Omega_e^2}{\omega_e} = \frac{\Omega_i^2}{\omega_i}\right)$ reduce to

$$\epsilon_1 = \left(1 + \frac{\Omega_e^2}{\omega_e^2} + \frac{\Omega_i^2}{\omega_i^2}\right)\epsilon_o = \frac{1}{\mu_o}\left(\frac{1}{V_a^2} + \frac{1}{V_c^2}\right) \approx \frac{1}{\mu_o V_a^2} \qquad \text{(IV-79a)}$$

$$\epsilon_2 = 0 \quad . \qquad \text{(IV-79b)}$$

The whistlers inhabit the next frequency range, $\omega_i \sim \omega \ll \omega_e$, where

$$\epsilon_1 = \left(\frac{\Omega_i^2}{\omega_i^2 - \omega^2}\right)\epsilon_o \qquad \text{(IV-80a)}$$

$$\epsilon_2 = \frac{i}{\omega}\left[\frac{\Omega_e^2}{\omega_e} - \frac{\Omega_i^2\,\omega_i}{\omega_i^2 - \omega^2}\right] = -\frac{\omega}{\omega_i}\epsilon_1 \quad . \qquad \text{(IV-80b)}$$

For $\omega \ll \omega_i$ these expressions agree with the Alfvén dielectric constants, because in a neutral plasma

$$\frac{\Omega_i^2}{\omega_i^2} = \frac{\omega_e}{\omega_i}\left(\frac{\Omega_e^2}{\omega_e^2}\right) \gg \frac{\Omega_e^2}{\omega_e^2} \gg 1 \quad .$$

Near the electron cyclotron frequency a better approximation is

$$\epsilon_1 = \left(\frac{\Omega_e^2}{\omega_e^2 - \omega^2}\right)\epsilon_o \qquad \text{(IV-81a)}$$

$$\epsilon_2 = +\frac{\omega}{\omega_e}\epsilon_1 \quad . \qquad \text{(IV-81b)}$$

The transition from expressions IV-80 to IV-81 occurs at the geometric mean of cyclotron frequencies, $\sqrt{\omega_e\omega_i}$; there IV-80a and IV-81a are equal.

Alfvén waves. Using the transverse permittivities defined by IV-79, the

coupled wave equations II-10 and II-11 immediately separate into

$$\nabla_t^2 H_z + S^2 H_z = 0 \qquad S^2 = -\gamma_\perp = h^2 + \omega^2\left(\frac{1}{V_a^2} + \frac{1}{V_c^2}\right) \qquad \text{(IV-82)}$$

$$\nabla_t^2 E_z + T^2 E_z = 0 \qquad T^2 = -\frac{\epsilon_3}{\epsilon_1}\gamma_1 = \frac{\epsilon_3}{\epsilon_1}\left[h^2 + \omega^2\left(\frac{1}{V_a^2} + \frac{1}{V_c^2}\right)\right] . \qquad \text{(IV-83)}$$

A comparison of these relations with IV-63a and IV-63b confirms that the MHD and narrow waveguide approximations approach a common limit as $\omega \to 0$.

The TE modes that arise as solutions to equation IV-82 have

$$H_z = H_o J_n(Sr) e^{-jn\theta} \qquad \text{and} \qquad E_z = 0 \quad . \qquad \text{(IV-84)}$$

The transverse fields evaluated by means of equations II-8 and II-9 are simply

$$\underline{E}_t = \frac{-j\omega\mu_o}{h}(\underline{e}_z \times \underline{H}_t) = \frac{-j\omega\mu_o}{\gamma_1}(\underline{e}_z \times \nabla_t H_z) \quad . \qquad \text{(IV-85)}$$

For $E_\theta = H_r = 0$ on the conducting wall at r_o , it is necessary to choose an S which satisfies $J_n'(Sr_o) = 0$. Then, according to equation IV-82, the TE Alfvén wave dispersion is

$$-h^2 = \omega^2\left(\frac{1}{V_a^2} + \frac{1}{V_c^2}\right) - S^2 \qquad \text{with} \qquad J_n'(Sr_o) = 0 \quad . \qquad \text{(IV-86)}$$

This wave does not propagate at zero frequency but cuts off $(h = 0)$ when

$$\omega = S\left(\frac{1}{V_a^2} + \frac{1}{V_c^2}\right)^{-1/2} = SV_c\left(1 + \frac{\Omega_e^2}{\omega_e^2} + \frac{\Omega_i^2}{\omega_i^2}\right)^{-1/2} \approx \frac{\omega_i}{\Omega_i} SV_c \quad . \qquad \text{(IV-87)}$$

This is the MHD behavior of cut-off frequency $\omega_{\perp,n}$ (cf. equations

III-39 and III-40.)

The solutions to the TM wave equation IV-83 which are regular on the waveguide axis are

$$E_z = E_o J_n(Tr)e^{-jn\theta} \qquad \text{and} \qquad H_z = 0 \quad . \tag{IV-88}$$

Since H_z and ϵ_2 are both zero, the transverse fields given by equations II-8 and II-9 become

$$\underline{E}_t = \frac{jh}{\omega \epsilon_1}(\underline{e}_z \times \underline{H}_t) = \frac{+h}{\gamma_1}\nabla_t E_z \quad . \tag{IV-89}$$

The boundary conditions $E_z = E_\theta = H_r = 0$ at r_o are conveniently satisfied if $J_n(Tr_o) = 0$. Equation IV-83 then yields the TM Alfvén wave dispersion relation

$$-n^2 = \omega^2\left(\frac{1}{V_a^2} + \frac{1}{V_c^2}\right) - \frac{\epsilon_1}{\epsilon_3}T^2 \qquad \text{with} \qquad J_n(Tr_o) = 0 \; . \tag{IV-90}$$

In accordance with the approximation that $\epsilon_2 = 0$ as $\omega \to 0$, note that

$$\epsilon_3 = \left(1 - \frac{\Omega_p^2}{\omega^2}\right)\epsilon_o \to -\infty \quad .$$

As a result equation IV-90 reduces to

$$\beta = \omega\left(\frac{1}{V_a^2} + \frac{1}{V_c^2}\right)^{1/2} \approx \frac{\omega}{V_a} \quad , \qquad \alpha = 0 \quad . \tag{IV-91}$$

The same expression also characterizes the dispersionless propagation of a plane Alfvén wave in an infinite plasma. Unlike the plane wave, the displacement vector of the waveguide mode has a longitudinal component $D_z = \epsilon_3 E_z$ which, to remain finite as $\epsilon_3 \to -\infty$, requires $E_z \to 0$. The transverse fields do not vanish with E_z because by equation IV-83,

$\gamma_1 = -\frac{\epsilon_1}{\epsilon_3} T^2$, so that IV-89 reads

$$\underline{E}_t = \frac{-\beta}{\omega \epsilon_1} (\underline{e}_z \times \underline{H}_t) = \frac{-j\beta}{\epsilon_1 T^2} \nabla_t D_z \quad . \tag{IV-92}$$

Thus as ω nears zero, both the electric and magnetic vectors of this mode become transverse to the guide axis; although the displacement vector continues to retain a longitudinal component.

The guided TM Alfvén wave also differs from the plane wave by having a transverse spatial dependence that satisfies certain boundary conditions, viz. $E_z\big|_{r_o} = E_\theta\big|_{r_o} = H_r\big|_{r_o} = 0$. The circular symmetric mode, however, is an exception because according to equation IV-92 these three field components are identically zero. The remaining fields are

$$\underline{E}_r = \frac{\beta}{\omega \epsilon_1} H_\theta = \frac{j\beta D_o}{\epsilon_1 T} J_1(Tr) \tag{IV-93}$$

where $D_o = \epsilon_3 E_o$. T is determined entirely by the source currents. If $T = 0$

$$H_\theta = \frac{\omega \epsilon_1}{\beta} E_r = \frac{1}{2}(j\omega D_o) r \quad . \tag{IV-94}$$

The source for this field is a uniform axial current

$$\underline{I} = \nabla \times \underline{H} = \frac{1}{r} \frac{\partial}{\partial r} (rH_\theta) \underline{e}_z = (j\omega D_o) \underline{e}_z \quad . \tag{IV-95}$$

Other studies of this MHD range have been conducted by R. W. Gould (11) and by J. Schmoys and E. Mishkin (12).

<u>The whistler mode of propagation.</u> Above the Alfvén range, the permittivity ϵ_1 is no longer a constant and ϵ_2 is different from zero, although if $\Omega_p \gg \omega$, ϵ_3 remains large and negative. In fact, ϵ_3 will be assumed infinite with the

justification that it is generally much larger than ϵ_1 and ϵ_2, and that this assumption results in a considerable simplification of the problem.

For $\epsilon_3 = -\infty$ the coupled equations II-10 and II-11 reduce to $E_z = 0$ and

$$\nabla_t^2 H_z + S^2 H_z = 0 \qquad \text{with} \qquad S^2 = \frac{\omega\mu_o}{d} = -\frac{\gamma_1^2 - \gamma_2^2}{\gamma_1} \quad . \tag{IV-96}$$

According to equations II-8 and II-9 the transverse fields produced by H_z are

$$\underline{E}_t = \frac{j\omega\mu_o}{-h}(\underline{e}_z \times \underline{H}_t) = b\nabla_t H_z + jd(\underline{e}_z \times \nabla_t H_z) \quad . \tag{IV-97}$$

The solution

$$H_z = H_o J_n(Sr) e^{-jn\theta} \tag{IV-98}$$

must satisfy the boundary condition

$$\underline{E}_\theta\Big|_{r_o} = \frac{j\omega\mu_o}{-h} H_r\Big|_{r_o} = \frac{-j\omega\mu_o}{\gamma_1^2 - \gamma_2^2}\frac{H_o}{r_o}\left[\gamma_2 n\, J_n(Sr_o) + \gamma_1(Sr_o)J_n'(Sr_o)\right]e^{-jn\theta} = 0 \quad .$$

Thus TE magnetohydrodynamic dispersion is defined by

$$\gamma_2 n\, J_n(Sr_o) + \gamma_1(Sr_o)\, J_n'(Sr_o) = 0 \tag{IV-99a}$$

and by equation IV-96 for S^2 which, when simplified using equation II-3 and the quadratic formula, becomes

$$-h^2 = (\omega^2\mu_o\epsilon_1 - \frac{S^2}{2}) \pm \sqrt{(\frac{S^2}{2})^2 + (\omega^2\mu_o\epsilon_2)^2} \quad . \tag{IV-99b}$$

If ϵ_1 and ϵ_2 are described by IV-79, the lower sign of equation IV-99b provides the TE dispersion relation IV-86, while the upper sign yields the

TEM dispersion relation IV-91 of the Alfvén domain. This illustrates that propagation of the principal (TEM) mode (9) near zero frequency may be treated as the limit of either a TM or a TE wave. Note further that with $\epsilon_2 = 0$ the sign of n does not enter into equation IV-99a. However, at higher frequencies where $\epsilon_2 \neq 0$ the first term produces a shift in the TE wave dispersion which takes opposite directions for each sign of n .

Using the transverse permittivities of equation IV-80 for the region $\omega \sim \omega_i$, equation IV-99b becomes

$$-h^2 = \left(\frac{\omega}{V_c}\right)^2 \left| \frac{\Omega_i^2}{\omega_i^2 - \omega^2} \right| - \frac{S^2}{2} \pm \sqrt{\left(\frac{S^2}{2}\right)^2 + \left(\frac{\omega}{V_c}\right)^4 \left(\frac{\omega}{\omega_i}\right)^2 \left(\frac{\Omega_i^2}{\omega_i^2 - \omega^2}\right)^2} \quad . \quad \text{(IV-100)}$$

As $\omega \to 0$, this statement agrees with the Alfvén dispersion relations. Near the ion cyclotron frequency the wave dispersion is approximately

$$-h^2 \approx \left(\frac{\omega}{V_c}\right)^2 \frac{\Omega_i^2}{\omega_i(\omega_i \mp \omega)} \quad . \quad \text{(IV-101)}$$

As a result the principal mode (upper sign) resonates at the ion cyclotron frequency; above resonance this mode is evanescent, since h is real. As ω is increased from 0 to ω_i , the phase velocity of the principal wave decreases monotonically from the Alfvén velocity $V_a \approx \frac{\omega_i}{\Omega_i} V_c$ to zero at resonance.

The other TE wave (lower sign) does not resonate with the gyrating ions but exhibits a cut-off at $\omega_{1,n} = \frac{\omega_i}{\Omega_i} SV_c$ in accordance with equation IV-87 of the Alfvén limit. Above cut-off the wave propagates with a phase velocity which has nearly a parabolic frequency behavior. This is the waveguide equivalent of the whistler mode. In the range $\omega_i < \omega \ll \omega_e$ where S^2 is negligible relative to $\omega^2 \mu_o \epsilon_2$, equation IV-100 can be approximated by

$$-h^2 = \left[\left(\frac{\omega}{V_c}\right)^2 \frac{\Omega_i^2}{\omega_i(\omega_i + \omega)} - \frac{S^2}{2} \right] \approx \frac{1}{V_c^2} \frac{\Omega_e^2}{\omega_e} \left[\omega - \frac{\omega_{l,n}^2}{2\omega_i} \right] \qquad \text{(IV-102)}$$

because in a neutral plasma $\frac{\Omega_i^2}{\omega_i} = \frac{\Omega_e^2}{\omega_e}$. This wave has a phase velocity

$$V_{ph} = \frac{\omega}{\beta} = V_c \sqrt{\frac{\omega \omega_e}{\Omega_e^2}} \Bigg/ \sqrt{1 - \frac{\omega_{l,n}^2}{2\omega\,\omega_i}} \qquad \text{(IV-103)}$$

and a group velocity

$$V_g = \left(\frac{d\beta}{d\omega}\right)^{-1} = 2V_c \sqrt{\frac{\omega\omega_e}{\Omega_e^2}} \sqrt{1 - \frac{\omega_{l,n}^2}{2\omega\,\omega_i}} \quad . \qquad \text{(IV-104)}$$

These expressions should be compared to equations IV-56 and IV-57. Note that the product of the group and phase velocities for the guided whistler modes and for the plane wave whistlers are equal.

$$(V_{ph} V_g)_{\text{waveguide}} = 2V_c^2 \left(\frac{\omega\omega_e}{\Omega_e^2}\right) = (V_{ph} V_g)_{\text{plane wave}} \quad . \qquad \text{(IV-105)}$$

Dellis and Weaver (26) have observed the whistler mode in a waveguide. The results they report were analyzed only qualitatively on the basis of a plane wave theory neglecting ion motion. The theory developed here should provide additional insight to the interpretation of their experiment.

In the third frequency range characterized by the permittivities of equation IV-81, equation IV-99b is

$$-h^2 = \left(\frac{\omega}{V_c}\right)^2 \left(\frac{\Omega_e^2}{\omega_e^2 - \omega^2}\right) - \frac{S^2}{2} \pm \sqrt{\left(\frac{S^2}{2}\right)^2 + \left(\frac{\omega}{\omega_e}\right)^2 \left(\frac{\omega}{V_c}\right)^4 \left(\frac{\Omega_e^2}{\omega^2 - \omega_e^2}\right)^2} \quad . \qquad \text{(IV-106)}$$

At $\omega = \sqrt{\omega_i \omega_e}$ this and equation IV-100 are identical.

It follows from IV-100 and IV-106 that the wave which propagates at the ion cyclotron frequency resonates at ω_e . Above the electron cyclotron frequency both this wave and the principal mode are evanescent.

The MHD dispersion curves. The field and dispersion relations IV-97 through IV-99b are valid over the entire MHD range if the complete expressions I-18 for the permittivities are used. Equations IV-99 can be derived directly from the exact dispersion relations II-16 and II-36:

$$\left[\gamma_1^2 - \gamma_2^2 + \gamma_1 T^2\right] - \frac{T^2}{\omega^2 \mu_o \epsilon_3}\left[\gamma_1^2 - \gamma_2^2 + \gamma_1 T^2 + k^2(\gamma_1 + T^2)\right] = 0 \qquad \text{(II-16)}$$

$$bn(T_1^2 - T_2^2) + (\omega\mu_o - dT_1^2)\frac{(T_2 r_o)J_n'(T_2 r_o)}{J_n(T_2 r_o)} - (\omega\mu_o - dT_2^2)\frac{(T_1 r_o)J_n'(T_1 r_o)}{J_n(T_1 r_o)} = 0 \qquad \text{(II-36)}$$

through a limiting process. Evidently allowing ϵ_3 to become infinite reduces II-16 to

$$T_1^2 = -\frac{\gamma_1^2 - \gamma_2^2}{\gamma_1} = \frac{\omega\mu_o}{d} \quad .$$

Substituting $T_1^2 = S^2 = \frac{\omega\mu_o}{d}$ into equation II-36 and cancelling the common $(\omega\mu_o - dT_2^2)$ factor leaves

$$\frac{bn}{d} - \frac{(Sr_o)\,J_n'(Sr_o)}{J_n(Sr_o)} = 0 \quad .$$

Upon replacing b and d according to equations II-4, this becomes equation IV-99a.

Using equations IV-99, the dispersion curves for the lowest circular symmetric and the first angular dependent modes are sketched on the following page. Indicated on the sketches are the critical frequencies,

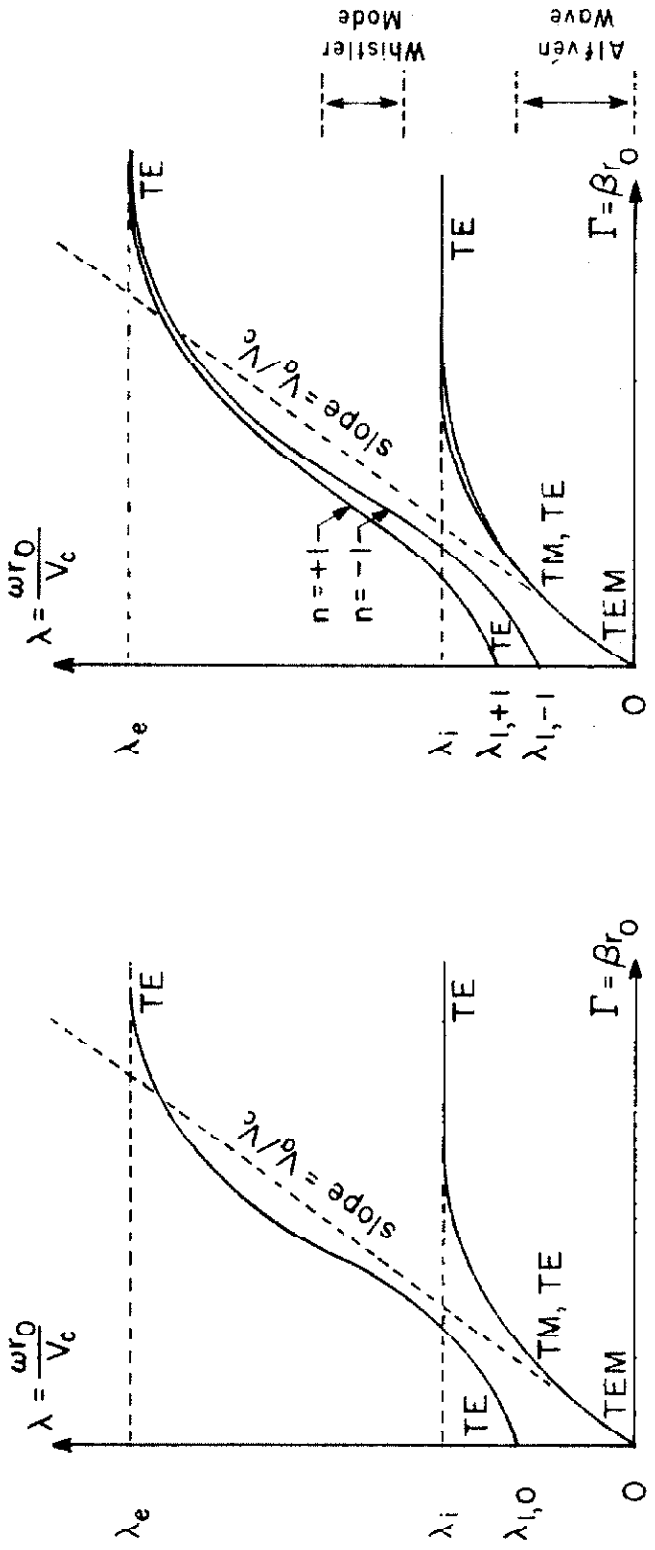

Figure IV-8. The MHD dispersion limit, equations IV-99a,b

the domains of analysis, and the primary character of the fields. Observe that according to equations III-40b and III-26 the cut-off frequencies $\omega_{2,n}$, $\omega_{3,n}$ and $\omega_{4,n}$ are removed to infinity along with Ω_p in the MHD limit.

These diagrams indicate that the TE branch which resonates at λ_i blends at smaller frequencies into a wave which may be excited in either the TE or TM mode. At the lowest frequencies, the longitudinal electric and magnetic components of these modes vanish and TEM waves result. A distinctive feature of the angular dependent waves is that both the left ($n = -1$) and the right ($n = +1$) "circular" polarizations of the fields resonate at each cyclotron frequency. This contrasts with the plane wave limit for which only the left circular polarized wave resonates with the ions, and only the right circular polarized wave resonates with the electrons. The following physical explanation is offered.

The transverse field configuration of the first angular dependent TE mode may be resolved into two components, a uniform field and a correction field, Figure IV-9. Both field components are necessary in order to fulfill the boundary conditions, but each resonates with a different type of charge. When the uniform field rotates in the same sense and at the same rate as one of the charge species, the electromagnetic energy of the wave is converted into the cyclotron motion of that species. Propagation halts and the wave is evanescent. The details of this resonance are exactly like the cyclotron interaction experienced by a plane wave. The anomalous cyclotron wave resonance is explained by the correction pattern which accounts for the curvature of

the TE_{11} field. As the correction pattern rotates, it periodically reverses at each observation point at the same rate at which the uniform field rotates. The correction field is capable of accelerating either type of charge provided that it has the proper phase and frequency relative to the orbiting particle. If the guide radius is increased, the correction field vanishes leaving only the selective resonance of a uniform plane wave.

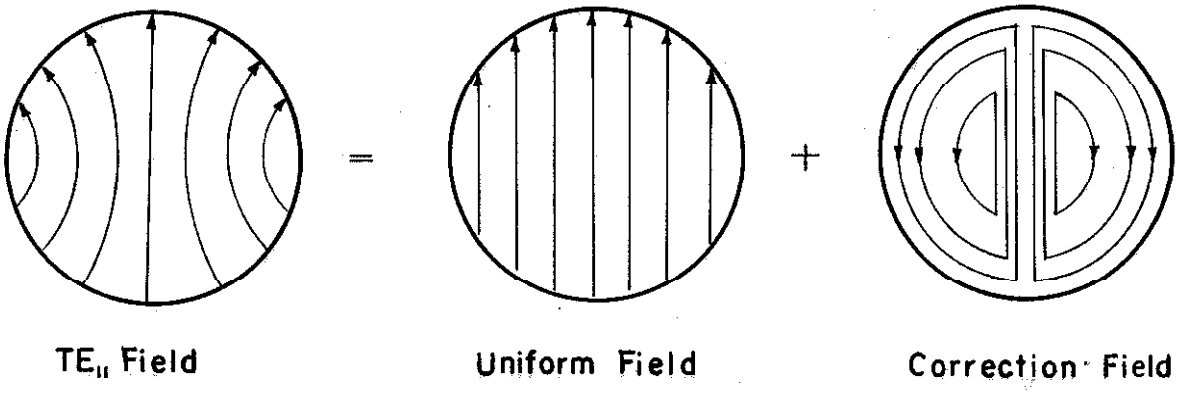

Figure IV-9. The resolution of the TE_{11} electric field into two component fields.

CHAPTER V. WAVE DISPERSION IN THE CIRCULAR PLASMAGUIDE

Various limiting conditions were introduced in Chapter IV for which the dispersion reduced to simple TE, TM, or plane wave propagation. In this chapter these limiting cases are compared numerically with several representative solutions of the exact dispersion relation. Once again the equations of primary interest are

$$\left[\gamma_1^2 - \gamma_2^2 + \gamma_1 T^2\right] - \frac{T^2}{\omega^2 \mu_o \epsilon_3}\left[\gamma_1^2 - \gamma_2^2 + \gamma_1 T^2 + h^2(\gamma_1 + T^2)\right] = 0 \qquad \text{(II-16)}$$

$$\frac{bn(T_1^2 - T_2^2)}{(\omega\mu_o - dT_1^2)(\omega\mu_o - dT_2^2)} + \frac{(T_2 r_o)\, J_n'(T_2 r_o)}{(\omega\mu_o - dT_2^2) J_n(T_2 r_o)} - \frac{(T_1 r_o)\, J_n'(T_1 r_o)}{(\omega\mu_o - dT_1^2) J_n(T_1 r_o)} = 0 \,. \qquad \text{(II-36)}$$

Equation II-16 is biquadratic in T with coefficients that are either real or complex, depending upon the nature of h. If h is real or purely imaginary, the coefficients are real and the two values of T^2 are either real or complex conjugates. The T's are either both real, both imaginary, one real and one imaginary, or else complex conjugates of one another.

When both roots are real, or else T_1 is real and T_2 is imaginary, the magnitude of T_2 is found to exceed T_1. For the ranges of propagation considered in Chapter IV, T_1 is either very nearly a solution of $J_n(T_1 r_o) = 0$ or else of $J_n'(T r_o) = 0$. Accordingly, the second root is many orders of magnitude larger than T_1. If T_2 is large and real, $J_n(T_2 r)$ is small. If T_2 is imaginary, Φ_2 decays rapidly toward the plasma interior until within the main body of the plasma the fields have a spatial dependence characteristic

of T_1 . Whether T_2 is real or imaginary, $\tau_2 = j(\frac{\omega\mu_o}{cT_2^2} - \frac{d}{c})$ is considerably smaller than τ_1 and the longitudinal electric field is primarily determined by T_1 , i.e., $E_z \approx \tau_1 \Phi_1 \approx \tau_1 H_z$. Depending upon whether τ_1 is much smaller or much larger than unity, E_z or H_z may be neglected. The field configuration is then predominantly TE or TM, although the finite size of T_2 guarantees that the fields are always mixed.

The conditions under which T_1 and T_2 are both imaginary are particularly restrictive. As an example, consider the circular symmetric modes. When both radial constants are imaginary and $n = 0$, equation II-36 becomes

$$\frac{F(|T_2 r_o|)}{F(|T_1 r_o|)} = \frac{\omega\mu_o + d|T_2|^2}{\omega\mu_o + d|T_1|^2} \tag{V-1}$$

where

$$F(|x|) = \frac{|x|\, I_1(|x|)}{I_o(|x|)} \tag{V-2}$$

and $I_n(|x|)$ is the modified Bessel function of the first kind. The left hand side of dispersion relation V-1 is a monotonically increasing function of the waveguide radius with unit initial value at $r_o = 0$ and asymptotic limit $\left|\frac{T_2}{T_1}\right|$ at $r_o = \infty$. The right hand side is independent of the radius, so that unless:

$$1 < \frac{\omega\mu_o + d|T_2|^2}{\omega\mu_o + d|T_1|^2} < \left|\frac{T_2}{T_1}\right| \tag{V-3}$$

the two functions will not intersect and the equality demanded by V-1 cannot be satisfied. Since equation V-1 has at most one solution, the

number of modes existing at each frequency is also limited to one. As illustrated in Figures V-1c and V-1f, this mode has a maximum amplitude nearest the waveguide wall. Surface waves of this sort are usually associated with ripples on the plasma-air interface of a partially filled plasmaguide (8,27). This is the first indication that such a wave might exist in a completely filled plasmaguide.

The conditions under which waves with complex conjugate T values propagate are not as restrictive as one might suspect. Equation II-36 for the circular symmetric mode having $T_1 = T_2^* = T$ is

$$\frac{F(T^* r_o)}{F(T r_o)} = \frac{\omega\mu_o - d(T^*)^2}{\omega\mu_o - d(T)^2} \qquad (V\text{-}4)$$

with

$$F(x) = \frac{x\, J_1(x)}{J_o(x)} \quad . \qquad (V\text{-}5)$$

The left hand side of V-4 varies from 1 to $\frac{T^*}{T}$ as r_o ranges from zero to infinity. As in equation V-1, the right hand side is independent of r_o. However, unlike V-1, the real part of T introduces damped oscillations into the function $\frac{F(T^* r_o)}{F(T r_o)}$ with the result that numerous intersections now occur where formerly (with T_1 and T_2 imaginary) only one solution existed. A necessary condition for the existence of a pair of complex conjugate radial constants is obtained, using equation II-3, by writing equation II-16 in standard form:

$$T^4 + \left[\gamma_1\left(1 + \frac{\epsilon_3}{\epsilon_1}\right) + \gamma_2 \frac{\epsilon_2}{\epsilon_1}\right] T^2 + \frac{\epsilon_3}{\epsilon_1}\left(\gamma_1^2 - \gamma_2^2\right) = 0 \quad , \qquad (V\text{-}6)$$

and requiring the discriminant to be negative:

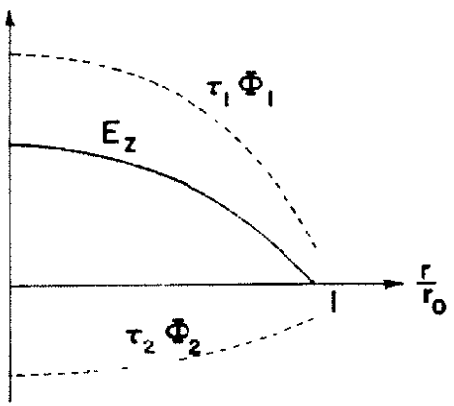

a) n=0, T_1 and T_2 real

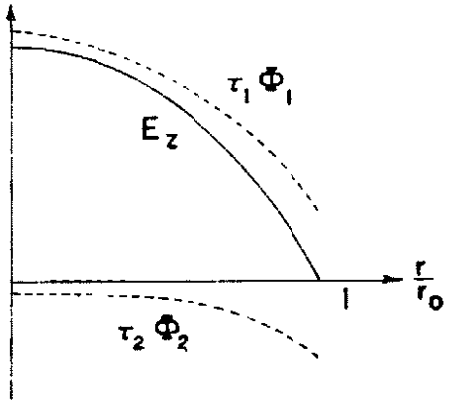

b) n=0, T_1 real, T_2 imaginary

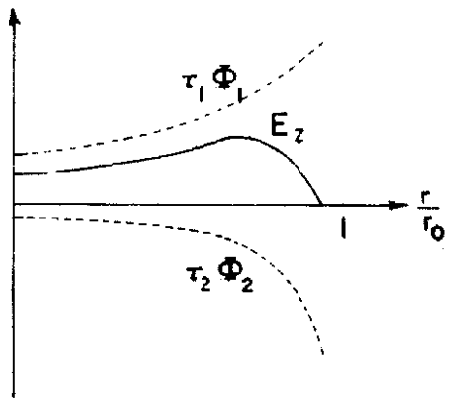

c) n=0, T_1 and T_2 imaginary

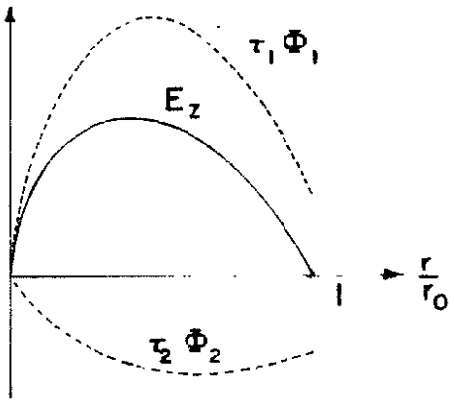

d) n=±1, T_1 and T_2 real

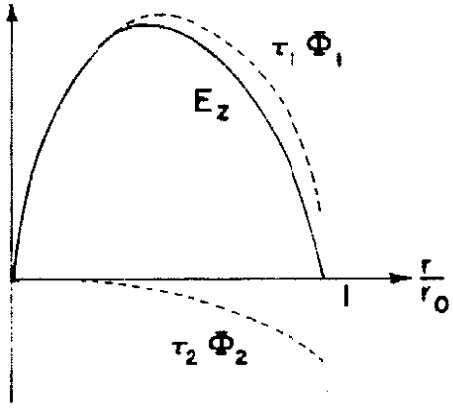

e) n=±1, T_1 real, T_2 imaginary

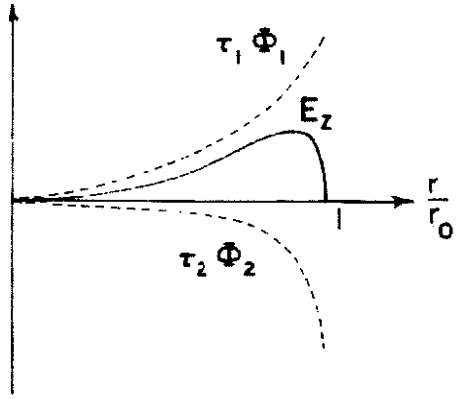

f) n=±1, T_1 and T_2 imaginary

Figure V-1. The radial variation of the longitudinal electric field for the lowest modes of the circularly symmetric and first angularly dependent waves

$$\left[\gamma_1\left(1 + \frac{\epsilon_3}{\epsilon_1}\right) + \gamma_2 \frac{\epsilon_2}{\epsilon_1} \right]^2 - 4 \frac{\epsilon_3}{\epsilon_1} (\gamma_1^2 - \gamma_2^2) < 0 \qquad \text{(V-7)}$$

Sketches of the possible radial variations of the longitudinal electric field appear in Figure V-1 for the circular symmetric and first angular dependent modes. In contrast to the TM and TE modes of Chapter IV whose boundary conditions require $J_n(Tr_o) = 0$ or $J_n'(Tr_o)=0$, respectively, the field distributions pictured in Figure V-1 are dependent upon the frequency through equation II-36.

The contour of the dispersion surface defined by equation II-16 and II-36 is in most cases very irregular and the roots are usually discovered only by laborious effort. Nevertheless, by means of a perturbation expansion about the MHD dispersion limit IV-99a,b, D. G. Swanson (28) has developed a FORTRAN program which calculates the circular symmetric (n = 0) wave dispersion for very dense plasmas in strong magnetostatic fields. Figures V-2a,b,c for $\lambda_e = 50$ and $\Lambda_e = 800$ were evaluated using this program on the IBM 7090 digital computer at C.I.T. For situations remote from the MHD limit this program fails and one is forced to use less automated programs which require continual monitoring during computation. The propagation characteristics summarized in Figure V-3 for $\lambda_e = 1$, $\Lambda_e = 2$ were evaluated in this manner. The close correspondence between this diagram and the narrow waveguide approximation, Figure V-4, suggests that a perturbation analysis of the narrow waveguide limit may yield the exact solutions more efficiently. This figure also compares the quasi-static approximation.

The normalized parameters $\lambda_e = 50$, $\Lambda_e = 800$ are pertinent to recent shock tube investigations here (28) and at other laboratories (26,

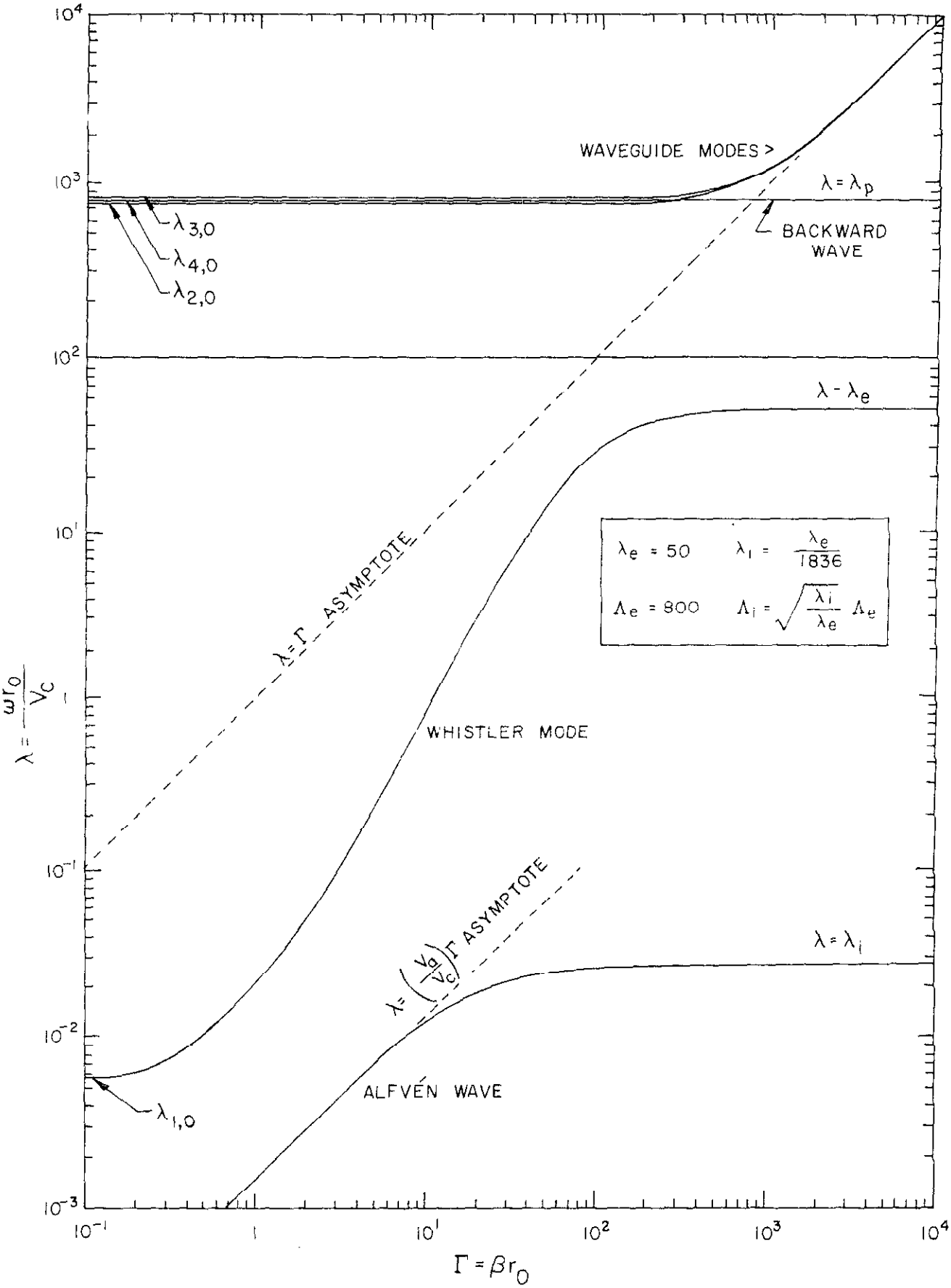

Figure V-2a. The dispersion diagram for the lowest radial order, circularly symmetric (n = 0) mode

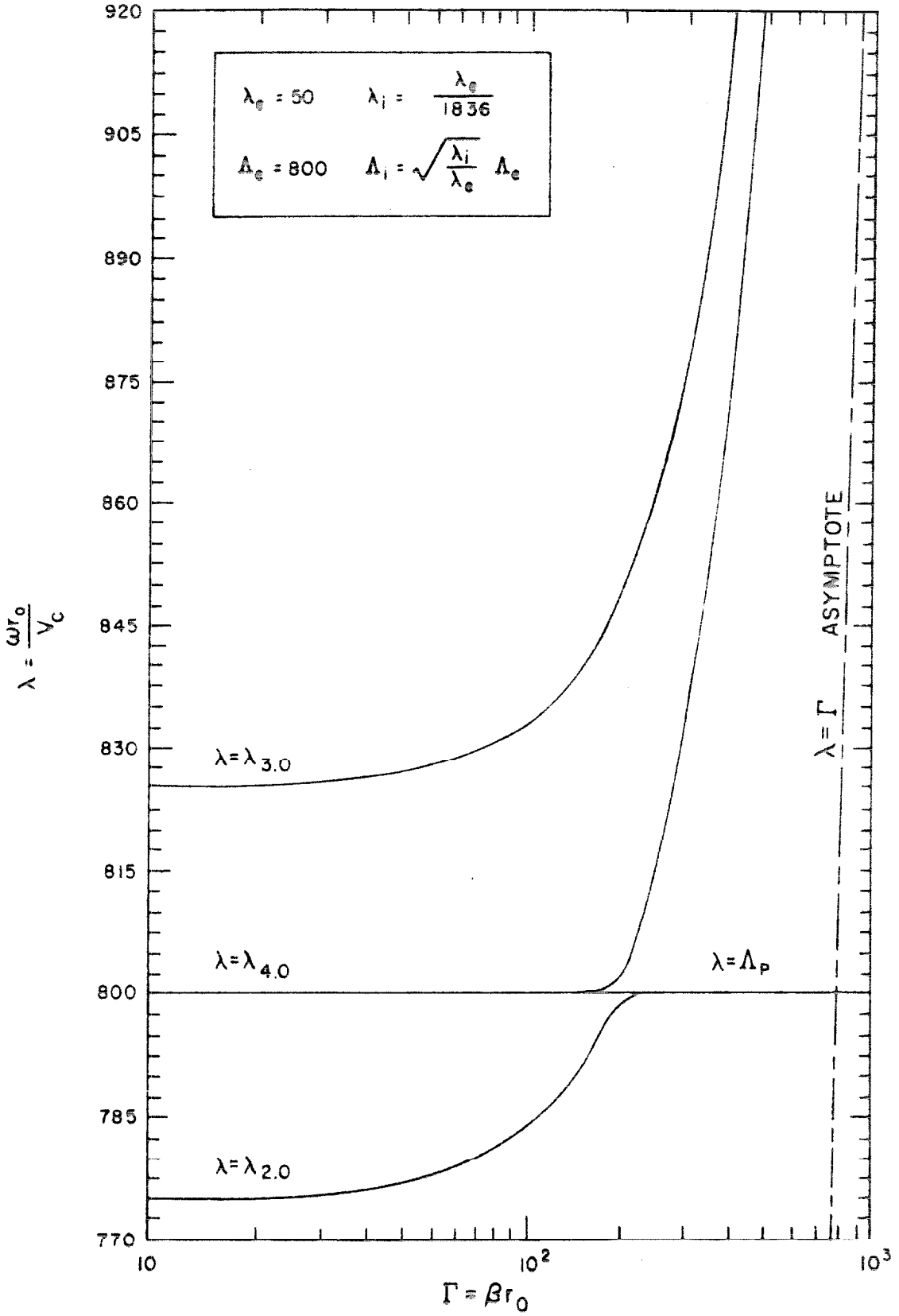

Figure V-2b. The waveguide modes of Figure V-2a

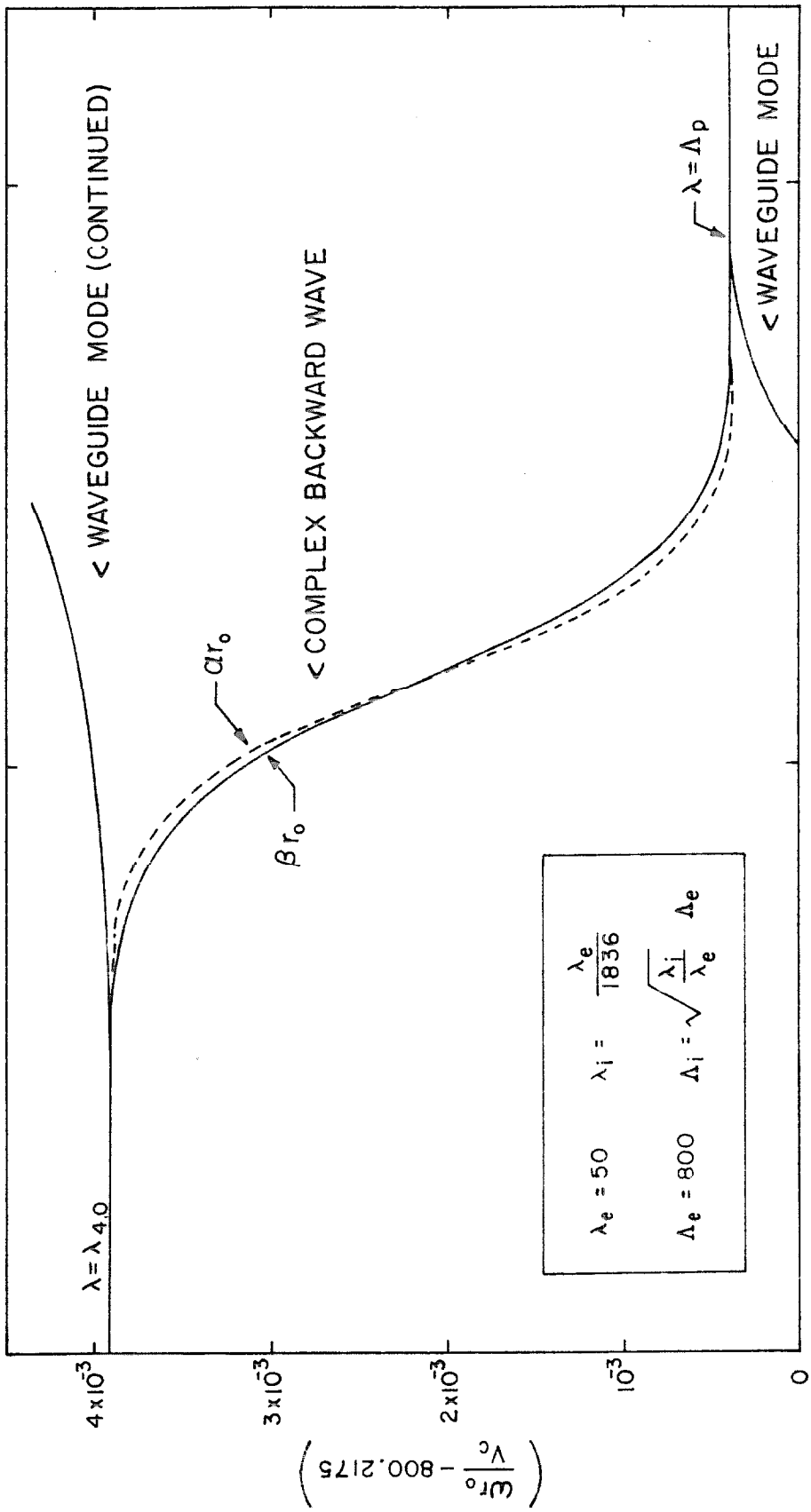

Figure V-2c. The complex backward wave of Figure V-2a.

29,30). The Alfvén wave and the whistler mode appear at the lowest frequencies of Figure V-2a as anticipated. The agreement between the exact dispersion and the MHD limit is so good that to the scale of this drawing the two are indiscernible. At the higher frequencies the inertia of the particles acts to prevent the ions and electrons from following the variation of the field. As a result, $\epsilon_1 \to \epsilon_3 \to \epsilon_o$ and $\epsilon_2 \to 0$ as $\omega \to \infty$, and the dispersion becomes that of an empty waveguide. The waves that occur near Λ_p are reminiscent of plane wave dispersion (cf. Figure IV-4). However, the effect of the waveguide surface is to couple the electrostatic plasma oscillation at Λ_p to the "ordinary" plane wave. The backward wave which results between $\lambda_{4,0}$ and Λ_p has a complex propagation constant whose real and imaginary parts are nearly equal. The existence of a complex wave at these frequencies was predicted by Chorney (14). In addition to the wave with propagation constant h, the symmetry of $\underline{\underline{\epsilon}}$ requires the existence of waves with propagation constants $\pm h$ and $\pm h^*$. As will be shown in Chapter VI, a single complex wave cannot by itself transmit power. However, if a pair of complex modes corresponding to h and h^* is present, power may be transmitted. Since the structure is passive, the fields at infinity must remain finite. Consequently the spatially growing wave is never excited within an infinite, unobstructed waveguide. Because the plasma is lossless, the spatially attenuated complex wave is not the result of dissipation.

The dispersion diagram of Figure V-3 for $\lambda_e = 1$, $\Lambda_e = 2$ has a completely different nature. These values of the normalized parameters are appropriate for microwave tube design where smaller magnetic fields,

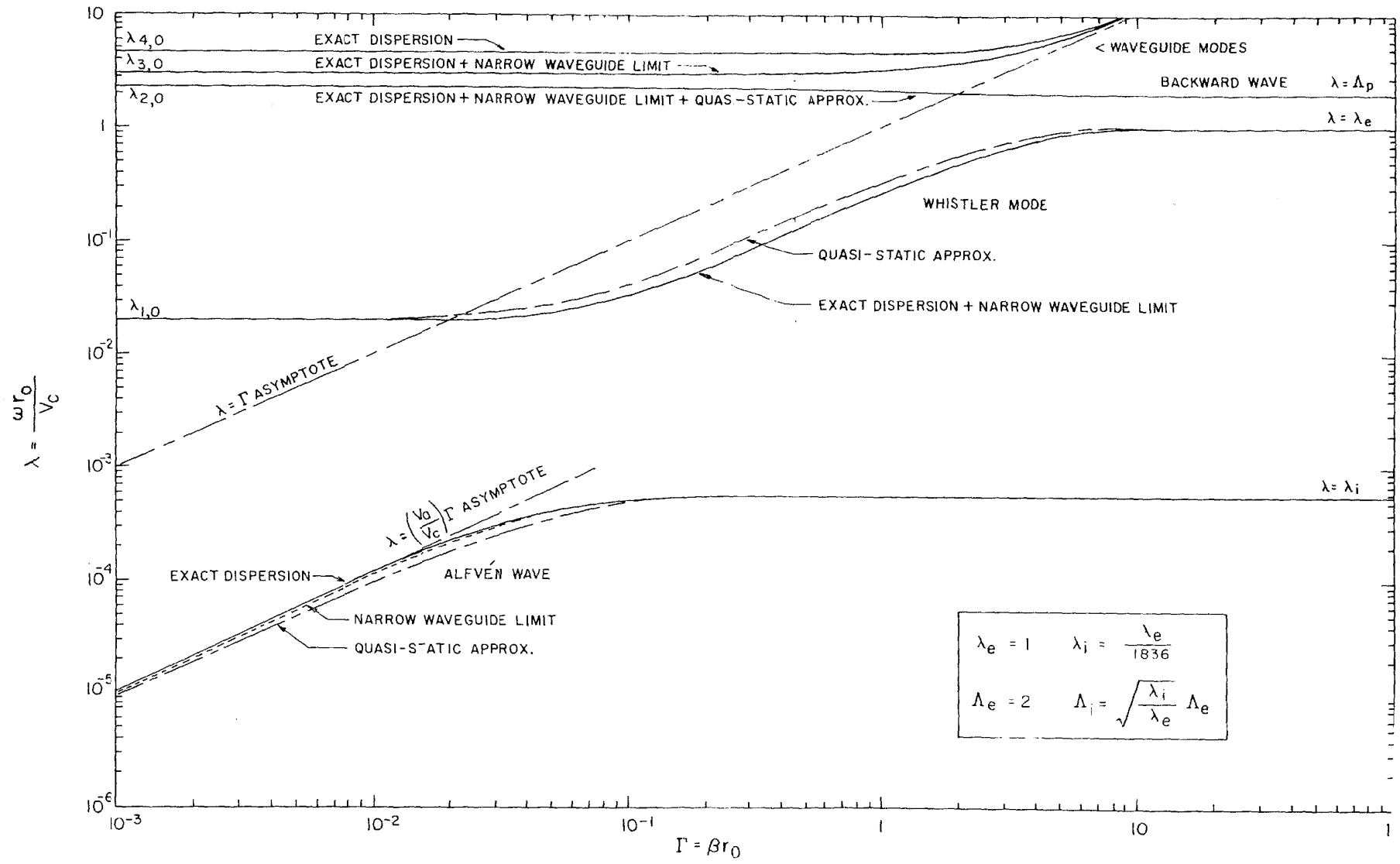

Fig. 2-2. A comparison of the exact dispersion relation with the quasi-static approximation and the narrow waveguide limit, for the whistler mode, the Alfvén wave, and the backward wave (slow wave) mode.

lower densities, and narrower cross sections are usual. The Alfvén wave occurs near zero frequency and, somewhat higher, the whistler mode is also present. At very large frequencies the plasmaguide again behaves like an empty waveguide. Unlike Figure V-2a, $\lambda_{1,0}$ now exceeds λ_1 and the dispersion is single valued. The occurrence of cut-off frequency $\lambda_{2,0}$ above plasma resonance results in a backward wave having a real propagation constant. The transition from plane wave to backward wave is pictured in Figure IV-5. Meanwhile, the waves associated with $\lambda_{3,0}$ and $\lambda_{4,0}$ correspond quite well to the TE and TM modes of an isotropic waveguide. Although one recognizes many features of plane wave dispersion, the resemblance to the TM narrow waveguide limit illustrated in Figure IV-7(1a) is even more remarkable.

The dispersion of the angular dependent modes closely resembles the dispersion of the circular symmetric modes. However, the magnetostatic field removes the degeneracy existing between the $+n$ and $-n$ modes by splitting each dispersion curve in two as $\underline{B}_o$ is increased. This is evident from equation II-36, but it can also be observed from Figure III-10 that the right and left wave polarizations have different cut-off frequencies. Since $+n$ and $-n$ modes of the same radial order propagate with different velocities, their superposition results in a wave which exhibits Faraday rotation. Faraday rotation in gyrotropic waveguides has been thoroughly investigated by several researchers (1, 2, 3, 4, 5).

CHAPTER VI. MODE ORTHOGONALITY, POWER FLOW, AND PLASMAGUIDE EXCITATION

This chapter deals with the orthogonal properties of the waveguide modes, their interpretation in terms of power flow, and finally, their application. The orthogonality relations are derived for a lossless plasma, then generalized to include dissipation. A substitution is also discovered which transforms the lossless description into the dissipative formulation. The orthogonality relation for a lossless plasma was first obtained by Walker (31); later Bressler et al. (32) derived the orthogonality relation for a dissipative plasma. Due to reflection symmetry these orthogonality relations can be substantially simplified. The simplified relations are used to study the fields excited by a coaxial current loop in a circular plasmaguide.

Notation

The modes of an empty waveguide are specified by the character of the field (whether TM or TE) and by two integers which designate the mode order. For a circular waveguide, the field character determines whether T is a root of $J_n(Tr_o) = 0$ (TM mode) or of $J_n'(Tr_o) = 0$ (TE mode). The angular integer n prescribes the order of the Bessel function; the radial order determines which of the multiple Tr_o roots should be chosen. Once the signal frequency, field character and mode number are given, the axial propagation factor may be calculated from

$$h = \pm j \sqrt{\left(\frac{\omega}{V_c}\right)^2 - T^2} \quad .$$

Alternatively, given ω and h, T can be calculated. The character of the wave can be deduced unambiguously from T only if n is known. It therefore takes all three quantities, n, ω and h, to completely

determine a mode.

The anisotropic waveguide modes are likewise completely specified by n, ω and h, after the waveguide radius, plasma parameters and magnetostatic field intensity are fixed. Since E_z and F_z are coupled, the waves are no longer TE or TM. Instead, two values of T need to be considered now. Once n, ω, and h are specified, T_1 and T_2 are determined by equation II-16.

To facilitate further study a notation must be adopted which unambiguously distinguishes each mode. The notation must make the reader aware of n, ω and h.

Because the frequency is understood to be the same as that of the source, only n and h need to appear explicitly. Therefore, let $\underline{E}(h_n)$ and $\underline{H}(h_n)$ correspond to the fields of angular mode order n, propagating as $e^{j(\omega t - n\theta) - h_n z}$, due to a source frequency ω.

Mode Orthogonality for a Lossless Plasma

Consider two coexisting modes $\underline{E}(h_n)$, $\underline{H}(h_n)$ and $\underline{E}(h_m)$, $\underline{H}(h_m)$ excited at the same frequency ω. At a source-free location within the guide, the first mode satisfies Maxwell's equations

$$\nabla \times \underline{E}(h_n) = - j\omega \mu_o \underline{H}(h_n) \qquad \text{(VI-1a)}$$

$$\nabla \times \underline{H}(h_n) = + j\omega \underline{\underline{\epsilon}} \cdot \underline{E}(h_n) \qquad \text{(VI-1b)}$$

The conjugate fields $\underline{E}^*(h_m)$, $\underline{H}^*(h_m)$ satisfy the complex conjugate of Maxwell's equations, namely

$$\nabla \times \underline{E}^*(h_m) = + j\omega \mu_o \underline{H}^*(h_m) \qquad \text{(VI-2a)}$$

$$\nabla \times \underline{H}^*(h_m) = - j\omega \underline{\underline{\epsilon}}^* \cdot \underline{E}^*(h_m) \; . \qquad \text{(VI-2b)}$$

An integral of the fields is formed using the identity

$$\nabla\cdot\left[\underline{E}(h_n)\times\underline{H}^*(h_m)\right] = \underline{H}^*(h_m)\cdot\nabla\times\underline{E}(h_n) - \underline{E}(h_n)\cdot\nabla\times\underline{H}^*(h_m) \qquad \text{(VI-3)}$$

and substituting equations VI-1a and VI-2a to yield

$$\nabla\cdot\left[\underline{E}(h_n)\times\underline{H}^*(h_m)\right] = -j\omega\left[\mu_o\underline{H}(h_n)\cdot\underline{H}^*(h_m) - \underline{E}(h_n)\cdot\underline{\underline{\epsilon}}^*\cdot\underline{E}^*(h_m)\right] \qquad \text{(VI-4)}$$

The complex conjugate of equation VI-4 with n and m interchanged is

$$\nabla\cdot\left[\underline{E}^*(h_m)\times\underline{H}(h_n)\right] = +j\omega\left[\mu_o\underline{H}^*(h_m)\cdot\underline{H}(h_n) - \underline{E}^*(h_m)\cdot\underline{\underline{\epsilon}}\cdot\underline{E}(h_n)\right]. \qquad \text{(VI-5)}$$

When losses are neglected $\underline{\underline{\epsilon}}$ is Hermitian, i.e.,

$$\underline{E}(h_n)\cdot\underline{\underline{\epsilon}}^*\cdot\underline{E}^*(h_m) = \underline{E}^*(h_m)\cdot\underline{\underline{\epsilon}}\cdot\underline{E}(h_n) \qquad \text{(VI-6)}$$

with the result that the permittivity tensor can be eliminated by adding equations VI-4 and VI-5. Thus

$$\nabla\cdot\left[\underline{E}(h_n)\times\underline{H}^*(h_m) + \underline{E}^*(h_m)\times\underline{H}(h_n)\right] = 0 \quad . \qquad \text{(VI-7)}$$

Integrating VI-7 over a volume V surrounded by the surface S consisting of the waveguide cross sections at z_1 and z_2 plus the waveguide wall between (see Figure VI-1) we obtain via Gauss' theorem:

$$\int_V \nabla\cdot\left[\underline{E}(h_n)\times\underline{H}^*(h_m) + \underline{E}^*(h_m)\times\underline{H}(h_n)\right] dV =$$

$$\oint_S \left[\underline{E}(h_n)\times\underline{H}^*(h_m) + \underline{E}^*(h_m)\times\underline{H}(h_n)\right]\cdot d\underline{S} = 0 \qquad \text{(VI-8)}$$

Let $\underline{n}$ be a local vector normal to the waveguide wall. If the electric field tangential to the perfectly conducting surface is to

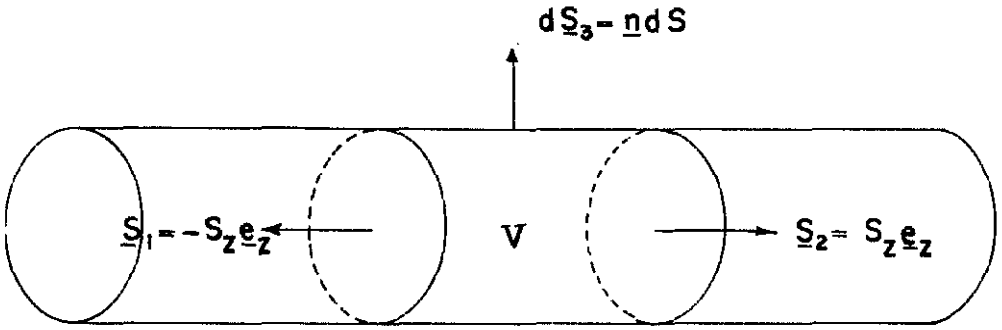

Figure VI-1. The surface of integration for equation VI-8

vanish, then $(\underline{n} \times \underline{E}) = 0$. As a result, products like $(\underline{E} \times \underline{H}^*)\cdot\underline{n}\,dS = (\underline{n} \times \underline{E}) \cdot \underline{H}^* dS$ vanish along the waveguide wall leaving behind, in VI-8, only the surface integrations at z_1 and z_2 . The fields at z_1 and z_2 are proportional because the z dependence of the wave can be separated from the transverse dependence as an exponential factor, viz.

$$\underline{E}(h_n) = \breve{\underline{E}}(h_n)e^{-h_n z} \qquad \text{and} \qquad \underline{H}(h_n) = \breve{\underline{H}}(h_n)e^{-h_n z} \quad .$$

Hence equation VI-8 becomes

$$\left[e^{-(h_n + h_m^*)z_2} - e^{-(h_n + h_m^*)z_1}\right] \int_{\substack{\text{cross}\\ \text{section}}} \left[\breve{\underline{E}}(h_n) \times \breve{\underline{H}}^*(h_m) + \breve{\underline{E}}^*(h_m) \times \breve{\underline{H}}(h_n)\right] \cdot \underline{e}_z dS_z = 0 \qquad \text{(VI-9)}$$

For $h_n \neq -h_m^*$ the first factor of VI-9 can never be zero; therefore the integral must vanish. This condition is conveniently summarized by writing

$$\int_{\substack{\text{cross}\\ \text{section}}} \left[\underline{E}(h_n) \times \underline{H}^*(h_m) + \underline{E}^*(h_m) \times \underline{H}(h_n)\right] \cdot \underline{e}_z\, dS_z = 0 \qquad \text{for} \quad h_n \neq -h_m^* \quad . \qquad \text{(VI-10)}$$

The breve has been deleted from the field vectors because the integration is independent of z. Orthogonality relation VI-10, first obtained by Walker (31), is the basis for expanding arbitrary $\underline{E}$ and $\underline{H}$ fields in terms of the waveguide modes.

Since the longitudinal fields do not contribute to the integral, orthogonality relation VI-10 can be restated as follows

$$\int_{\substack{\text{cross}\\ \text{section}}} \left[\underline{E}_t(h_n) \times \underline{H}_t^*(h_m) + \underline{E}_t^*(h_m) \times \underline{H}_t(h_n) \right] \cdot \underline{e}_z dS_z = 4P(h_n)\, \delta_{-h_n, h_m^*} \quad . \quad \text{(VI-11)}$$

The right side contains the normalization constant $P(h_n)$ followed by the Kronecker delta symbol which has unit value when both subscripts are alike $(h_n = -h_m^*)$ and zero value otherwise. The subscript t refers to the transverse components of the field.

A longitudinally invariant waveguide filled with an axially magnetized plasma exhibits reflection symmetry. Corresponding to each modal solution with transverse fields $\underline{E}_t(h_n)$, $\underline{H}_t(h_n)$, longitudinal field components $E_z(h_n)$, $H_z(h_n)$ and propagation constant h_n, there can exist a wave traveling in the opposite direction with propagation constant $-h_n$ and field components

$$\underline{E}_t(-h_n) = \underline{E}_t(h_n) \qquad \underline{H}_t(-h_n) = -\underline{H}_t(h_n)$$

$$E_z(-h_n) = -E_z(h_n) \qquad H_z(-h_n) = H_z(h_n) \quad .$$

Reflection symmetry was discussed at the conclusion of Chapter II but this property is also evident from equations II-8 through II-11. By substituting the reflected wave variables $\left\{ \underline{E}_t(h_n),\ -\underline{H}_t(h_n),\ -h_n \right\}$ for the initial variables $\left\{ \underline{E}_t(h_n),\ \underline{H}_t(h_n),\ h_n \right\}$ in VI-11, a new orthogonality relation is obtained:

$$\int_{\substack{\text{cross}\\ \text{section}}} \left[\underline{E}_t(h_n) \times \underline{H}_t^*(h_m) - \underline{E}_t^*(h_m) \times \underline{H}_t(h_n) \right] \cdot \underline{e}_z dS_z = j4Q(h_n)\, \delta_{h_n, h_m^*} \qquad \text{(VI-12)}$$

$Q(h_n)$ replaces $P(h_n)$ as the normalization constant for VI-12. Upon adding expressions VI-11 and VI-12 a somewhat simpler orthogonality relation results:

$$\int_{\substack{\text{cross}\\ \text{section}}} \underline{E}_t(h_n) \times \underline{H}_t^*(h_m) \cdot \underline{e}_z dS_z = 2 \left[P(h_n) \delta_{-h_n, h_m^*} + jQ(h_n)\, \delta_{h_n, h_m^*} \right] . \qquad \text{(VI-13)}$$

Subtracting VI-12 from VI-11 produces the following integral

$$\int_{\substack{\text{cross}\\ \text{section}}} \underline{E}_t^*(h_m) \times \underline{H}_t(h_n) \cdot \underline{e}_z dS_z = 2 \left[P(h_n) \delta_{-h_n, h_m^*} - jQ(h_n)\, \delta_{h_n, h_m^*} \right] . \qquad \text{(VI-14)}$$

Taken individually, these orthogonality relations fail to resolve between the incident and reflected (h_n and $-h_n$) waves of a field expansion. Consequently VI-13 and VI-14 are useful only if no reflected waves are present, e.g., in an infinite, unobstructed waveguide. In a waveguide section containing obstacles or improper terminations both waves are present and one is forced to use either orthogonality relation VI-11 or VI-12 to uniquely evaluate the amplitudes of the modes.

Power Flow

In a lossless plasma, the orthogonality integrals assume an added importance when interpreted in terms of power flow. In this connection note that because n and m are dummy variables, the integrals contained in VI-13 and VI-14 are complex conjugates. It therefore follows that $P(h_n)$ and $Q(h_n)$ are real constants.

For $h_n = h_m = \alpha_n + j\beta_n$, the orthogonality relations VI-11 and VI-12 can be written as

$$\mathrm{Re}\ \frac{1}{2} \int_{\substack{\text{cross} \\ \text{section}}} \left[\underline{E}_t(h_n) \times \underline{H}_t^*(h_n) \right] \cdot \underline{e}_z dS_z = P(h_n)\ \delta_{\alpha_n, 0} \qquad \text{(VI-15)}$$

$$\mathrm{Im}\ \frac{1}{2} \int_{\substack{\text{cross} \\ \text{section}}} \left[\underline{E}_t(h_n) \times \underline{H}_t^*(h_n) \right] \cdot \underline{e}_z dS_z = Q(h_n)\ \delta_{\beta_n, 0} \qquad \text{(VI-16)}$$

because

$$\delta_{-h_n, h_n^*} = \delta_{-\alpha_n - j\beta_n, \alpha_n - j\beta_n} = \delta_{\alpha_n, 0} \qquad \text{(VI-17a)}$$

and

$$\delta_{+h_n, h_n^*} = \delta_{\alpha_n + j\beta_n, \alpha_n - j\beta_n} = \delta_{\beta_n, 0} \quad . \qquad \text{(VI-17b)}$$

Since $\underline{E} \times \underline{H}^*$ is the complex Poynting vector, $P(h_n)$ and $Q(h_n)$ are immediately recognized as the real and reactive powers of the wave. The power transported by a propagating mode $(\alpha_n = 0)$ is real; for an evanescent mode $(\beta_n = 0)$ it is reactive. A single mode having a complex propagation constant $(\alpha_n \neq 0,\ \beta_n \neq 0)$ carries neither a real nor a reactive power through any cross section of the guide.

If both members of a pair of modes having complex propagation constants h_n and $h_m = -h_n^*$ are present, the right side of equation VI-11 equals $4P(h_n)$ while the delta function of equation VI-12 vanishes. Consequently, the power delivered by a pair of complex modes is always real, if the pair consists of an exponentially increasing member $(-\alpha_n + j\beta_n)$ and an exponentially decreasing member $(\alpha_n + j\beta_n)$. As $\alpha_n \to 0$, this pair degenerates into a single propagating mode whose power flow is real.

In contrast, for the pair of modes described by h_n and $h_m = +h_n^*$ the integral of equation VI-11 vanishes while the integral of equation

VI-12 equals $j4Q(h_n)$. As a result, the power transported by the pair of modes $\alpha_n + j\beta_n$ and $\alpha_n - j\beta_n$ is entirely reactive.

Finally, for the pair of modes consisting of an incident wave having $h_n = \alpha_n + j\beta_n$ and a reflected wave having $h_m = -h_n = -\alpha_n - j\beta_n$ ($\alpha_n \neq 0$, $\beta_n \neq 0$), the integrals in both VI-11 and VI-12 vanish. In other words this pair of modes does not convey any real or reactive power.

These deductions can be summarized by the following statements:

1) The total real power transmitted by the waveguide equals the algebraic sum of the real partial powers carried by each propagating mode ($\alpha_n = 0$), plus the algebraic sum of the real mutual powers carried by each pair h_n, $h_m = -h_n^*$ of complex modes.

2) The total reactive power transmitted by the waveguide equals the algebraic sum of the reactive partial powers carried by each evanescent mode ($\beta_n = 0$), plus the algebraic sum of the reactive mutual powers carried by each pair h_n, $h_m = +h_n^*$ of complex modes.

Wave Excitation in the Lossless Plasma

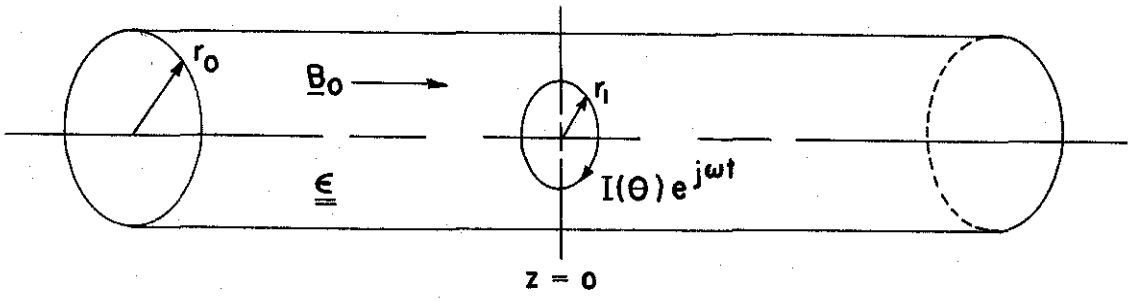

Figure VI-2. A coaxial current loop in an infinite circular plasmaguide

A circular waveguide of infinite extent is excited at $z = 0$ by a coaxial current loop. The loop, located at radius r_1, is of infinitesimal thickness and carries a current $I(\theta)e^{j\omega t}$. The current and magnetic field at this plane are related by Ampere's law. Therefore the discontinuity in the transverse magnetic field at the plane of excitation equals the current flowing in that surface.

$$\Delta(\underline{e}_z \times \underline{\mathcal{H}}_t)\Big|_{z=0} = I(\theta)\,\delta(r - r_1)\underline{e}_\theta \qquad \text{(VI-18a)}$$

A more convenient form of this relation is

$$\Delta\underline{\mathcal{H}}_t\Big|_{z=0} = I(\theta)\,\delta(r - r_1)\underline{e}_r \quad . \qquad \text{(VI-18b)}$$

According to the principle of reflection symmetry, the transverse electric field is continuous across the plane of excitation while $\underline{\mathcal{H}}_t\Big|_{z=-\xi} = -\underline{\mathcal{H}}_t\Big|_{z=+\xi}$ so that

$$\Delta\underline{\mathcal{H}}_t\Big|_{z=0} = \underline{\mathcal{H}}_t\Big|_{z=+\xi} - \underline{\mathcal{H}}_t\Big|_{z=-\xi} = 2\underline{\mathcal{H}}_t\Big|_{z=0+} \qquad \text{as} \quad \xi \to 0 \ , \qquad \text{(VI-19)}$$

and VI-18b becomes

$$I(\theta)\,\delta(r - r_1)\underline{e}_r = 2\underline{\mathcal{H}}_t\Big|_{z=0+} \qquad \text{(VI-20)}$$

The excited fields in the plane $z = 0+$ can be expressed in terms of the following mode expansions

$$\underline{\mathcal{E}}_t = \sum_{h_n} \underline{E}_t(h_n) = \sum_{h_n} A(h_n)\, \hat{\underline{E}}_t(h_n) e^{-jn\theta} \tag{VI-21}$$

$$\underline{\mathcal{H}}_t = \sum_{h_n} \underline{H}_t(h_n) = \sum_{h_n} A(h_n)\, \hat{\underline{H}}_t(h_n) e^{-jn\theta} \tag{VI-22}$$

$$\mathcal{E}_z = \sum_{h_n} E_z(h_n) = \sum_{h_n} A(h_n)\, \hat{E}_z(h_n) e^{-jn\theta} \tag{VI-23}$$

$$\mathcal{H}_z = \sum_{h_n} H_z(h_n) = \sum_{h_n} A(h_n)\, \hat{H}_z(h_n) e^{-jn\theta} \quad . \tag{VI-24}$$

For convenience the common $e^{j\omega t}$ dependence has been suppressed, and in compliance with equations II-29 and II-34

$$\hat{\underline{E}}_t(h_n) = \Big\{(ja\tau_1 + b)\, \underline{\Psi}(T_1 r) + k_o(ja\tau_2 + b)\, \underline{\Psi}(T_2 r) + \\ + (c\tau_1 + jd)\, \underline{e}_z \times \underline{\Psi}(T_1 r) + k_o(c\tau_2 + jd) \underline{e}_z \times \underline{\Psi}(T_2 r)\Big\} \tag{VI-25}$$

$$\hat{\underline{H}}_t(h_n) = \Big\{(f\tau_1 + ja)\, \underline{\Psi}(T_1 r) + k_o(f\tau_2 + ja)\, \underline{\Psi}(T_2 r) + \\ + (jg\tau_1 + c) \underline{e}_z \times \underline{\Psi}(T_1 r) + k_o(jg\tau_2 + c) \underline{e}_z \times \underline{\Psi}(T_2 r)\Big\} \tag{VI-26}$$

$$\hat{E}_z(h_n) = \Big\{\tau_1 J_n(T_1 r) + k_o \tau_2 J_n(T_2 r)\Big\} \tag{VI-27}$$

$$\hat{H}_z(h_n) = \Big\{J_n(T_1 r) + k_o J_n(T_2 r)\Big\} \tag{VI-28}$$

$$\underline{\Psi}(T_i r) = \Big\{T_i J_n'(T_i r) \underline{e}_r - \frac{jn}{r} J_n(T_i r) \underline{e}_\theta\Big\} \quad . \tag{VI-29}$$

The quantity

$$k_o = - \frac{\tau_1 J_n(\tau_1 r_o)}{\tau_2 J_n(\tau_2 r_o)} \qquad \text{(VI-30)}$$

results from making $E_z(h_n)$ vanish on the conducting waveguide wall at r_o. The coefficients a through g are functions of h_n according to equations II-3 and II-4.

The expansion coefficients $A(h_n)$ are determined by the source currents. Upon substituting VI-22 for $\mathcal{H}_t$ in equation VI-20

$$I(\theta)\, \delta(r - r_1)\underline{e}_r = 2 \sum_{h_n} \underline{H}_t(h_n) \qquad \text{(VI-31)}$$

and taking note of orthogonality relation VI-14, the method for evaluating $A(h_n)$ becomes clear. Vector multiplication by $\underline{E}_t^*(h_m)$ and integration over the cross section yields

$$\int_{\substack{\text{cross}\\ \text{section}}} \left[\underline{E}_t^*(h_m) \times \underline{e}_r\, I(\theta)\, \delta(r - r_1) \right] \cdot \underline{e}_z\, r dr\, d\theta = - 2 \sum_{h_n} \int_{\substack{\text{cross}\\ \text{section}}} \left[\underline{E}_t^*(h_m) \times \underline{H}_t(h_n) \right] \cdot \underline{e}_z\, dS_z \quad . \qquad \text{(VI-32)}$$

By virtue of the triple scalar product and the Dirac delta function, only the θ component of the electric field evaluated at r_1 remains on the left side. The right side is determined by orthogonality relation VI-14.

$$-r_1 A^*(h_m) \hat{E}_\theta^*(h_m)\Big|_{r_1} \int_0^{2\pi} I(\theta) e^{jm\theta}\, d\theta = 4 \sum_{h_n} \left[P(h_n)\delta_{-h_n, h_m^*} - jQ(h_n)\delta_{h_n, h_m^*} \right]. \qquad \text{(VI-33)}$$

Further simplification of equation VI-33 requires the introduction of two boundary conditions:

1. The fields at infinity must be bounded. This demands that waves with an $e^{-(\alpha_n + j\beta_n)z}$ axial dependence have $\alpha_n \geq 0$ in the region $z > 0$.

2. Power must always flow away from the source, i.e., the group velocity $\frac{d\omega}{d\beta_n}$ must be positive for $z > 0$.

Figure VI-3 illustrates various possible types of propagation factors. The diagram is drawn symmetric about the ω axis because the plasma-guide exhibits reflection symmetry.

At ω' two evanescent modes appear having propagation factors $h_1 = \alpha_1 > 0$ and $h_1' = -\alpha_1$. These modes are not mutually orthogonal because $h_1' = -h_1^*$. Nevertheless, by boundary condition 1, the spatially growing wave (h_1') is eliminated from the positive z region. Consequently the first mode (h_1) becomes orthogonal to all modes occurring at this frequency. It also follows that $\alpha_n \neq -\alpha_m$ for all evanescent modes in either half of an infinite plasmaguide.

At ω'' the dispersion diagram shows four propagating modes with exponents $h_1 = j\beta_1$, $h_1' = -j\beta_1$, $h_2 = +j\beta_2$ and $h_2' = -j\beta_2$. The modes associated with h_1 and h_1' are forward waves, whereas h_2 and h_2' correspond to backward waves. The forward wave at h_1' and the backward wave at h_2 carry power in the negative direction $(\frac{d\omega}{d\beta} < 0)$ and therefore do not appear in the region $z > 0$. The two remaining modes are mutually orthogonal since $h_2' \neq \pm h_1^*$. As a result $\beta_n \neq -\beta_m$ for all propagating modes in either

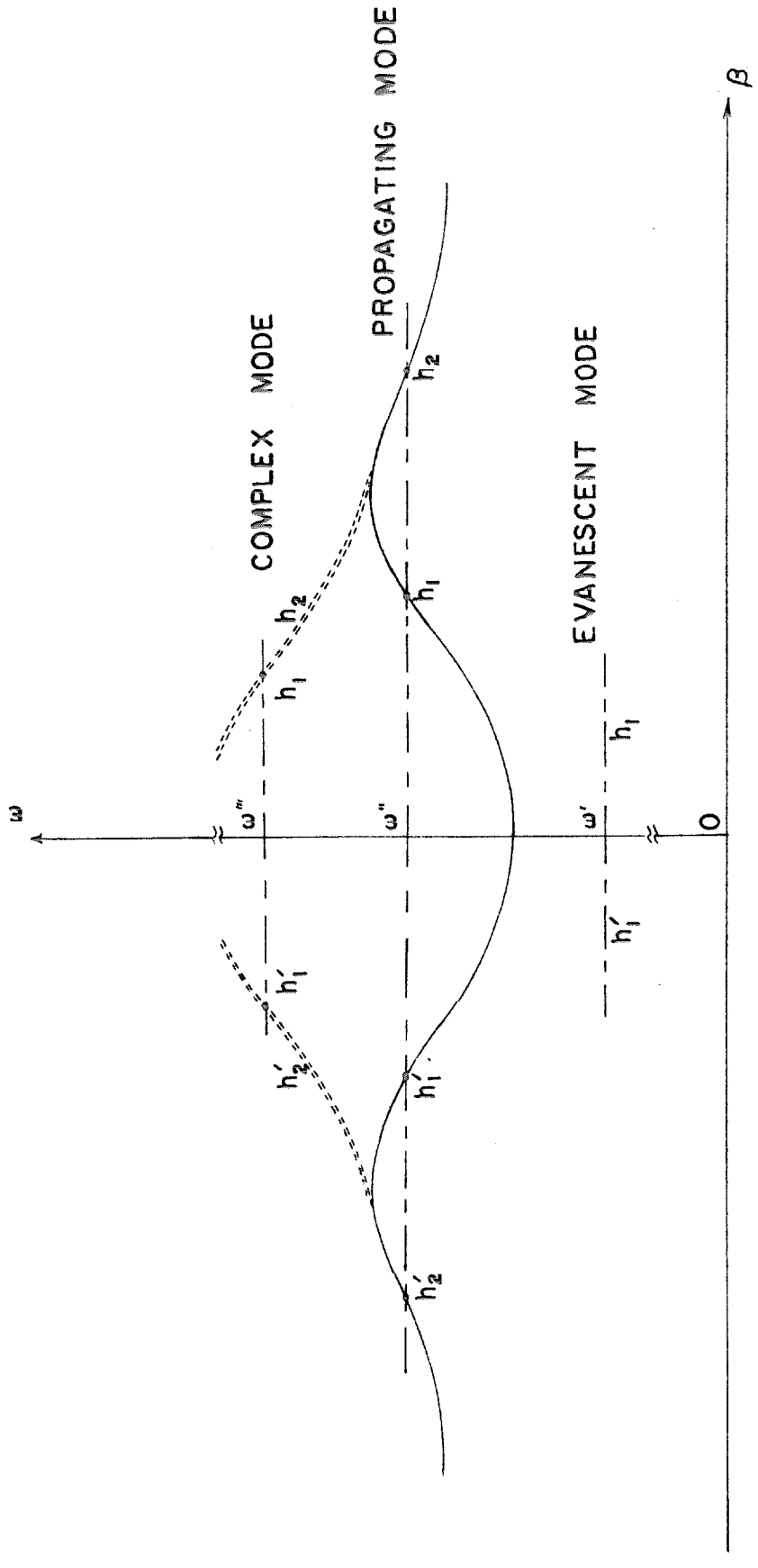

Figure VI-3. A segment of a dispersion diagram illustrating the variety of waves which occur in the lossless plasmaguide.

half of an infinite plasmaguide.

At ω''' four complex modes are accommodated with $h_1 = \alpha + j\beta$, $h_1' = -\alpha - j\beta$, $h_2 = -\alpha + j\beta$ and $h_2' = \alpha - j\beta$. The waves belonging to h_1' and h_2 are rejected (for $\alpha > 0$) according to boundary condition 1. The remaining modes corresponding to h_1 and h_2' are not mutually orthogonal because $h_2' = +h_1^*$. However, $h_n \neq -h_m^*$ for all complex modes in either half of an infinite plasmaguide.

These observations permit the following simplifications. First, because $\alpha_n \neq -\alpha_m$ unless $\alpha_n = \alpha_m = 0$ (propagating mode),

$$\delta_{-h_n,h_m^*} = \delta_{-\alpha_n,\alpha_m}\,\delta_{\beta_n,\beta_m} = \delta_{\alpha,0}\,\delta_{\beta_n,\beta_m} \tag{VI-34a}$$

where $\alpha = \alpha_n = \alpha_m$. Then, since $\beta_n \neq -\beta_m$ unless $\beta_n = \beta_m = 0$ (evanescent mode),

$$\delta_{h_n,h_m^*} = \delta_{\alpha_n,\alpha_m}\,\delta_{\beta_n,-\beta_m} = \delta_{\beta,0}\,\delta_{\alpha_n,\alpha_m} \tag{VI-34b}$$

where $\beta = \beta_n = \beta_m$. Finally, for the complex modes, the inequality $h_n \neq -h_m^*$ eliminates the delta function

$$\delta_{-h_n,h_m^*} = 0 \tag{VI-35}$$

the other delta function δ_{h_n,h_m^*} remains unaltered.

The expansion coefficients for the evanescent ($\alpha_n = 0$) and propagating ($\beta_n = 0$) modes are evaluated by substituting VI-34a,b into equation VI-33. Thus

$$-r_1 A^*(h_m)\hat{E}^*_\theta(h_m)\Big|_{r_1}\int_0^{2\pi} I(\theta)e^{jm\theta}d\theta = 4\sum_{h_n}\left[P(h_n)\delta_{\alpha,0}\delta_{\beta_n,\beta_m} - jQ(h_n)\delta_{\beta,0}\delta_{\alpha_n,\alpha_m}\right]$$

$$= 4\sum_{h_n}\left[P(h_n)\delta_{\alpha_m,0} - jQ(h_n)\delta_{\beta_m,0}\right]\delta_{h_n,h_m}$$

$$= 4\left[P(h_m)\delta_{\alpha_m,0} - jQ(h_m)\ \delta_{\beta_m,0}\right] \quad \text{(VI-36)}$$

However, according to equations VI-15, VI-16, VI-21 and VI-22,

$$\left[P(h_m)\delta_{\alpha_m,0} - jQ(h_m)\delta_{\beta_m,0}\right] = \left[P(h_m)\delta_{\alpha_m,0} + jQ(h_m)\ \delta_{\beta_m,0}\right]^*$$

$$= \frac{1}{2}\left|A(h_m)\right|^2 \int_{\substack{\text{cross}\\ \text{section}}} \left[\underline{\hat{E}}^*_t(h_m) \times \underline{\hat{H}}_t(h_m)\right]\cdot \underline{e}_z\, dS_z \ . \quad \text{(VI-37)}$$

Hence the expansion coefficient is

$$A(h_m) = \frac{-r_1\hat{E}^*_\theta(h_m)\Big|_{r_1}\int_0^{2\pi} I(\theta)\ e^{jm\theta}\ d\theta}{2\int_{\substack{\text{cross}\\ \text{section}}}\left[\underline{\hat{E}}^*_t(h_m) \times \underline{\hat{H}}_t(h_m)\right]\cdot \underline{e}_z\, dS_z} \quad \text{(VI-38)}$$

when h_m^2 is real.

For complex modes, the substitution of VI-35 reduces equation VI-33 to

$$-r_1 A^*(h_m)\hat{E}^*_\theta(h_m)\Big|_{r_1}\int_0^{2\pi} I(\theta)e^{jm\theta}d\theta = -j\,4\sum_{h_n} Q(h_n)\delta_{h_n,h_m^*} = -j\,4Q(h_m^*) \quad \text{(VI-39)}$$

where, according to equations VI-12, VI-21 and VI-22,

$$Q(h_m^*) = \frac{1}{j4} A(h_m^*)A^*(h_m) \int_{\substack{\text{cross}\\ \text{section}}} \left[\hat{\underline{E}}_t(h_m^*) \times \hat{\underline{H}}_t^*(h_m) - \hat{\underline{E}}_t^*(h_m) \times \hat{\underline{H}}_t(h_m^*) \right] \cdot \underline{e}_z dS_z \quad . \tag{VI-40}$$

As a result,

$$A(h_m^*) = \frac{r_1 \hat{E}_\theta^*(h_m)\Big|_{r_1} \int_0^{2\pi} I(\theta)\, e^{jm\theta}\, d\theta}{\int_{\substack{\text{cross}\\ \text{section}}} \left[\hat{\underline{E}}_t(h_m^*) \times \hat{\underline{H}}_t^*(h_m) - \hat{\underline{E}}_t^*(h_m) \times \hat{\underline{H}}_t(h_m^*) \right] \cdot \underline{e}_z dS_z} \quad . \tag{VI-41}$$

Replacing h_m by h_m^* yields the expansion coefficient corresponding to the <u>complex</u> propagation constant h_m.

$$A(h_m) = \frac{r_1 \hat{E}_\theta^*(h_m^*)\Big|_{r_1} \int_0^{2\pi} I(\theta)\, e^{jm\theta}\, d\theta}{\int_{\substack{\text{cross}\\ \text{section}}} \left[\hat{\underline{E}}_t(h_m) \times \hat{\underline{H}}_t^*(h_m^*) - \hat{\underline{E}}_t^*(h_m^*) \times \hat{\underline{H}}_t(h_m) \right] \cdot \underline{e}_z dS_z} \quad . \tag{VI-42}$$

To illustrate the use of these formulas for $A(h_m)$, the input impedance of a uniform current loop is calculated next. The complex power delivered by the loop to the plasma is

$$N = -\frac{1}{2} \int \underline{\mathcal{E}} \cdot \underline{J}^*\, dv = -\frac{1}{2} \int \mathcal{E}_\theta\, I^*(\theta)\, \delta(r - r_1)\, \delta(z) dv$$

$$= -\frac{1}{2} \int_0^{2\pi} \mathcal{E}_\theta \Big|_{\substack{r=r_1\\ z=0}} I^*(\theta)\, r_1 d\theta \quad . \tag{VI-43}$$

For $I(\theta) = I_o$ (a constant), and $\mathcal{E}_\theta$ defined by VI-21

$$N = -\frac{1}{2} r_1 I_o^* \sum_{h_n} A(h_n)\, \hat{E}_\theta(h_n) \int_0^{2\pi} e^{jn\theta}\, d\theta = -\pi r_1 I_o^* \sum_{h_o} A(h_o) \hat{E}_\theta(h_o) \Big|_{r_1} . \tag{VI-44}$$

If the frequency of operation lies in a range where complex waves do not propagate, then equation VI-38 suffices. The expansion coefficients for $I(\theta) = I_o$ are then

$$A(h_o) = \frac{-\pi r_1 I_o\, \hat{E}_\theta^*(h_o)\Big|_{r_1}}{\int_{\substack{\text{cross}\\ \text{section}}} \left[\underline{\hat{E}}_t^*(h_o) \times \underline{\hat{H}}_t(h_o)\right] \cdot \underline{e}_z dS_z} \tag{VI-45}$$

$$A(h_m) = 0 \qquad \text{for} \quad m \neq 0 \quad .$$

Whereupon

$$N = \pi^2 r_1^2 \left|I_o\right|^2 \sum_{h_o} \frac{\left|\hat{E}_\theta(h_o)\right|^2_{r_1}}{\int_{\substack{\text{cross}\\ \text{section}}} \left[\underline{\hat{E}}_t^*(h_o) \times \underline{\hat{H}}_t(h_o)\right] \cdot \underline{e}_z dS_z} . \tag{VI-46}$$

The input impedance of the loop is therefore

$$Z = \frac{2N}{\left|I_o\right|^2} = 2\pi^2 r_1^2 \sum_{h_o} \frac{\left|\hat{E}_\theta(h_o)\right|^2_{r_1}}{\int_{\substack{\text{cross}\\ \text{section}}} \left[\underline{\hat{E}}_t^*(h_o) \times \underline{\hat{H}}_t(h_o)\right] \cdot \underline{e}_z dS_z} . \tag{VI-47}$$

Consider the MHD range of propagation where h^2 is always real. For $\epsilon_3 \to \infty$, equation II-16 shows that $T_1 \to \frac{\omega\mu_o}{d}$ while $T_2 \to \infty$; in accordance with equation II-17a it follows that $\tau_1 \to 0$ and $\tau_2 \to -j\frac{d}{c}$. Hence by equation VI-30 $k_o \to 0$ so that equations II-25 and II-26 become

$$\hat{\underline{E}}_t(h_o) = b\underline{\Psi}(T_1 r) + jd\, \underline{e}_z \times \underline{\Psi}(T_1 r)$$

$$= \frac{-\omega\mu_o}{\gamma_1^2 - \gamma_2^2} (\gamma_2 \underline{e}_r - j\gamma_1 \underline{e}_\theta) T_1 J_1(T_1 r) \qquad \text{(VI-48a)}$$

$$\hat{\underline{H}}_t(h_o) = ja\, \underline{\Psi}(T_1 r) + c\, \underline{e}_z \times \underline{\Psi}(T_1 r)$$

$$= \frac{h_o}{\gamma_1^2 - \gamma_2^2} (-\gamma_1 \underline{e}_r + j\gamma_2 \underline{e}_\theta) T_1 J_1(T_1 r) \qquad \text{(VI-48b)}$$

Obviously the dispersion reduces to $J_1(T_1 r_o) = 0$ in order that $E_z\Big|_{r_o} = E_\theta\Big|_{r_o} = \underline{H}_r\Big|_{r_o} = 0$. To distinguish between T_1's and γ_1's corresponding to different h_o's the subscripts os will be appended to these variables. Thus

$$T_1 \rightarrow T_{os} \qquad \text{and} \qquad \gamma_1 \rightarrow \gamma_{1os} \quad ;$$

the first letter corresponds to the angular order $n = 0$, the s refers to the radial order. Hence

$$\left|\hat{E}_\theta(h_o)\right|^2_{r_1} = \left(\frac{\omega\mu_o\gamma_{1os}}{\gamma_{1os}^2 - \gamma_2^2}\right)^2 T_{os}^2\, J_1^2(T_{os}\, r_1) \qquad \text{(VI-49)}$$

and

$$\int_{\substack{\text{cross}\\ \text{section}}} \left[\hat{\underline{E}}_t^*(h_o) \times \hat{\underline{H}}_t(h_o) \right] \cdot \underline{e}_z \, dS_z =$$

$$= \frac{-j\omega\mu_o h_o (\gamma_{los}^2 + \gamma_2^2)}{(\gamma_{los}^2 - \gamma_2^2)^2} 2\pi \int_0^{(T_{os} r_o)} (T_{os} r) J_1^2(T_{os} r) \, d(T_{os} r)$$

$$= \frac{-j\omega\mu_o h_o (\gamma_{los}^2 + \gamma_2^2)}{(\gamma_{los}^2 - \gamma_2^2)^2} \pi (T_{os} r_o)^2 J_o^2(T_{os} r_o) \, . \qquad \text{(VI-50)}$$

The impedance of the uniform current loop in the MHD frequency range is obtained by substituting equations VI-49 and VI-50 into VI-47 . Hence

$$Z = 2\pi \sum_s \frac{\omega\mu_o}{-jh_o} \frac{\gamma_{los}^2}{(\gamma_{los}^2 + \gamma_2^2)} \left[\frac{r_1 J_1(T_{os} r_1)}{r_o J_o(T_{os} r_o)} \right]^2 \, . \qquad \text{(VI-51)}$$

The summation extends over all circularly symmetric modes. If the Hall effect is also negligible, i.e., $\gamma_2^2 \ll |\gamma_{los}|^2$ this reduces to the result obtained by R. W. Gould (11) for the Alfvén range, viz.

$$Z = 2\pi \sum_s \frac{\omega\mu_o}{-jh_o} \left[\frac{r_1 J_1(T_{os} r_1)}{r_o J_o(T_{os} r_o)} \right]^2 \, . \qquad \text{(VI-52)}$$

Mode Orthogonality for a Dissipative Plasma

The orthogonality relations for a dissipative plasma are derived by a scheme analogous to the one employed for the lossless case. Once again consider two modes having fields $\underline{E}(h_n)$, $\underline{H}(h_n)$ and $\tilde{\underline{E}}(h_m)$, $\tilde{\underline{H}}(h_m)$ excited at the same frequency. The fields of the first mode propagate in a medium of permittivity $\underline{\underline{\epsilon}}$ according to Maxwell's equations

$$\nabla \times \underline{E}(h_n) = -j\omega\mu_o \underline{H}(h_n) \qquad \text{(VI-53a)}$$

$$\nabla \times \underline{H}(h_n) = j\omega \underline{\underline{\epsilon}} \cdot \underline{E}(h_n) \quad , \tag{VI-53b}$$

However, the fields of the second mode propagate in a medium whose permittivity $\underline{\underline{\tilde{\epsilon}}}$ is the transpose of $\underline{\underline{\epsilon}}$. This mode satisfies the equations

$$\nabla \times \underline{\tilde{E}}(h_m) = - j\omega \mu_o \underline{\tilde{H}}(h_m) \tag{VI-54a}$$

$$\nabla \times \underline{\tilde{H}}(h_m) = j\omega \underline{\underline{\tilde{\epsilon}}} \cdot \underline{\tilde{E}}(h_m) \quad . \tag{VI-54b}$$

Evidently

$$\begin{aligned} \nabla \cdot \left[\underline{E}(h_n) \times \underline{\tilde{H}}(h_m) \right] &= \underline{\tilde{H}}(h_m) \cdot \nabla \times \underline{E}(h_n) - \underline{E}(h_n) \cdot \nabla \times \underline{\tilde{H}}(h_m) \\ &= - j\omega\mu_o \underline{\tilde{H}}(h_m) \cdot \underline{H}(h_n) - j\omega \underline{E}(h_n) \cdot \underline{\underline{\tilde{\epsilon}}} \cdot \underline{\tilde{E}}(h_m) \end{aligned} \tag{VI-55}$$

and

$$\begin{aligned} \nabla \cdot \left[\underline{\tilde{E}}(h_m) \times \underline{E}(h_n) \right] &= \underline{H}(h_n) \cdot \nabla \times \underline{\tilde{E}}(h_m) - \underline{\tilde{E}}(h_m) \cdot \nabla \times \underline{H}(h_n) \\ &= - j\omega\mu_o \underline{H}(h_n) \cdot \underline{\tilde{H}}(h_m) - j\omega \underline{\tilde{E}}(h_m) \cdot \underline{\underline{\epsilon}} \cdot \underline{E}(h_n) . \end{aligned} \tag{VI-56}$$

By subtracting VI-56 from VI-55 the following is obtained

$$\begin{aligned} \nabla \cdot \left[\underline{E}(h_n) \times \underline{\tilde{H}}(h_m) - \underline{\tilde{E}}(h_m) \times \underline{H}(h_n) \right] &= \\ &= - j\omega \left[\underline{E}(h_n) \cdot \underline{\underline{\tilde{\epsilon}}} \cdot \underline{\tilde{E}}(h_m) - \underline{\tilde{E}}(h_m) \cdot \underline{\underline{\epsilon}} \cdot \underline{E}(h_n) \right] \\ &= - j\omega \underline{E}(h_n) \cdot \left[\underline{\underline{\tilde{\epsilon}}} - \underline{\underline{\epsilon}} \right] \cdot \underline{\tilde{E}}(h_m) = 0 . \end{aligned} \tag{VI-57}$$

Integrating this expression over the volume V contained within some

surface S , and then applying Gauss' theorem to the volume integral on the left produces

$$\oint_S \left[\underline{E}(h_n) \times \underline{\tilde{H}}(h_m) - \underline{\tilde{E}}(h_m) \times \underline{H}(h_n) \right] \cdot d\underline{S} = 0 . \qquad \text{(VI-58)}$$

According to equation I-19, reversing the magnetostatic field $\underline{B}_o$ transposes the permittivity tensor of the dissipative plasma, i.e., $\underline{\underline{\epsilon}}(-\underline{B}_o) = \underline{\underline{\tilde{\epsilon}}}(+\underline{B}_o)$. Consequently, $\underline{\tilde{E}}(h_m)$ and $\underline{\tilde{H}}(h_m)$ are the fields of the plasmaguide mode having propagation constant $h_m(-\underline{B}_o) \equiv \tilde{h}_m$ when the magnetostatic field points in the negative z direction. An examination of equations II-16 and II-36 reveals that reversing $\underline{B}_o$ has the same effect as reversing the sign of the angular integer. Thus

$$h_m(-\underline{B}_o) = h_{-m}(+\underline{B}_o) \qquad \text{(VI-59a)}$$

or simply

$$\tilde{h}_m = h_{-m} . \qquad \text{(VI-59b)}$$

Physically the polarization of the wave is referred to $\underline{B}_o$ while the positive θ direction is defined relative to the z axis by a right hand relation ($\underline{e}_\theta = \underline{e}_z \times \underline{e}_r$) . As a result, reversing $\underline{B}_o$ changes the sign of n which specifies the rotational sense of the field relative to the z axis.

Since a wave traveling anti-parallel to $\underline{B}_o$ has the same propagation factor as a wave traveling parallel to $\underline{B}_o$ with the opposite circular polarization, it follows that replacing n by -n , B_o by $-B_o$ in VI-25 through VI-29 yields the proper expressions for $\underline{\tilde{E}}(h_n)$ and $\underline{\tilde{H}}(h_n)$. Thus

$$\underline{\tilde{E}}(h_n) = (-1)^{n+1}\left[\hat{E}_r(h_n)\underline{e}_r - \hat{E}_\theta(h_n)\underline{e}_\theta + \hat{E}_z(h_n)\underline{e}_z\right] e^{jn\theta}$$

$$\underline{\tilde{H}}(h_n) = (-1)^{n}\left[\hat{H}_r(h_n)\underline{e}_r - \hat{H}_\theta(h_n)\underline{e}_\theta + \hat{H}_z(h_n)\underline{e}_z\right] e^{jn\theta} \quad .$$

Use was made of the identity: $J_{-n}(Tr) = (-1)^n J_n(Tr)$ plus the fact γ_2, b, c, f and τ change sign with $\underline{B}_o$, while γ_1, a, d and g remain fixed.

The tilde can be thought of as an operator which replaces $\underline{B}_o$ by $-\underline{B}_o$ in the same respect that the asterisk, denoting complex conjugation, replaces $j = \sqrt{-1}$ by $-j$. For example,

$$\underline{\underline{\tilde{\epsilon}}}(+\underline{B}_o) = \underline{\underline{\epsilon}}(-\underline{B}_o)$$

or else, since

$$\underline{E}(h_n) - \underline{E}(h_n(+\underline{B}_o), +\underline{B}_o) \qquad \text{(VI-60a)}$$

then

$$\underline{\tilde{E}}(h_n) = \underline{E}(h_n(-\underline{B}_o), -\underline{B}_o) = \underline{E}(h_{-n}(+\underline{B}_o), -\underline{B}_o) = \underline{E}(\tilde{h}_n, -\underline{B}_o) \qquad \text{(VI-60b)}$$

If, as in the lossless case, the z dependence of the wave is separated from its transverse behavior according to

$$\underline{E}(h_n) = \underline{\breve{E}}(h_n)e^{-h_n z} \qquad \underline{H}(h_n) = \underline{\breve{H}}(h_n)e^{-h_n z} \qquad \text{(VI-61a)}$$

then

$$\underline{\tilde{E}}(h_m) = \left[\underline{\breve{E}}(h_m)e^{-h_m z}\right]_{-\underline{B}_o} = \underline{\breve{\tilde{E}}}(h_m)e^{-\tilde{h}_m z}$$

$$\underline{\tilde{H}}(h_m) = \left[\underline{\breve{H}}(h_m)e^{-h_m z}\right]_{-\underline{B}_o} = \underline{\breve{\tilde{H}}}(h_m)e^{-\tilde{h}_m z} \quad . \qquad \text{(VI-61b)}$$

By fitting the surface of integration S in equation VI-58 to the surface illustrated in Figure VI-1 and using expressions VI-61 for the fields, equation VI-58 reduces to

$$\left[e^{-(h_n+\tilde{h}_m)z_2} - e^{-(h_n+\tilde{h}_m)z_1}\right] \int_{\substack{\text{cross}\\\text{section}}} \left[\underline{\breve{E}}(h_n) \times \underline{\breve{\tilde{H}}}(h_m) - \underline{\breve{\tilde{E}}}(h_m) \times \underline{\breve{H}}(h_n)\right] \cdot \underline{e}_z dS_z = 0 \quad . \tag{VI-62}$$

As earlier, only the end surfaces contribute to VI-61 because $(\underline{n} \times \underline{E}) = 0$ on the perfectly conducting waveguide wall. For $h_n \neq -\tilde{h}_m$ the first factor of VI-61 can never be zero, and the integral must therefore vanish.

$$\int_{\substack{\text{cross}\\\text{section}}} \left[\underline{E}(h_n) \times \underline{\tilde{H}}(h_m) - \underline{\tilde{E}}(h_m) \times \underline{H}(h_n)\right] \cdot \underline{e}_z dS_z = 0 \quad \text{for} \quad h_n \neq -\tilde{h}_m \; . \tag{VI-63}$$

The breve has been deleted because the integration is independent of z. Since the longitudinal field components do not enter into the triple scalar product, this integral simplifies still further.

$$\int_{\substack{\text{cross}\\\text{section}}} \left[\underline{E}_t(h_n) \times \underline{\tilde{H}}_t(h_m) - \underline{\tilde{E}}_t(h_m) \times \underline{H}_t(h_n)\right] \cdot \underline{e}_z dS_z = 4\tilde{P}(h_n)\delta_{-h_n,\tilde{h}_m} \; . \tag{VI-64}$$

$P(h_n)$ is the normalization for this orthogonality integral. A complementary orthogonality relation is immediately obtained from VI-64 by introducing the principle of reflection symmetry. If the initial variables $\left\{\underline{E}_t(h_n),\ \underline{H}_t(h_n),\ h_n\right\}$ are replaced by the reflected variables $\left\{\underline{E}_t(h_n),\ -\underline{H}_t(h_n), -h_n\right\}$, equation VI-64 becomes

$$\int_{\substack{\text{cross}\\\text{section}}} \left[\underline{E}_t(h_n) \times \underline{\tilde{H}}_t(h_m) + \underline{\tilde{E}}_t(h_m) \times \underline{H}_t(h_n) \right] \cdot \underline{e}_z dS_z = j4\tilde{Q}(h_n)\delta_{h_n,\tilde{h}_m} \quad \text{(VI-65)}$$

$\tilde{Q}(h_n)$ replaces $\tilde{P}(h_n)$ as the normalization constant for relation VI-65. Upon adding VI-64 and VI-65, a somewhat simpler orthogonality integral results.

$$\int_{\substack{\text{cross}\\\text{section}}} \left[\underline{E}_t(h_n) \times \underline{\tilde{H}}_t(h_m) \right] \cdot \underline{e}_z dS_z = 2\left[\tilde{P}(h_n)\delta_{-h_n,\tilde{h}_m} + j\tilde{Q}(h_n)\delta_{h_n,\tilde{h}_m} \right] \quad \text{(VI-66)}$$

Subtracting VI-64 from VI-65 produces

$$\int_{\substack{\text{cross}\\\text{section}}} \left[\underline{\tilde{E}}_t(h_m) \times \underline{H}_t(h_n) \right] \cdot \underline{e}_z dS_z = -2\left[\tilde{P}(h_n)\delta_{-h_n,\tilde{h}_m} - j\tilde{Q}(h_n)\delta_{h_n,\tilde{h}_m} \right] \quad \text{(VI-67)}$$

Orthogonality integrals VI-63 through VI-66 are generalizations of similar relations obtained by Bressler et al (32), because through $\tilde{P}(h_n)\delta_{-h_n,\tilde{h}_m}$ we include the possibility of having reflected waves.

Wave Excitation in a Dissipative Plasma

Reconsider the coaxial current loop of Figure VI-2 now located in a lossy plasma. Equations VI-18a through VI-31 are still valid. However, in place of VI-32 we now have

$$\int_{\substack{\text{cross}\\\text{section}}} \left[\underline{\tilde{E}}_t(h_m) \times \underline{e}_r \, I(\theta) \, \delta(r - r_1) \right] \cdot \underline{e}_z \, r \, dr \, d\theta =$$

$$= 2 \sum_{h_n} \int_{\substack{\text{cross}\\\text{section}}} \left[\underline{\tilde{E}}_t(h_m) \times \underline{H}_t(h_n) \right] \cdot \underline{e}_z dS_z \quad \text{(VI-68)}$$

The integral on the right is evaluated by means of orthogonality relation VI-67, while on the left $\underline{\tilde{E}}_t(h_m)$ is replaced by $\tilde{A}(h_m)\underline{\hat{\tilde{E}}}_t(h_m)e^{-jm\theta}$ according to equation VI-21. Hence

$$- r_1 \tilde{A}(h_m)\hat{\tilde{E}}_\theta(h_m)\Big|_{r_1} \int_0^{2\pi} I(\theta)e^{-jm\theta}d\theta = -4\sum_{h_n}\left[\tilde{P}(h_n)\delta_{-h_n,\tilde{h}_m} - j\tilde{Q}(h_n)\delta_{h_n,\tilde{h}_m}\right] . \tag{VI-69}$$

Because all modes are attenuated as they pass through the dissipative plasma, it follows that $\alpha_n > 0$ for $z > 0$ and that h_n can never equal $-\tilde{h}_m$. Equation VI-69 therefore reduces to

$$- r_1 \tilde{A}(h_m)\hat{\tilde{E}}_\theta(h_m)\Big|_{r_1} \int_0^{2\pi} I(\theta)e^{-jm\theta}d\theta = j4\sum_{h_n}\tilde{Q}(h_n)\delta_{h_n,\tilde{h}_m} = j4\tilde{Q}(\tilde{h}_m) . \tag{VI-70}$$

According to VI-65, VI-21, and VI-22

$$j4\tilde{Q}(\tilde{h}_m) = A(\tilde{h}_m)\tilde{A}(h_m)\int_{\substack{\text{cross}\\\text{section}}}\left[\underline{\hat{\tilde{E}}}_t(\tilde{h}_m)\times\underline{\hat{\tilde{H}}}_t(h_m) + \underline{\hat{\tilde{E}}}_t(h_m)\times\underline{\hat{H}}_t(\tilde{h}_m)\right]\cdot\underline{e}_z dS_z . \tag{VI-71}$$

Consequently

$$A(\tilde{h}_m) = \frac{-r_1\,\hat{\tilde{E}}_\theta(\tilde{h}_m)\Big|_{r_1}\int_0^{2\pi} I(\theta)e^{-jm\theta}\,d\theta}{\int_{\substack{\text{cross}\\\text{section}}}\left[\underline{\hat{\tilde{E}}}_t(\tilde{h}_m)\times\underline{\hat{\tilde{H}}}_t(h_m) + \underline{\hat{\tilde{E}}}_t(h_m)\times\underline{\hat{H}}_t(\tilde{h}_m)\right]\cdot\underline{e}_z dS_z} . \tag{VI-72}$$

Since two consecutive reversals of $\underline{B}_o$ leaves this magnetostatic field unchanged, then $\tilde{\tilde{h}}_m = h_m$. Substituting h_m for $\tilde{h}_m$ in equation VI-72

the expansion coefficient corresponding to h_m is obtained

$$A(h_m) = \frac{-r_1 \hat{\tilde{E}}_\theta(\tilde{h}_m)\Big|_{r_1} \int_0^{2\pi} I(\theta)\, e^{-jm\theta}\, d\theta}{\int_{\substack{\text{cross}\\ \text{section}}} \left[\underline{\hat{E}}_t(h_m) \times \underline{\hat{\tilde{H}}}_t(\tilde{h}_m) + \underline{\hat{\tilde{E}}}_t(\tilde{h}_m) \times \underline{\hat{H}}_t(h_m) \right] \cdot \underline{e}_z dS_z} \quad . \qquad \text{(VI-73)}$$

In accordance with equation VI-60b the tilde is an operator which reverses $\underline{B}_o$; hence,

$$\underline{\hat{\tilde{E}}}_t(\tilde{h}_n) = \underline{\hat{E}}_t(\tilde{\tilde{h}}_n, -\underline{B}_o) = \underline{\hat{E}}_t(h_n(+\underline{B}_o), -\underline{B}_o) \qquad \text{(VI-74a)}$$

$$\underline{\hat{\tilde{H}}}_t(\tilde{h}_n) = \underline{\hat{H}}_t(\tilde{\tilde{h}}_n, -\underline{B}_o) = \underline{\hat{H}}_t(h_n(+\underline{B}_o), -\underline{B}_o) \quad . \qquad \text{(VI-74b)}$$

In other words $\underline{\hat{\tilde{E}}}_t(\tilde{h}_n)$ and $\underline{\hat{\tilde{H}}}_t(\tilde{h}_n)$ are constructed from $\underline{\hat{E}}_t(h_n)$ and $\underline{\hat{H}}_t(h_n)$ by replacing $\underline{B}_o$ by $-\underline{B}_o$ in equations VI-25 and VI-26 and then substituting the propagation factor $h_n(+\underline{B}_o)$ pertaining to the wave whose excitation coefficient is sought. Note that $\underline{\tilde{E}}(\tilde{h}_n)$ and $\underline{\tilde{H}}(\tilde{h}_n)$ are not solutions to Maxwell's equations nor do they satisfy the boundary conditions; rather, they are functions constructed from the wave solutions.

Once a particular mode is decided upon, n, h and ω are given, whereas T_1 and T_2 are fixed by equation II-16. In accordance with equations II-3, II-4, and II-17, the coefficients γ_2, b, c, f and τ change sign with $\underline{B}_o$, while γ_1, a, d, and g do not. Consequently, replacing $\underline{B}_o$ by $-B_o$ transforms equations II-25 and II-26 into

$$\hat{\underline{\underline{E}}}_t(\tilde{h}_n) = \Big\{ -(ja\,\tau_1 + b)\,\underline{\Psi}(T_1 r) - K_o(ja\,\tau_2 + b)\,\underline{\Psi}(T_2 r) + \\ + (c\tau_1 + jd)\,\underline{e}_z x \underline{\Psi}(T_1 r) + K_o(c\tau_2 + jd)\,\underline{e}_z \times \underline{\Psi}(T_2 r) \Big\} \qquad \text{(VI-75a)}$$

$$\hat{\underline{\underline{H}}}_t(\tilde{h}_n) = \Big\{ (f\tau_1 + ja)\,\underline{\Psi}(T_1 r) + K_o(f\tau_2 + ja)\,\underline{\Psi}(T_2 r) + \\ - (jg\,\tau_1 + c)\underline{e}_z \times \underline{\Psi}(T_1 r) - K_o(jg\,\tau_2 + c)\,\underline{e}_z \times \underline{\Psi}(T_1 r) \Big\} \qquad \text{(VI-75b)}$$

Coefficients a through g and τ in VI-75 are evaluated by means of equations II-3 and II-4 using the absolute value of $\underline{B}_o$. The expansion coefficients of equation VI-73 for the modes excited by a coaxial current loop in a dissipative plasma are thereby defined in terms of equations VI-25, VI-26, VI-29 and VI-75 for the fields and their derived functions.

Formula VI-73 includes losses, but reduces to formula VI-42 when dissipative effects are removed. In a lossless plasma, the solutions to Maxwell's equations in $\underline{\underline{\epsilon}}(-B_o) = \tilde{\underline{\underline{\epsilon}}}(+B_o) = \underline{\underline{\epsilon}}^*(+B_o)$ are just the complex conjugates of the solutions in $\underline{\underline{\epsilon}}(+B_o)$. In other words, if the quantities

$$\hat{\underline{\underline{E}}}\,,\ \hat{\underline{\underline{H}}}\,,\ \omega\,,\ m\,,\ \tilde{h}_m \text{ and } \tilde{\underline{\underline{\epsilon}}}$$

are replaced by

$$\pm\,\hat{\underline{\underline{E}}}^*,\ \mp\,\hat{\underline{\underline{H}}}^*\,,\ \omega\,,\ -m\,,\ h_m^* \text{ and } \underline{\underline{\epsilon}}^*$$

respectively, Maxwell's equations are satisfied and VI-73 reduces to VI-42.

CONCLUSION

The theory presented here does not pretend to be exhaustive; many simplifications have been introduced to make the problem tractable. Primarily it is assumed that the plasma is cold, collisionless and homogeneous; conditions which are not mutually independent. A few of the effects which have been neglected in the process of making these assumptions are Landau damping, dissipational damping, ion-acoustic waves and the plasma sheath which covers the inner surface of the guide. In spite of these simplifications the theory is still formidable.

This analysis presents several parameters which the experimentalist can easily observe and use as diagnostics for the plasma. These are the resonance and cut-off frequencies, the velocity of propagation, and the attenuation rate for evanescent modes when losses are negligible. As a result these parameters determine the ion masses, component densities, magnetostatic field intensity and mode number. Furthermore, they can be used to predict the waveform received at any point in the plasma-guide due to a given source.

A good test of the theory is obtained by measuring the wave dispersion. Propagating, evanescent and complex waves may be expected. The phase velocity of the propagating wave may exceed the velocity of light by many orders of magnitude, or else be very slow like that of the Alfvén wave. Near the plasma frequency a backward wave propagates which under certain conditions (14) acquires a complex axial wave number. The possibility of surface waves in a completely filled plasmaguide is also pointed out.

In order to measure the wave dispersion it is necessary to know the phase and amplitude of a mode at two longitudinally displaced

points. Usually it is convenient to choose one of these two points at the field source where the generated mode amplitudes and phases, i.e., excitation coefficients, are known. Formulas giving the excitation coefficients for a coaxial circular current loop within an infinite plasmaguide are derived for both lossy and lossless plasmas.

The theoretical dispersion characteristics are difficult to compute because of their intrinsic transcendental nature. To improve our understanding, and to obtain some asymptotic approximations to the dispersion relations, several limiting forms of wave propagation are investigated. The dispersion and field configuration at zero and infinite magnetostatic field intensities are discussed, as are the MHD, the plane wave and the narrow waveguide limits. The quasi-static approximation is shown to be a very restricted example of narrow waveguide propagation.

Further investigations should consider hot, dissipative, inhomogeneous plasmas having radial density distributions (sheaths). However, the dispersion relations for a hot, homogeneous plasma (33) are already so complex that their solution has been abandoned. The inclusion of nonlinear terms is another area which invites consideration. The advantages of linearizing the dynamical equations by the small signal assumption are numerous. The primary difficulties introduced by the nonlinear terms are in connection with the solution of the field equations and the inability to express an arbitrary field as a superposition of source-free modes.

BIBLIOGRAPHY

1. Kales, M.L., "Modes in Wave Guides Containing Ferrites", Jour. Appl. Phys. 24, 604-608 (1953)

2. Suhl, H. and L. R. Walker, "Topics in Guided Wave Propagation through Gyromagnetic Media", B.S.T.J. 33; Part I 579-659 Part II 939-986, Part III 1133-1194 (1953)

3. Gamo, H., "The Faraday Rotation of Waves in a Circular Waveguide", Jour. Phys. Soc. Japan 8, 176-182 (1953)

4. Van Trier, A. A. Th. M., "Guided Electromagnetic Waves in Anisotropic Media", Appl. Sci. Res. B3, 305-371 (1953)

5. Epstein, P.S., "Theory of Wave Propagation in a Gyromagnetic Medium", Rev. Mod. Phys. 28, 3-17 (1956)

6. Wang, C. C. and J. E. Hopson, "Electromagnetic Wave Propagation in Gyroelectric Plasmas", Second Scientific Report NA-8210-8191-2, Sperry Gyroscope Company, Great Neck, L.I., New York (1960)

7. Smullin, L. D. and P. Chorney, "Properties of Ion-Filled Waveguides", Proc. I.R.E. 46, 360-361 (1958)

8. Trivelpiece, A. W. and R. W. Gould, "Space Charge Waves in Cylindrical Plasma Columns", Jour. Appl. Phys. 30, 1784-1793 (1959)

9. Newcomb, W. A., "The Hydromagnetic Wave Guide", Magnetohydrodynamics: A Symposium, R.K.M. Landshoff, Ed., Stanford University Press, Palo Alto, California (1957), pp.109-115.

10. Gajewski, R., "Magnetohydrodynamic Waves in Wave Guides", Phys. Fluids 2, 633-641 (1959)

11. Gould, R. W., "Excitation of Alfvén Waves", STL/TR-60-0000-09143, Space Technology Laboratories, Inc., Los Angeles, Calif. (1960)

12. Schmoys, J. and E. Mishkin, "Hydromagnetic Waveguide with Finite Conductivity and Arbitrary Cross Section", Phys. Fluids 3, 473-475 (1960)

13. Gould, R. W. and A. W. Trivelpiece, "A New Mode of Wave Propagation on Electron Beams", Proceedings of the Symposium on Electronic Waveguides, Vol. VIII, Polytechnic Press, Polytechnic Institute of Brooklyn, Brooklyn, New York (1958), pp.215-228

14. Chorney, P., "Power and Energy Relations in Bidirectional Waveguides", Proceedings of the Symposium on Electronic Waveguides, Vol. XI, Polytechnic Press, Polytechnic Institute of Brooklyn, Brooklyn, New York (1961), pp.195-210

15. Spitzer, L., Physics of Fully Ionized Gases, Second Edition, Interscience Publishers, Inc., New York (1962)

16. Delcroix, J. L., Introduction to the Theory of Ionized Gases, Interscience Publishers, Inc., New York (1960)

17. Landau, L. D. and E. M. Lifshitz, Statistical Physics, Addison-Wesley Publishing Co., Inc., Reading, Massachusetts (1958), § 124, pp.403-408

18. Landau, L. D. and E. M. Lifshitz, Electrodynamics of Continuous Media, Addison-Wesley Publishing Co., Inc., Reading, Massachusetts (1960), § 82, pp.331-337

19. Bressler, A. D. and N. Marcuvitz, "Operator Methods in Electromagnetic Field Theory", Part I, Research Report R-495-56 (1956); Part II, Research Report R-565-57 (1957), Polytechnica Institute of Brooklyn, M.R.I., Brooklyn, New York

20. Morse, P. M. and H. Feshbach, Methods of Theoretical Physics, Part I, McGraw-Hill Book Co., Inc., New York (1953), p.499 ff.

21. Buchsbaum, S. J., L. Mower and S. C. Brown, "Interaction between Cold Plasmas and Guided Electromagnetic Waves", Phys. Fluids 3, 806-819 (1960)

22. Mower, L. and S. J. Buchsbaum, "Interaction of Cold Plasmas and Buided Electromagnetic Waves, II", Phys. Fluids 5, 1545-1551 (1962)

23. Jahnke, E. and F. Emde, Tables of Functions, 4th Edition, Dover Publications, New York (1945), p.143, items 4 and 6.

24. Alfvén, H., Cosmical Electrodynamics, Clarendon Press, Oxford (1950), Chapter IV.

25. Storey, L.R.O., "An Investigation of Whistling Atmospherics", Phil. Trans. Roy. Soc. 246A, 113-141 (1953)

26. Dellis, A. N. and J. M. Weaver, "Measurement of a High Refractive Index for Transmission of 3 cm. Microwaves through a Plasma", Nature 193, 1274-1275 (1962)

27. Rigrod, W. W. and J. A. Lewis, "Wave Propagation along a Magnetically Focused Cylindrical Electron Beam", B.S.T.J. 33, 399-416 (1954)

28. Swanson, D. G., "An Experimental Study of Compressional Hydrodynamic Waves", Technical Report No. 1, Plasma Physics Laboratory, California Institute of Technology, Pasadena, California (1963)

29. Wilcox, J. M., F. I. Boley, and A. W. DeSilva, "Experimental Study of Alfvén Wave Properties", Phys. Fluids 3, 15-19 (1960)

30. Hooke, W. M. et al, "Experiments on Ion Cyclotron Waves", Phys. Fluids 4, 1131-1141 (1961)

31. Walker, L. R., "Orthogonality Relation for Gyrotropic Wave Guides", Jour. Appl. Phys. 28, 377 (1957)

32. Bressler, A. D., G. H. Joshi and N. Marcuvitz, "Orthogonality Properties for Modes in Passive and Active Uniform Wave Guides", Jour. Appl. Phys. 29, 794-799 (1958)

33. Kantor, M., "On Guided Waves in Hot, Gyrotropic Plasma", STL/TR 60-0000-GR11, Space Technology Laboratories, Inc., Los Angeles, Calif. (1960)

APPENDIX. THE QUASI-STATIC APPROXIMATION

Whenever one of the following conditions is satisfied, Maxwell's equations

$$\nabla \times \underline{E} = - j\omega \mu_c \underline{H} \qquad \text{and} \qquad \nabla \times \underline{H} = j\omega \underline{\underline{\epsilon}} \cdot \underline{E}$$

can be reduced to static expressions.

1) The fields have a slow temporal variation, i.e., $\omega \to 0$
2) The spatial dimensions of the structure are small compared to a wavelength
3) The phase velocity of the wave is much less than the velocity of light
4) The fields actually have an electrostatic configuration, e.g., the longitudinal oscillations of an infinite plasma.

Then, if the magnetic field is neglected in the first Maxwell equation,

$$\nabla \times \underline{E} = 0 \qquad \text{or} \qquad \underline{E} = - \nabla \varphi \quad .$$

Because the divergence of the curl of any vector is identically zero, the divergence of the second Maxwell equation yields

$$\nabla \cdot \underline{\underline{\epsilon}} \cdot \underline{E} = 0 \qquad \text{or} \qquad \nabla \cdot \underline{\underline{\epsilon}} \cdot \nabla \varphi = 0 \quad .$$

This is Laplace's equation for an anisotropic medium. The magnetic field is determined by the second Maxwell equation, $\nabla \times \underline{H} = j\omega \underline{\underline{\epsilon}} \cdot \underline{E}$.

For a circular cylindrical geometry and a permittivity tensor as defined in equations I-17 and I-18, Laplace's equation assumes the form

$$\frac{1}{r} \frac{\partial}{\partial r} \left(r \frac{\partial \varphi}{\partial r} \right) + \frac{1}{r^2} \frac{\partial^2 \varphi}{\partial \theta^2} + \frac{\epsilon_3}{\epsilon_1} \frac{\partial^2 \varphi}{\partial z^2} = 0 \; .$$

Defining $\zeta = \sqrt{\frac{\epsilon_1}{\epsilon_3}}\, z$ reduces this to Laplace's equation for an isotropic medium:

$$\frac{1}{r}\frac{\partial}{\partial r}\left(r\frac{\partial \varphi}{\partial r}\right) + \frac{1}{r^2}\frac{\partial^2 \varphi}{\partial \theta^2} + \frac{\partial^2 \varphi}{\partial \zeta^2} = 0$$

for which the solutions are well known.

$$\varphi = \left[AJ_n(Tr) + BY_n(Tr)\right] e^{\pm jn\theta}\, e^{\pm jT\zeta}$$

$$= \left[AJ_n(Tr) + BY_n(Tr)\right] e^{\pm jn\theta}\, e^{\pm j\sqrt{\epsilon_1/\epsilon_3}\,Tz} .$$

Obviously the propagation constant in the z direction is $h = \pm j\sqrt{\frac{\epsilon_1}{\epsilon_3}}\, T^2$. The boundary conditions require φ to remain finite on the axis and to vanish on the conducting surface $r = r_o$ of the waveguide. Therefore B must be zero and $J_n(Tr_o) = 0$. It follows that the quasi-static dispersion relation is

$$h^2 = -\frac{\epsilon_1}{\epsilon_3} T^2 \quad \text{where } T \text{ satisfies } \quad J_n(Tr_o) = 0 .$$

LIST OF SYMBOLS

Those symbols which appear repeatedly throughout the manuscript are listed below, together with their usual meanings. Symbols which are used at isolated places, perhaps with different meanings from the ones listed below, are defined at the points where they are introduced.

A_1, A_2	Arbitrary constants
$A(h_n)$	Amplitude of the mode corresponding to propagation factor h_n
$\underline{B}$	Magnetic induction
$\underline{B}_o = B_o \underline{e}_z$	Axial magnetostatic field
$\underline{D}$	Electric displacement
$\underline{E}$	Electric field intensity. A t or z subscript denotes, respectively, the transverse or axial component of the field
$\underline{F}_e, \underline{F}_i$	Lorentz force on an electron, on an ion.
$\underline{H}$	Magnetic field intensity. A t or z subscript denotes, respectively, the transverse or axial component of the field
$\underline{I}$	Electric current
$\underline{J}$	Electric current density
$J_n(x)$	Bessel function of the first kind, of order n and argument x
K	Defined by equations II-25 and II-26
N	Complex radiated power
$P(h_n)$	Real power transmitted in a lossless plasma by the modes whose propagation factors are h_n and $-h_n^*$
$\tilde{P}(h_n)$	The generalization of $P(h_n)$ to include dissipative plasmas
$Q(h_n)$	Reactive power transmitted in a lossless plasma by the modes whose propagation factors are h_n and $+h_n^*$
$\tilde{Q}(h_n)$	The generalization of $Q(h_n)$ to include dissipative plasmas

R	Plasma reduction factor
$\underline{S}, S_z$	A closed surface and its z component (Chapter VI)
$S, \bar{S} = Sr_o$	TE radial wave number and its normalization
$T, \bar{T} = Tr_o$	TM radial wave number and its normalization
$T_1, \bar{T}_1 = T_1 r_o$ $T_2, \bar{T}_2 = T_2 r_o$	Radial wave numbers, and their normalizations, for the coupled fields
$U_1(u), U_2(u)$	Separated functions of the generalized coordinate u
$V_1(v), V_2(v)$	Separated functions of the generalized coordinate v
$V_a = \frac{B_o}{\sqrt{\mu_o \rho_m}}$	Alfvén velocity
$V_c = \frac{1}{\sqrt{\mu_o \epsilon_o}}$	Velocity of light in vacuum
$V_g = V_{group} = \frac{d\omega}{d\beta}$	Group velocity
$V_{ph} = V_{phase} = \frac{\omega}{\beta}$	Phase velocity
a, b, c d, f, g	Coefficients of the fields defined by equation II-4
e	Magnitude of the electronic charge
$\underline{e}_z$, etc.	Unit coordinate vector in the z direction, etc.
$h_n = \alpha_n + j\beta_n$	Longitudinal propagation factor for modes of angular order n
h_+, h_-	Propagation factor for the right and left circularly polarized plane waves
$j = \sqrt{-1}$	Imaginary unit
k	Defined by equation III-4
k_o	Defined by equation VI-30
ℓ_u, ℓ_v	Metric coefficients corresponding, respectively, to generalized coordinates u and v

m_e, m	Mass of an electron, of an ion
$n = n_e + n_i$	Total particle density
n_e, n_i	Density of electrons, of ions
$\underline{n}$	Unit normal vector at the waveguide wall
q_i	Charge on an ion
r	Radial coordinate of a cylindrical system
$\underline{r}$	Three-dimensional position vector
r_o	External radius of the plasmaguide
$S = \lvert\bar{S}\rvert$	Magnitude of the normalized TE radial wave number when $\bar{S}$ is imaginary
t	Time
u, v	Generalized coordinates
$\underline{v}_e, \underline{v}_i$	Electron and ion velocities
x, y, z	Rectilinear coordinates
α_n	Real part of propagation factor h_n
β_n	Imaginary part of propagation factor h_n
β_+, β_-	Propagation factors for the right and left circularly polarized plane waves
$\underline{\beta}$	Plane wave propagation vector
$\Gamma_n = \beta_n r_o$	Normalized β_n
γ_1, γ_2	Defined by equation II-3
ϵ_o	Permittivity of vacuum
$\underline{\underline{\epsilon}}$	Permittivity tensor of the magnetoactive plasma
$\epsilon_1, \epsilon_2, \epsilon_3$	Elements of the permittivity tensor as described by equations I-17 and I-18
θ	Polar coordinate
$\Lambda_e, \Lambda_i, \Lambda_p$	Normalized electron, ion, and total plasma frequencies
$\lambda = \frac{\omega r_o}{V_c}$	Normalized signal frequency

λ_a, λ_b	Normalized narrow waveguide cut-off frequencies
λ_e, λ_i	Normalized electron and ion cyclotron frequencies
λ_L, λ_R	Normalized cut-off frequencies for the left and right circularly polarized plane waves
$\lambda_{1,n}\ \lambda_{2,n}\ \lambda_{3,n}$	Normalized TE waveguide cut-off frequencies
$\lambda_{4,n}$	Normalized TM waveguide cut-off frequency
μ_o	Permeability of vacuum
π	$= 3.14159\ldots$
ρ	Total charge density
ρ_m	Total mass density
$\underline{\underline{\sigma}}$	Conductivity tensor of the magnetoactive plasma
$\sigma_1, \sigma_2, \sigma_3$	Elements of the conductivity tensor as described by equations I-11 and I-12
τ_1, τ_2	Defined by equations I-17a,b
Φ_1, Φ_2	Scalar potential functions for the coupled longitudinal fields, cf. equations II-13 and II-14
ϕ	Azimuthal angle between $\underline{\beta}$ and $\underline{B}_o$
φ	Quasi-static potential function (Appendix)
Ψ_1, Ψ_2	Vector potential functions of equation II-30 for the transverse fields
$\Omega_e, \Omega_i, \Omega_p$	Electron, ion and total plasma frequencies
ω	Signal frequencies
ω_a, ω_b	Narrow waveguide cut-off frequencies
ω_e, ω_i	Electron and ion cyclotron frequencies
ω_L, ω_R	Cut-off frequencies for the left and right circularly polarized plane waves
$\omega_{1,n}\ \omega_{2,n}\ \omega_{3,n}$	TE waveguide cut-off frequencies

$\omega_{4,n}$	TM waveguide cut-off frequency

Punctuation

*	The asterisk denotes complex conjugation
$\breve{}$	The breve denotes a suppression of the exponential z dependence of a field
$\hat{}$	The caret denotes a suppression of the exponential θ,z and τ dependences of a field
′	The prime denotes differentiation of a function with respect to its argument
$\sim$	The tilde denotes a reversed magnetostatic field